Characterisation of atypical Rho GTPases of the RhoBTB family and their binding partners

Inaugural-Dissertation

zur

Erlangung des Doktorgrades

der Mathematisch-Naturwissenschaftlichen Fakultät

der Universität zu Köln

vorgelegt von

Kristína Schenková

aus Nitra, Slowakei

Köln 2010

Berichterstatter/in: Prof. Dr. Angelika A. Noegel

                              Prof. Dr. Jürgen Dohmen

Tag der mündlichen Prüfung: 30. Juni 2010

Die vorliegende Arbeit wurde in der Zeit von November 2006 bis Mai 2010 unter Anleitung von Prof. Dr. Angelika A. Noegel und der Betreuung von PD Dr. Francisco Rivero am Institut für Biochemie I der Medizinischen Fakultät der Universität zu Köln und Centre for Biomedical Research, Hull York Medical School, University of Hull, Großbritannien angefertigt.

Acknowledgement

I would like to thank all people that that by any means contribute to the successful completion of this dissertation thesis. Especially I would like to thank:

- PD Dr. Francisco Rivero for the opportunity to work in his group on the interesting topic, for sharing his knowledge and experience, for never ending helpfulness, for long discussions and for the opportunity to present my research at various international meetings.

- Prof. Dr. Angelika A. Noegel for the opportunity to conduct my work in her renowned institute.

- Prof. Dr. Jürgen Dohmen, Prof. Dr. Matthias Hammerschmidt and Prof. Dr. Ludwig Eichinger for their willingness and time to read this thesis and participate in the committee during my exam.

- Prof. Dr. Pontus Aspenström for providing RhoBTB constructs and one cullin construct, Prof. Dr. Reinhard Fässler for providing kindlin constructs, Dr. Manabu Furukawa for providing cullin constructs, Prof. Dr. Martin Bähler for myosin construct and to Dr. Michael Gmachl for providing the ubiquitin construct.

- All my colleagues and co-workers in the Institute for Biochemistry I, Medical Faculty, University of Cologne and in the Centre for Biomedical Research, Hull York Medical School, University of Hull for help and advices, especially to Anja and Nils. Thank you for the great time in Hull ☺!

- My family for support.

- Vlasta for encouragement, emotional support and faith in me.

Table of contents

1 Introduction

1.1 The Ras superfamily of small GTPases

The Ras superfamily, named after the most studied oncogene in human carcinogenesis, Ras, represents a group of small guanosine triphosphatases (GTPases), which comprises over 150 members in humans but can be found in all eukaryotes (Colicelli 2004, Wennerberg et al. 2005). The common feature of these proteins (with few exceptions) is their ability to bind and hydrolyse GTP due to the presence of a ~20 kDa G-domain. The G-domain consists of a six-stranded β-sheet and five α-helices and contains four to five conserved G-box motif elements (G1-G5), which are responsible for binding GTP. The so-called switch domains I and II bind γ-phosphate oxygens of GTP and after GTP hydrolysis and release of γ-phosphate, the switch domains relax into the GDP-specific conformation (Bourne et al. 1991).

Ras proteins act as molecular switches, cycling between an active GTP-bound state and an inactive GDP-bound state. Guanine nucleotide exchange factors (GEFs) and GTPase activating proteins (GAPs) regulate the activation/inactivation cycle (Figure 1.1). The dissociation of GDP from the inactive GDP-bound form is promoted by an upstream signal and conversion to the GTP-bound state is catalysed by GEFs. In the GTP-bound state, small GTPases are active and interact with downstream effector proteins. Hydrolysis of GTP to GDP is very slow and is accelerated by GAPs. In addition, GDP-dissociation inhibitors (GDIs) regulate cycling of Rho and Rab GTPases between cytosol and membranes by capturing them in both GTP- and GDP-bound states (Colicelli 2004, Takai et al. 2001).
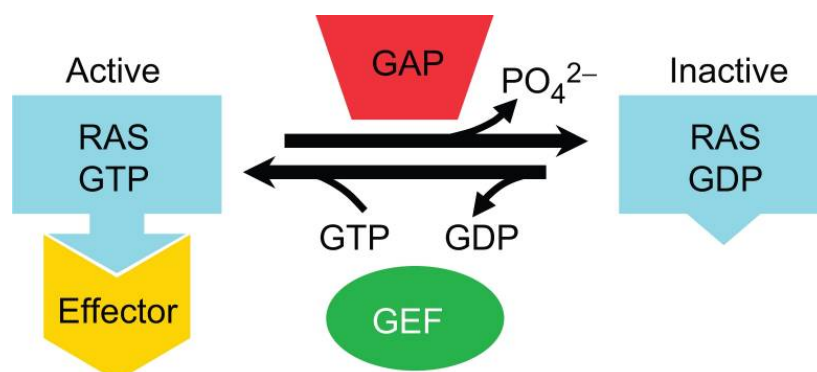
Figure 1.1: Regulation of activity of small GTPases. In the active state, the GTPase binds GTP and interacts with effectors of signalisation. GAPs accelerate the hydrolysis of bound GTP. In GDP-bound state, small GTPases are inactive. GEFs catalyse the release of GDP. Due to the higher cytosolic concentration of GTP than GDP, the GTPase can again bind GTP. Taken from Colicelli (2004).

The Ras superfamily can be subdivided into five families according to the sequence and known functions of their members: Ras (Rat sarcoma oncoproteins), Rho (Ras homologous proteins), Rab (Ras-like proteins in brain), Ran (Ras-like nuclear protein), Arf (ADP-ribosylation factor) and Miro (mitochondrial Rho) (Colicelli 2004, Wennerberg et al. 2005). Members of the Ras superfamily are involved in a variety of cellular processes like gene expression (Ras, Rho), regulation of cell proliferation, differentiation and survival (Ras), actin organisation and cell cycle progression (Rho), vesicular transport and trafficking of proteins (Rab, Arf), transport between nucleus and cytoplasm and microtubule organisation (Ran) (Colicelli 2004, Takai et al. 2001, Wennerberg et al. 2005).

1.2 The Rho-family

The Rho family is characterised by an insertion (so-called Rho insert) of usually 13 residues with high sequence variability between the fifth ß-strand and the fourth α-helix in the GTPase domain (Valencia et al. 1991). To date, 21 proteins of the Rho family have been described in vertebrates (Figure 1.2): Cdc42-like (Cdc42, TC10, TCL, Chp/Wrch2, Wrch1), Rac-like (Rac1-3, RhoG), Rho-like (RhoA-C), Rnd (Rnd1-2, Rnd3/RhoE), RhoD (RhoD und Rif), RhoH/TTF and RhoBTB (RhoBTB1-3) (Wennerberg and Der 2004). RhoBTB3 is very often not considered as a member of the Rho family because of its divergent GTPase domain. Members of the Rho family are present from lower eukaryotes up to mammals and have not been identified in eubacteria and archaea.

The most studied Rho GTPases are RhoA, Rac1 and Cdc42. The members of the Rho, Rac and Cdc42 subfamilies are involved in regulation of cytoskeleton reorganisation in response to extracellular signals. Rho proteins are responsible for the formation of stress fibres and focal adhesions, Rac proteins for the formation of lamellipodia and Cdc42 proteins are involved in filopodia formation. They also have been implicated in many other cytoskeleton-dependent processes like cell growth (G1 cell cycle progression), cytokinesis, morphogenesis, cell-cell interaction, cell polarity and cell migration. In addition, Rho proteins are involved in cellular processes such a membrane trafficking, endocytosis and gene expression (Jaffe and Hall 2005, Takai et al. 2001). Other Rho GTPases have been also identified in cytoskeleton-dependent processes like loss or formation of stress fibres (Rnd1, Rnd3, RhoD and Rif), focal adhesions (Rnd1, Rnd3, and RhoD), cell migration and cell-cell adhesion (Rnd3), formation of Cdc42-independent filopodia (Rif)

and cell migration and cytokinesis (RhoD) (Vega and Ridley 2007). For others, like Rnd2 and RhoBTB1, 2 and 3 an effect on the actin cytoskeleton has not been observed.
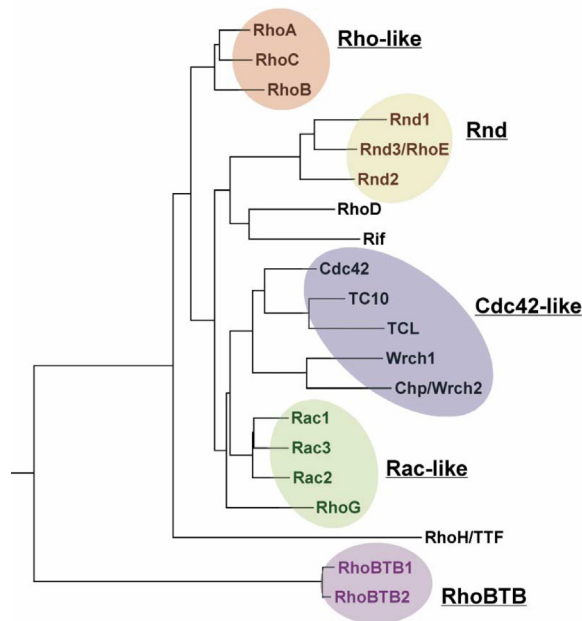
Figure 1.2: Phylogenetic tree of the Rho family of small GTPases. The family can be divided into six subfamilies: RhoA-related, Rac-related, Cdc42-related, Rnd proteins, RhoH/TTF and RhoBTB proteins. Note that RhoBTB3 is not shown in this tree because of its divergent GTPase domain. Taken from Burridge and Wennerberg (2004).

Some of the members of the Rho family are referred to as atypical Rho GTPases because their structure and functional characteristics differ from those of the classical ones. The atypical GTPases are Rnd proteins, RhoH, Wrch1, Chp/Wrch2 and RhoBTB (Aspenström et al. 2007). One of the most striking features that make these Rho GTPases atypical is the difference in the cycling between the GTP- and the GDP-bound state. For example, RhoH has been shown to be constitutively in the GTP-bound state (Li et al. 2002), as well as Rnd1 and Rnd3 (Chardin 2006). Wrch1 is predominantly in the GTP-bound state (Saras et al. 2004, Shutes et al. 2004). RhoBTB proteins seem to be even more different – RhoBTB2 does not bind GTP (Chang et al. 2006) and it was shown recently that RhoBTB3 can bind and hydrolyse ATP (Espinosa et al. 2009).

1.3 RhoBTB proteins

The RhoBTB subfamily constitutes the more recent addition to the Rho family. It was identified during the study of Rho-related protein-encoding genes in *Dictyostelium discoideum* (Rivero et al. 2001). In humans, the RhoBTB subfamily is composed of three

isoforms: RhoBTB1, RhoBTB2 (also named DBC2, <u>d</u>eleted in <u>b</u>reast <u>c</u>ancer <u>2</u>) and RhoBTB3. RhoBTB1 and RhoBTB2 are very similar to each other (79% similarity) and to the *Drosophila* orthologue (Dm RhoBTB), whereas RhoBTB3 (43% similarity to human RhoBTB1 and RhoBTB2) and the *Dictyostelium discoideum* orthologue (RacA) are the most divergent members. Orthologues of RhoBTB have been found in numerous eukaryotes, but they are absent in fungi and plants.

1.3.1 Structure of RhoBTB proteins

RhoBTB proteins consist of a GTPase domain followed by a proline-rich region, a tandem of two BTB domains and a C-terminal domain (Figure 1.3).
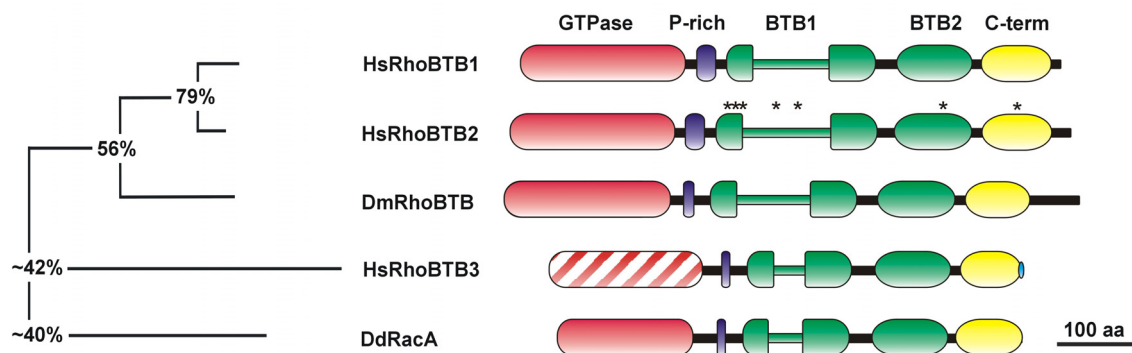
Figure 1.3: Domain architecture of RhoBTB proteins. The GTPase domain of RhoBTB3 is barely recognisable as such. The first BTB domain is interrupted by an insertion of variable length. Only RhoBTB3 has a CAAX motif at the C-terminus. The simplified phylogenetic tree on the left illustrates the relationship among the proteins. Figures denote overall percentage similarity between branches, but the degree of similarity is higher when the comparisons are restricted to particular domains (not shown). Asterisks denote the positions of mutations in RhoBTB2 found in tumours. Hs: *Homo sapiens*, Dm: *Drosophila melanogaster,* Dd: *Dictyostelium discoideum*. Taken from Berthold et al. (2008a).

1.3.1.1 The GTPase domain

The GTPase domain is perhaps the region where most divergence is found among members of the RhoBTB subfamily. Early analyses revealed that this domain is typically Rac-like in RacA and divergent, but recognisable as Rho-related in RhoBTB1 and RhoBTB2 as well as in Dm RhoBTB (Rivero et al. 2001).

The GTPase domain of RhoBTB proteins other than RhoBTB3 and RacA also contains a Rho insert, which is characteristic for Rho proteins. This insert is longer than usual (18 residues or more) and rich in charged residues. Moreover, the GTPase domain of these RhoBTB proteins contains two insertions and one deletion, as well as a few deviations from the GTPase consensus of most Rho GTPases (Rivero et al. 2001). The deletion affects the phosphate/magnesium binding region within the switch II; in particular, one of

the deleted residues is the glutamine equivalent to Q61 in Ras. Also of importance, the glycine residue equivalent to G12 in Ras appears substituted by asparagine in RhoBTB1 and RhoBTB2 or threonine in Dm RhoBTB. Because these two residues are essential for GTP hydrolysis, these proteins would predictably display impaired enzyme activity. Indeed, using a blot overlay approach, Chang et al. (2006) have shown that the GTPase domain of RhoBTB2 appears not to bind GTP at all.

In RhoBTB3, the GTPase domain appears extensively erased, to the point that it is virtually unrecognisable as a GTPase. Only a short stretch at the end of the domain can be reliably aligned to the GTPase domain of other subfamily members. Interestingly, it has been shown recently that RhoBTB3 can bind and hydrolyse ATP (Espinosa et al. 2009). Small GTPases usually contain the sequence NKXD in the G4 box motif within the GTPase domain and the aspartic acid confers specificity for guanosine (Hwang and Miller 1987, Zhong et al. 1995). In RhoBTB3 this aspartic acid is mutated to asparagine and this is the crucial residue for ATP binding and hydrolysis (Espinosa et al. 2009).

In phylogenetic analyses, the GTPase domain of RacA groups together with GTPases of the Rac subfamily and all relevant residues for nucleotide binding and enzymatic activity are conserved (Rivero et al. 2001). In RacA the so-called Rho insert is shorter (6 amino acids) than the usual 13 amino acids of most Rac proteins. As far as it has been examined, the GTPase domain of RacA behaves like other Rac proteins (see section 1.3.3.4).

1.3.1.2 The proline-rich region

The proline-rich region links the GTPase to the first BTB domain. Sequences rich in proline are very common recognition motifs involved in protein-protein interactions. Among the modules that bind proline-rich regions are the SH3 (Src homology 3) domain, the WW domain, the Ena/VASP homology 1 domain, profilin, the GYF domain, ubiquitin enzyme variant (Uev), and the cytoskeleton-associated protein glycine-rich domain (Kay et al. 2000, Li 2005). The SH3 domain is often present in proteins involved in signal transduction and cytoskeleton organisation. The proline-rich region of some RhoBTB proteins could act as a SH3 domain binding site (Figure 1.4). Nevertheless, albeit the sequence analysis strongly suggests that the proline-rich region of several RhoBTB proteins is a potential SH3 domain-binding site, this still needs to be verified experimentally.

```
DdRacA      SVPIPPVMPPAGKAPWIDIITS-
HsRhoBTB1   PLLQAPFLPPKAPPPVIKIPECP
HsRhoBTB2   PLLQAPFLPPKPPPPIIVVPDPP
DmRhoBTB    PLLQAPFRPPKPPPPEVTVMVG-
HsRhoBTB3   HGIRPPQLEQPEKMPVLKAEAS-
```

Figure 1.4: Alignment of proline-rich region sequences of RhoBTB proteins. The P*xx*P motif (where *x* denotes any amino acid) described initially as the core binding motif of the SH3 domain can be found in RhoBTB1, RhoBTB2, DmRhoBTB and Rac1. In RhoBTB3 this region is very poorly preserved. Subsequent analyses have defined proline-rich motifs for a number of different SH3 domains more precisely as +*x*FP*x*FP (class I ligands), FP*x*FP*x*+ (class II ligands) and $^R/_K xx ^K/_R$ (class III ligands); where F is a hydrophobic and + is in most cases a basic residue) (Kay et al. 2000, Li 2005, Mayer 2001). RhoBTB1 and RhoBTB2 have a conserved class II motif and DmRhoBTB has class III motif. Proline residues are marked in grey background. Class II motif and R*xx*K sequence are underlined.

1.3.1.3 The BTB domain

The BTB domain (<u>B</u>road-Complex, <u>T</u>ramtrack, <u>B</u>ric à brac) was named after *Drosophila* transcription factors where this domain was first described. It is also known as a <u>po</u>xvirus and <u>z</u>inc finger domain (POZ). The BTB domain is an evolutionarily conserved domain that is widespread among eukaryotes. In humans, nearly 200 different proteins bear BTB domains, in most cases in combination with other domains. The BTB domain is a protein-protein interaction domain participating in homomeric and heteromeric associations with other BTB domains (Aravind and Koonin 1999) and RhoBTB proteins are also capable of forming homodimers and heterodimers (Berthold et al. 2008b). The crystal structure of some BTB domains has been solved. The BTB core fold consists of a 95 amino acid globular cluster of 5 α-helices flanked by 3 short β-strands (Figure 1.4). The BTB domain of the RhoBTB proteins contains an N-terminal extension that folds into one α-helix and one β-strand, and this extension mediates the formation of dimers and oligomers (Stogios et al. 2005).

More recently, it was shown that proteins containing BTB domains are components of cullin 3 (Cul3)-dependent ubiquitin ligase complexes (Furukawa et al. 2003, Geyer et al. 2003, Pintard et al. 2003, Xu et al. 2003) (see section 1.4.2). The role of RhoBTB proteins as components of Cul3-dependent complexes will be also discussed below (see section 1.4.3).

The BTB domains of RhoBTB have some special features. A tandem of two BTB domains as in RhoBTB is not found within the BTB protein family. Moreover, the first BTB domain is bipartite, being interrupted by an extension of unknown function that is rich in charged residues.
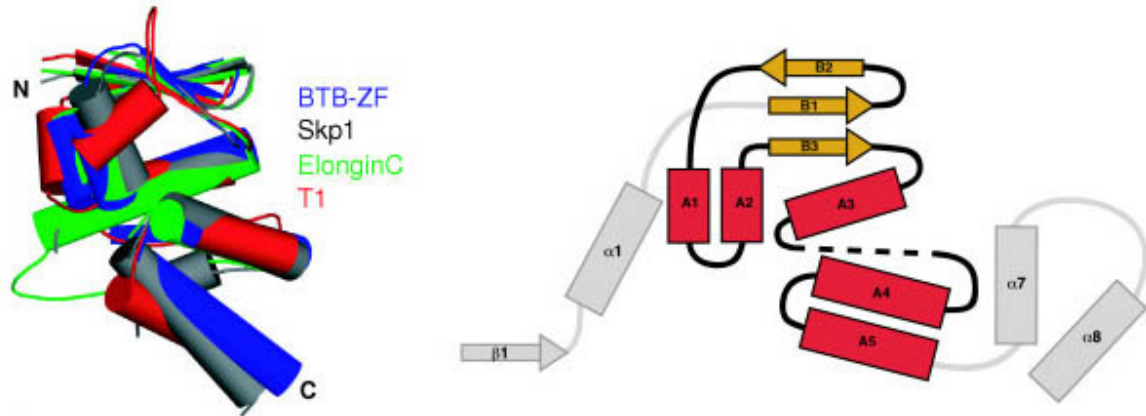
Figure 1.4: Structure of the BTB domain. The BTB core folds from the structures of BTB-Zinc-Finger (BTB-ZF), Skp1, Elongin C and T1 are shown on the left hand panel. The core of the BTB fold consists of three conserved β-strands (B1 to B3) and five α-helices (A1 to A5). The 'long form' of BTB proteins has additionally one α-helix α1 and one β-strand β1. Skp1 protein has two additional α-helices at the carboxyl terminus (α7 and α8). Taken from Stogios et al. (2005).

1.3.1.4 The C-terminal region

Following the second BTB domain, there is a region conserved in all members of the RhoBTB subfamily that may constitute a novel domain, but has not been found so far in any other protein apart from RhoBTB. The core of the C-terminal domain consists of approximately 80 amino acids that predictably folds as four consecutive α-helices. The last helix ends close before the prenylation signal of RhoBTB3, but prolongs further in a predicted β-strand in RhoBTB1, RhoBTB2, and Dm RhoBTB (Ramos et al. 2002). RhoBTB are atypical Rho GTPases – in contrast to the classical Rho family members they do not undergo any known post-translational modification, and almost all of them lack the C-terminal CAAX prenylation motif that is recognised by a set of enzymes that introduce a post-translational modification, isoprenylation, responsible for the targeting of the modified protein to membranes. Only RhoBTB3 ends with the CAAX prenylation motif. Closely upstream of this motif is an additional cysteine residue, which suggests that RhoBTB3 might be also palmitoylated (Ramos et al. 2002).

1.3.2 Expression of RhoBTB proteins

The expression of both, mouse and human *RHOBTB* genes has been studied using different approaches. All three *RHOBTB* genes are ubiquitously expressed although with notable differences in the pattern of tissue levels among the three genes. Interestingly, while *RHOBTB1* and *RHOBTB3* showed high expression levels in many tissues examined, *RHOBTB2* was very weakly expressed in both, human and mouse tissues. *RHOBTB* genes are also expressed in foetal tissues (Nagase et al. 1998a, Nagase et al. 1998b, Ramos et al.

2002). In addition, the expression of one or more *RHOBTB* genes has been reported in numerous human and mouse cell lines using RT–PCR. *RHOBTB3* was found expressed in human cancer cell lines: in leukaemia cell lines, in cervical carcinoma and in colorectal carcinoma (Ramos et al. 2002).

Expression of *RHOBTB2* has been also studied during mammogenesis. St-Pierre et al. (2004) found that during mammary gland development in mice, *RHOBTB2* transcripts are expressed at low but constant levels. However, attempts to study the spatial pattern of the expression of *RHOBTB2* in the mammary gland using *in situ* hybridisation were inconclusive because of undetectable mRNA levels.

1.3.3 Function of RhoBTB proteins

Over the past years it has been shown that RhoBTB is involved in several cellular processes. However, the connection between these processes is largely unknown. The role of RhoBTB proteins as components of the Cul3-dependent complexes will be discussed below (see section 1.4.3).

1.3.3.1 RhoBTB, cell growth, and apoptosis

Overexpression of RhoBTB2 in the breast cancer cell line T-47D (a cell line that lacks RhoBTB2 transcripts) effectively suppressed cell growth *in vitro* (Hamaguchi et al. 2002). More recently, Freeman and co-workers have shown that the overexpression of RhoBTB2 leads to a short-term increase in cell cycle progression and proliferation, but long-term expression has a negative effect on proliferation (Freeman et al. 2007). The growth arrest effect of RhoBTB2 has been explained by the downregulation of cyclin D1. Cyclin D1 is upstream of cyclin E, and the overexpression of any of both prevented the growth arrest effect of RhoBTB2 (Yoshihara et al. 2007). The effect on cyclin D1 is only partially dependent on proteasomal degradation. Moreover, it has not been investigated whether cyclin D1 is degraded by Cul3-dependent complexes through direct binding to RhoBTB2. The downregulation of cyclin D1 is essential for the cell proliferation suppression effect of RhoBTB2, but this works for T-47D cells and not for 293 cells. It therefore appears that the regulation of cyclin D1 is not a universal tumour suppressive mechanism used by RhoBTB2. The explanation has been put forward that resistance to RhoBTB2 in some cell lines may be achieved by rapid destruction of the protein through 26S proteasome-mediated degradation (Collado et al. 2007). Further support for the roles in cell cycle regulation has been provided recently with the identification of *RHOBTB2* as a target of

the E2F1 transcription factor (Collado et al. 2007). E2F1 is a member of a class of E2F implicated in the transcription of genes necessary for DNA replication and cell cycle progression and can also promote apoptosis (DeGregori and Johnson 2006). RhoBTB2 levels increase upon initiation of prophase and decrease at telophase, and this effect depends on E2F1 (Freeman et al. 2007). RhoBTB2 levels also increase during drug-induced apoptosis in an E2F1-dependent manner, and the downregulation of *RHOBTB2* delays the onset of apoptosis (Freeman et al. 2007). In agreement with an implication in this process, *RhoBTB* was found in *Drosophila* as one of several genes whose expression was significantly upregulated in a DNA microarray analysis aimed at identifying genes associated with cell death induced by the steroid hormone ecdysone (Lee et al. 2003). However, the role of RhoBTB as a possible cell death regulator was not investigated further.

1.3.3.2 RhoBTB and chemokine expression

It was shown recently that downregulation of *RHOBTB2* by RNA interference in primary lung epithelial cells causes a decrease in mRNA expression of CXCL14 (a chemokine that controls leukocyte migration and angiogenesis). The same effect was observed in keratinocytes. Apparently, this effect is independent of Cul3-mediated protein degradation (McKinnon et al. 2008).

1.3.3.3 RhoBTB and vesicle transport

Chang et al. (2006) have addressed the potential role of RhoBTB2 in vesicle transport in a fluorescent recovery after photobleaching analysis with the help of a vesicular stomatitis virus glycoprotein (VSV-G) fused to GFP. VSV-G is extensively used to study anterograde transport from the endoplasmic reticulum (ER) to the Golgi apparatus (GA). Knockdown of endogenous RhoBTB2 hindered the ER to GA transport and resulted in the altered distribution of the fusion protein.

More recently, it was reported that RhoBTB3 binds the GTP-bound conformation of Rab9 through the second BTB domain and the C-terminal domain (Espinosa et al. 2009). Rab9 localises to late endosomes and vesicles travelling towards the Golgi apparatus (GA). It is required for the trafficking of the mannose 6-phosphate receptors (MPRs) from late endosomes to the GA (Lombardi et al. 1993, Riederer et al. 1994). Using siRNA depletion of RhoBTB3 Espinosa et al. (2009) demonstrated that RhoBTB3 is required for retrograde transport of MPRs to the GA. Interestingly, these authors did not observe any alteration in

transport of VSV-G from ER to GA as it was reported for RhoBTB2 (Chang et al. 2006). By measuring ATPase activity of purified proteins Espinosa et al. (2009) demonstrated that Rab9 enhances ATP hydrolysis of RhoBTB3. Moreover, RhoBTB3 binds TIP47 (tail-interacting protein of 47 kDa), that is recruited by Rab9 from the cytosol to late endosomes to package MPRs cargo for transport (Carroll et al. 2001, Ganley et al. 2004). Espinosa et al. (2009) proposed a model in which Rab9 activates RhoBTB3 on the GA, which removes TIP47 from the vesicles and permits membrane fusion of vesicles with the GA. Further, in support of a role in vesicle trafficking, *RhoBTB* has been identified as one of the genes that suppress the neuromuscular junction overgrowth phenotype induced in *Drosophila* larvae by the expression of a dominant negative form of the N-ethylmaleimide sensitive factor (NSF) (Laviolette et al. 2005). NSF is an ATPase that participates in vesicle trafficking through binding to the SNARE complex and is also important for the regulation of receptor trafficking (Zhao et al. 2007).

1.3.3.4 RhoBTB and the actin filament system

Although very atypical, RhoBTB proteins are members of the Rho family, therefore, the first aspect that was investigated was their effect on the organisation of the actin filament system. Aspenström et al. (2004) observed only a moderate influence on the morphology and actin organisation of porcine aortic endothelial cells upon the ectopic expression of RhoBTB1 and RhoBTB2. Not surprisingly, neither RhoBTB1 nor RhoBTB2 were found to interact with the GTPase-binding domain of WASP, PAK1, or Rhotekin, three well-known effectors of many typical Rho GTPases. Confirming that, at least in metazoa, RhoBTB proteins do not play a major role in the organisation of the actin filament system, Dm RhoBTB was found among the proteins whose depletion had no effect on lamellae morphology in *Drosophila* S2 cells (Rogers et al. 2003). Unlike metazoan RhoBTB, the *Dictyostelium* orthologue RacA may be directly implicated in the regulation of the actin cytoskeleton. The GTPase domain of RacA, which is very closely related to members of the Rac subfamily, is able to interact with the Rac-binding domain of WASP and kinases of the PAK family in yeast two-hybrid assays (de la Roche et al. 2005, Han et al. 2006, Park et al. 2004). Unlike metazoan RhoBTB, RacA is susceptible to regulation by RhoGEF and RhoGAP, and *in vitro* interaction with a RhoGEF, GxcDD, has been reported recently (Mondal et al. 2007). RacA probably represents a "primitive" cytoskeleton-regulating stage of the RhoBTB subfamily that was

replaced in the evolved metazoan RhoBTB proteins by roles in cell proliferation and vesicle trafficking.

1.3.4 RhoBTB in human diseases

Since the first report proposing *RHOBTB2* as a tumour suppressor gene, evidence is accumulating in support of members of the RhoBTB subfamily being implicated in tumorigenesis. The *RHOBTB2* gene was identified as the gene homozygously deleted at region 8p21 in breast cancer samples (Hamaguchi et al. 2002). This is a region commonly associated with loss of heterozygosity (LOH) in a wide range of cancers. Alterations found in *RHOBTB* genes in tumour tissues and cell lines are summarised in Table 1.1 and are also depicted in the Figure 1.3.

Tumour type	Genomic alterations (% cases)	Mutation and effect	Decreased expression (% cases)	Reference
RHOBTB1				
Head and neck	23% LOH (n=52 tumours)	None n = 52 tumours	37% (n=46 tumours)	(Beder et al. 2006)
RHOBTB2/DBC2				
Breast	3.5% HD (n=200 tumours)	E5 G>A D299N No growth inhibition when re-expressed E9 C>A P647T Unknown effect E5 A>C D368A Unknown effect n = 65 tumours + 65 cell lines of breast and lung cancer	42% (n=19 cell lines)	(Hamaguchi et al. 2002)
Lung	NA	E5 T>G Y284D Abolished binding to Cul3 n = 65 cell lines of breast and lung cancer	50% (n=14 cell lines)	(Hamaguchi et al. 2002) (Wilkins et al. 2004)
Breast (sporadic)	NA	Promoter –238G>A Altered expression? Promoter –121C>T Altered expression? 5' UTR +48G>A Altered expression? n = 100 tumours	NA	(Ohadi et al. 2007)
Breast (familial)	NA	None n = 17 tumours	NA	(Ohadi et al. 2007)
Stomach	29% LOH (n=95 tumours)	E5 C>T R275W Unknown effect n=95 tumours	NA	(Cho et al. 2007)
Bladder	42% LOH (n=54 tumours) 38% LOH (n=32 cell lines)	E5 G>C E349D Unknown effect E7 G>A G561S* Unknown effect (only cases with SSCP mobility shift were sequenced)	75% (n=12 cell lines)	(Knowles et al. 2005)

Table 1.1: Alterations found in *RHOBTB* genes in tumour tissues and cell lines. Only changes identified either as mutations or as polymorphisms that could result in functional alterations are shown in the table. The genomic structure of the *RHOBTB* genes is described in Ramos et al. (2002). Note that in the table exons are numbered from the first transcribed exon, whereas in Ramos et al. exon 1 was considered the exon with the ATG codon. *RHOBTB1* is placed in 10q21.2, *RHOBTB2/DBC2* in 8p21.3 and *RHOBTB3* in 5q15. HD - homologous deletion; LOH - loss of heterozygosity; NA - not analysed; SSCP - single strand conformation polymorphism; *Polymorphism with possible effect. Modified from Berthold et al. (2008a).

In some of these studies decreased expression of *RHOBTB1* and *RHOBTB2* in tumour samples was observed (Beder et al. 2006, Hamaguchi et al. 2002, Knowles et al. 2005). Although we still have limited information on the status of *RHOBTB* genes in tumours, the picture that emerges from the reports is one of rare mutations but common reduced or extinguished expression. This observation can be made extensive to the third family member, *RHOBTB3*. Berthold et al. (2008b) determined the expression of *RHOBTB3* in an array of tumour tissues and their matched normal tissues and have found a moderate but significant decrease of *RHOBTB3* expression in the breast, kidney, uterus, lung, and ovary tumours.

Recently, RhoBTB3 was proposed by Kurian et al. (2009) as a blood biomarker for psychosis that are accompanied by hallucinations, as decreased expression of RhoBTB3 mRNA in patients with high hallucinations states was observed.

1.4 RhoBTB proteins and proteasome-dependent degradation

1.4.1 General overview of the proteasome-dependent degradation pathway

Until 1980's, protein degradation was an unexplored area of cell biology. This process was considered as an unspecific phenomenon. Today it is clear that destruction of proteins is as important as their synthesis to achieve homeostasis in living organisms. The key molecule in this process is ubiquitin, a small (8.6 kDa) globular protein. It is highly conserved among eukaryotes (e.g. human and yeast ubiquitin differ only in three amino acids), but is absent in eubacteria and archaea. It is necessary to mention that besides degradation of proteins, ubiquitination is also involved in other non-proteolytical cellular processes like histone modification (Shukla et al. 2009) and viral budding (Patnaik et al. 2000, Schubert et al. 2000, Strack et al. 2000).

Degradation of unwanted or misfolded proteins by the proteasome-dependent degradation pathway is accomplished in two consecutive steps: 1) substrate tagging by a polyubiquitin chain and 2) recognition of the polyubiquitinated protein by the 26S proteasome. First, the ubiquitin-activating enzyme E1 activates ubiquitin in an ATP-requiring reaction to generate a high-energy E1-thiol-ester~ubiquitin intermediate E1-S~Ub (Haas et al. 1982). This activated thiol moiety is transferred to the ubiquitin-conjugating enzyme E2 (also called ubiquitin-carrier protein, UBC), forming a high-energy thiol ester intermediate E2-S~Ub (Hershko et al. 1983). Activated ubiquitin is then transferred from E2 to the substrate by the third enzyme called ubiquitin-ligase E3 (Hershko et al. 1983). It is the

E3, which specifically interacts with different substrates. E3s mediate this transfer by different mechanism and can be grouped in several classes. The two best known classes are HECT (homologous to the E6-AP COOH terminus) ligases and RING (Really Interesting New Genes) finger-containing ligases. In the case of HECT ligases, activated ubiquitin is transferred first to the E3 before it is conjugated to the ligase-bound substrate. RING finger-containing ligases catalyse the direct transfer of the ubiquitin to the substrate (Glickman and Ciechanover 2002) (Figure 1.5).
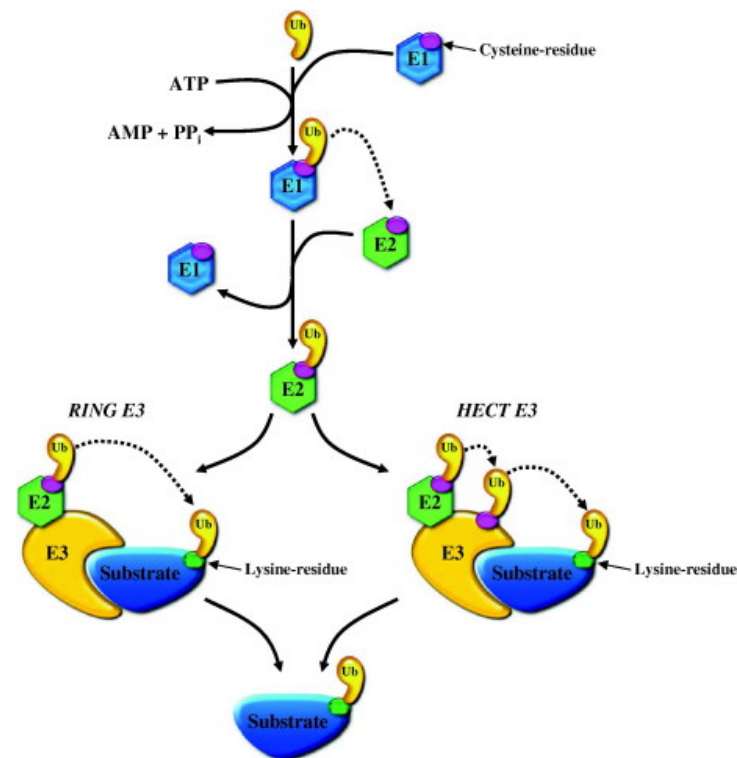
Figure 1.5: Proteasome-dependent degradation pathway. E1 activates ubiquitin in an ATP-requiring reaction. Activated ubiquitin is then transferred to E2 and from E2 to the substrate by the third enzyme called ubiquitin-ligase E3. RING finger-containing ligases catalyse the direct transfer of ubiquitin from E2 to a lysine-residue on the substrate protein. HECT-domain E3 enzyme transfers ubiquitin from E2 to a cysteine-residue on E3 and then to a lysine-residue in the substrate protein. Taken from Jung et al. (2009).

The ubiquitin molecule has seven lysine residues (K6, K11, K27, K29, K33, K48 and K63) and it has been shown that for formation of ubiquitin chains *in vivo* all lysine residues are used (Peng et al. 2003). Ubiquitin is attached to the protein substrate by a covalent isopeptide bond between the C-terminal glycine of ubiquitin and the ε-NH2 group of a lysine residue of the substrate protein (Hershko et al. 1980). A polyubiquitin chain is formed by subsequent attachment of the C-terminal glycine of the next ubiquitin to the lysine of the previous ubiquitin. The minimal and sufficient length of polyubiquitin

chain that serves as a tag for degradation in the proteasome is four ubiquitin molecules (Thrower et al. 2000). Up to date, the best described and characterised polyubiquitin chains are the Lys48- and Lys63-linked chains. Lys48-linked polyubiquitin chains constitute the major signal for targeting the substrates to the proteasome for degradation (Pickart 1997). Lys63-linked ubiquitination was believed to be involved in proteasome-independent processes such as DNA repair (Spence et al. 1995) and receptor endocytosis (Acconcia et al. 2009). However, nowadays there is also evidence that polyubiquitin chains linked through Lys63 to the protein may also serve as a signal for proteasome-dependent degradation (Kim et al. 2007, Saeki et al. 2009).

Ubiquitin-mediated degradation is a very complex process that is undoubtedly crucial for proper cell function. It has been implicated in a variety of cellular processes, like cell-cycle regulation, signal transduction, transcription factor regulation (Glickman and Ciechanover 2002, Weissman 2001), the quality control of newly synthesised proteins (ERAD) (Hirsch et al. 2009) and immune response (Bhoj and Chen 2009). Dysfunction of components of this pathway leads to the development of diseases like cystic fibrosis, atherosclerosis, diabetes, several neurodegenerative illnesses (e.g. Parkinson's disease, Alzheimer's disease) and has been linked also with the process of aging (Jung et al. 2009).

1.4.2 Cullin (Cul)-dependent E3 ligases

Cullins (of which there are 7 in mammals) function as scaffolding proteins that bring together the ubiquitin-conjugating enzyme and substrate-recognition components. The crystal structure revealed that they are composed of three repeats of five helix bundles and a globular C-terminal domain (Angers et al. 2006, Goldenberg et al. 2004, Zheng et al. 2002). Cullins belong to the group of RING-finger containing ligases. The core ligase of a Cul-dependent complex consists of a cullin protein that binds the RING-finger protein Roc1 (which recruits the ubiquitin-conjugating enzyme) through its C-terminus and a linker protein through its N-terminus. An adaptor protein then acts as a bridge between the linker protein and the substrates. The complex is positively regulated by covalent attachment of the Nedd8 ubiquitin-like protein to the cullin subunit. Each cullin family member interacts with a specific linker. The Cul1 complex contains the Skp1 linker and an F-box-containing adaptor (called SCF complex: Skp1/Cul1/F-box). The Cul2 and Cul5 complexes contain the linker Elongin C (along with Elongin B) and a SOCS-box-containing protein (called ECVcomplex: EloB/C-Cul2-VHL-box protein or ECS complex: EloB/C-Cul5-SOCS-box protein). The Cul3 complexes contain a BTB domain-bearing

protein that functions simultaneously as linker and adaptor (Petroski and Deshaies 2005) (Figure 1.6). Interestingly, comparison of the structure of the BTB domain with Skp1 and Elongin C demonstrated that Skp1 and Elongin C are in fact BTB proteins that display a similar interface for interaction with the corresponding cullin, despite a low degree of primary sequence conservation (Stogios et al. 2005).
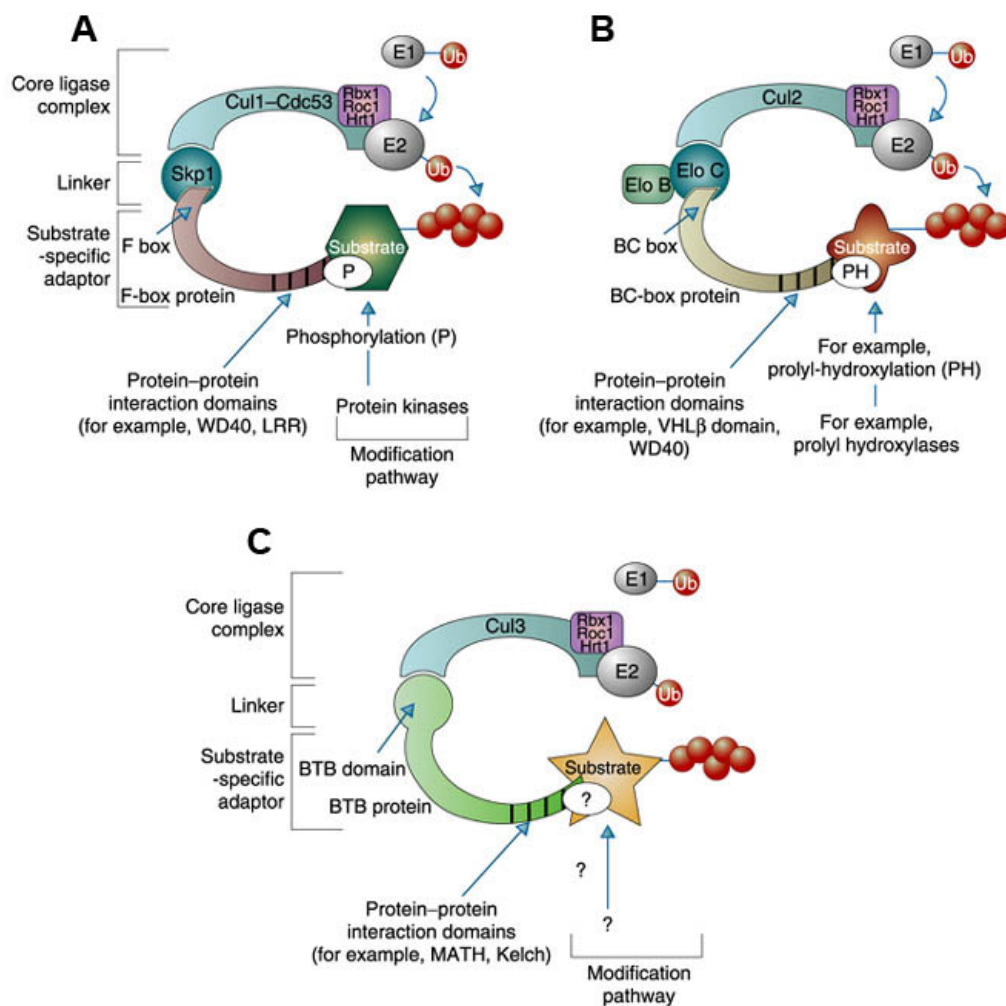
Figure 1.6: Cullin-dependent ubiquitin ligases share a similar architecture. A)   The archetypal SCF complex contains Cul1, Skp1 and Rbx1/Roc1/Hrt1 and an F-box protein. B) ECV/ECS complex contains Cul2 (or Cul5), Elongin B/C, Rbx1/Roc1/Hrt1 and a BC-box protein. C)   In the ubiquitin-ligase complex containing Cul3, Rbx1/Roc1/Hrt1 and BTB-domain protein, the BTB protein associates directly with Cul3 through its BTB domain without the help of a linker protein. Taken from Krek (2003).

1.4.3 RhoBTB proteins as adaptors of Cul3-dependent ubiquitin ligases

The identification of the BTB domain as adaptor in Cul3-dependent ubiquitin ligase complexes prompted Wilkins and co-workers to investigate whether RhoBTB2 may also take part in the formation of such complexes (Wilkins et al. 2004). They identified the N-terminal region of murine Cul3 as an interacting partner of RhoBTB2 in a yeast two-hybrid

screening (Wilkins et al. 2004). RhoBTB2 interacts specifically with Cul3, but not with other cullin family members *in vivo*. The interaction was mapped to the first BTB domain in a series of pull-down experiments with deletion constructs. Wilkins et al. (2004) also provided evidence that RhoBTB2 is itself a substrate for Cul3-based ubiquitin ligase complexes, as treatment with proteasomal inhibitor MG132 or shRNA ablation of Cul3 resulted in increased levels of RhoBTB2, and RhoBTB2 was polyubiquitinated by Cul3 complexes *in vitro*. RhoBTB3, similar to RhoBTB2 interacts with Cul3 through the first BTB domain and upon proteasomal inhibition accumulates in the cells (Berthold et al. 2008b). *RHOBTB2* was proposed as a candidate tumour suppressor gene based on the fact that its re-expression in T-47D (a breast cancer cell line that lacks *RHOBTB2* transcripts) caused growth inhibition, whereas the expression of the somatic mutant D299N did not have the same effect (Hamaguchi et al. 2002). This mutation is placed in the first BTB domain immediately before the insertion. In fact, it is interesting that almost all missense mutations found in the *RHOBTB2* locus reside in the first BTB domain of the protein (Figure 1.3). The question arises whether one or more of those mutations result in impaired interaction with Cul3. This has been investigated by Wilkins et al. (2004) who found that the Y284D mutant, but not the D299N and D368A mutants, failed to co-immunoprecipitate with Cul3, and consequently, had a longer half life than the wild-type protein. The Y284D mutation resides in the dimerisation interface of the first BTB domain and could prevent proper folding. Analogous mutants have been shown to abrogate function by impairing folding of the BTB domain, for example, in the transcription factor PLZF (Melnick et al. 2000).

1.5 MUF1/LRRC41

To date, no substrates have been shown to be degraded by RhoBTB-Cul3-dependent ligase complexes. Previous experiments performed in our laboratory identified a list of potential binding partners of RhoBTB3 that includes MUF1, kindlin-2 and Uev1a (S. Ramos, personal communication). However, these interactions have not been investigated extensively and are the object of this thesis.

MUF1/LRRC41 (leucine-rich repeat containing 41) is a largely uncharacterised protein that has an N-terminal SOCS-box motif and a C-terminal leucine-rich repeat (LRR) region (Figure 1.7A). It has been shown that MUF1 interacts with Elongin B/C through the BC-box subdomain of the SOCS-box. This interaction mediates binding to Cul5 and

the MUF1-Elongin B/C-Cul5-Rbx1 complex has ubiquitin ligase activity (Kamura et al. 2001). The expression, subcellular localisation and function of MUF1 have not been addressed so far.

Figure 1.7: Domain composition of MUF1. A) Schematic representation of MUF1. Numbering of amino acids is in respect to the murine MUF1. The SOCS-box is at the N-terminus of MUF1 and the leucine-rich repeat (LRR) region is C-terminal. B) Sequence alignment of MUF1 SOCS-box with representative SOCS-box sequences and SOCS-box consensus. Amino acids at position A42-P71 of MUF1 are shown. Red arrows indicate amino acid residues crucial for interaction with EloB/C. *SOCS3*, SH2 domain-containing SOCS-box protein 3; *WSB1*, WD repeat-containing SOCS-box protein 1; *ASB2*, ankyrin repeat-containing SOCS-box protein 2; *RAR*, Ras-related SOCS-box protein; *SSB1*, SPRY domain-containing SOCS-box protein. Modified from Kamura et al. (2001). C) The LRR of murine MUF1. The conserved regions $LxxLxLxx^N/_CxL$ are highlighted in grey.

1.5.1 The SOCS-box

The SOCS-box is a structural motif that has been initially characterised in the members of the suppressors of cytokines signalling (SOCS) family (Hilton et al. 1998). SOCS proteins have been originally identified as negative regulators of the JAK-STAT signalling pathway induced by cytokine stimulation (Endo et al. 1997, Naka et al. 1997, Starr et al. 1997). All SOCS proteins (SOCS1-7, CIS) share structural similarities: an N-terminal region of

variable length is followed by an SH2 domain and the SOCS-box, which is located at the C-terminus (Hilton et al. 1998, Starr et al. 1997). The SOCS-box is a ~40 amino acid motif composed of two well conserved blocks separated by 2 – 10 non-conserved residues (Figure 1.7B). The C-terminal conserved region is a cullin box motif, and the N-terminal conserved region is a consensus BC-box, a ~10 amino acid degenerate sequence motif with the consensus sequence (A,P,S,T)L*xxx*C*xxx*(A,I,L,V), where leucine at position 2 and cysteine at position 6 are highly conserved. SOCS-box proteins bind to the Elongin C through the BC-box (Kamura et al. 1998, Zhang J.G. et al. 1999), which is structurally similar to Skp1 and the BTB fold as already mentioned (Stogios et al. 2005). Binding of Elongin C to the BC-box is mediated by interaction with the highly conserved leucine at position 2 (Stebbins et al. 1999) and point mutations at conserved residues within the BC-box abolish this interaction (Kamura et al. 1998, Kamura et al. 2001). Elongin C interacts with ubiquitin like protein Elongin B (Garrett et al. 1994) and the whole complex can bind to Cul2 or Cul5, depending on the specific cullin box (Kamura et al. 2004). The ECV complex (EloB/C-Cul2-VHL-box) and the ECS complex (EloB/C-Cul5-SOCS box) resemble SCF complex and have ubiquitin ligase activity (De Sepulveda et al. 2000, Iwai et al. 1999, Kamizono et al. 2001, Kamura et al. 2001). A large number of SOCS-box containing proteins accommodate additional domains like WD-40 repeats, SPRY domains and ankyrin repeats (Hilton et al. 1998, Masuhara et al. 1997). In all these proteins the SOCS-box domain is C-terminal. With an N-terminal SOCS-box, MUF1 seems to be unique.

1.5.2 The LRR

The leucine-rich repeat (LRR) is a structural motif that has been implicated in mediating protein-protein interactions. It has been identified in thousands of proteins in eukaryotes, bacteria, viruses and archaea. LRRs are usually 20-29 residues long sequences repeating multiple times within the protein (2 to 52 times). LRRs are usually composed of a so-called conserved segment, which shows significant similarities in all known LRR containing proteins, and a variable segment whose sequence varies among the members of different subfamilies (Bella et al. 2008). The sequence of the conserved region is L*xx*L*x*L*xx*$^\mathrm{N}$/$_\mathrm{C}$*x*L, where *x* denotes any amino acid. Later it has been shown that there is certain variability in the conserved region and leucine can be substituted by valine, isoleucine or phenylalanine; asparagine/cysteine can be substituted by either serine or threonine (Kajava 1998). The first LRR protein that has been crystallised was the ribonuclease inhibitor (RI). RI

adopts a curved solenoid structure where the LRRs form β-sheets on the concave side of the solenoid and are connected by loops with α-helices that align on the convex side (Figure 1.8A) (Kobe and Deisenhofer 1993). Since the 3D structure of RI has been solved, nearly 90 structures of other LRR proteins have been determined indicating that all LRRs adopt a more or less perfect solenoid conformation (Bella et al. 2008).

LRR containing proteins have been implicated in wide range of cellular processes as cell adhesions, signalling, extracellular matrix assembly, platelet aggregation, neuronal development, RNA processing, invasion of pathogenic bacteria to the cell and immune response (Bella et al. 2008). Mutations in genes encoding LRR proteins have been associated with several human diseases such as schizophrenia, Parkinson's disease and Crohn's disease (Matsushima et al. 2005).
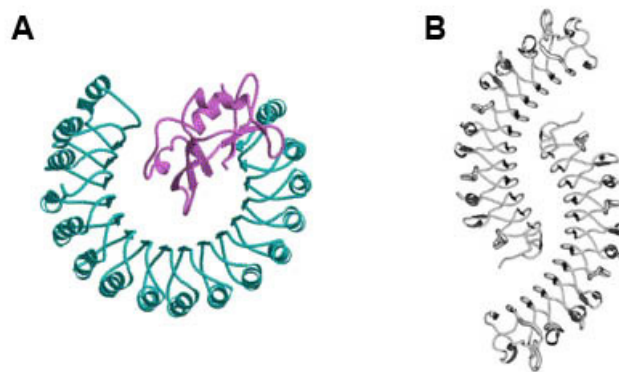
Figure 1.8: 3D structure of LRR proteins. A) 3D structure of ribonuclease inhibitor (RI). The LRR domains are shown in cyan, the other domains are shown in magenta. Taken from Kobe and Kajava (2001). B) 3D structure of decorin core protein (DCN). DCN is capable of homodimerisation, where the surface on the concave side is used as a homodimerisation interface. Taken from Bella et al. (2008).

It is the concave side of LRR domain that is mainly involved in protein-protein interactions and moreover, it has been demonstrated that proteins containing a LRR region form very often homo- and heterodimers (Figure 1.8B) (e.g. Toll-like receptor ectodomain, Ran GTPase-activating protein, monocyte differentiation antigen CD14) or even larger assemblies like tetramers (*Yersinia* outer membrane protein M, YopM) (Bella et al. 2008). Examination of the leucine rich repeat region of mouse MUF1 revealed at least four conserved 11 amino acids long LxxLxLxx^N/$_C x$L motifs (Figure 1.7C).

1.6 The kindlin protein family

The kindlin family consists of three members: kindlin-1, kindlin-2 and kindlin-3 (Siegel et al. 2003). Kindlins are encoded by the *FERMT* (fermitin family homologue) genes *FERMT1*, *FERMT2* and *FERMT3*. The first identified member of this family was kindlin-

2, which was identified among serum-inducible genes in serum-starved quiescent human fibroblasts and was initially named Mig-2 (<u>mi</u>togen-<u>i</u>nduced <u>gene 2</u>) (Wick et al. 1994). Kindlins are composed of a FERM (4.1, ezrin, radixin, moesin) domain, which is subdivided into four subdomains named F0, F1, F2 and F3 (Figure 1.9). The N-terminally localised F0 subdomain adopts an ubiquitin-like fold. The F1 subdomain is interrupted by an insert that has a similar size in kindlin-1 and kindlin-2, but is shorter in kindlin-3 (Goult et al. 2009). The F2 subdomain is interrupted by a pleckstrin homology (PH) domain and the F3 subdomain contains a phosphotyrosine binding fold (PTB) that is capable of recognising β integrin tails (Kloeker et al. 2004, Shi et al. 2007).

Figure 1.9: Domain structure of kindlins. Kindlins are composed of a FERM (4.1, ezrin, radixin, moesin) domain, which is subdivided into subdomains named F0, F1, F2 and F3. The F2 subdomain is interrupted by a pleckstrin homology domain (PH). This insertion does not interfere with FERM domain function. A nuclear localisation signal has been described in the F0 subdomain of kindlin-2.

1.6.1 The role of kindlins in integrin activation

All three kindlins have been shown to bind directly to cytoplasmic tails of β1 and β3 subunits of integrins (Figure 1.10) and have been identified as key regulators of integrin activation, together with talin (Harburger et al. 2009, Moser et al. 2008, Ussar et al. 2008). Integrins are heterodimeric transmembrane receptors that are composed of α and β subunits. There are 18 α and 8 β subunits in mammals that combine with each other to form 24 specific dimers. Each integrin subunit has a large extracellular domain, a short transmembrane domain and a cytoplasmic tail (Hynes 2002). Inactive integrins assume a bent conformation and are in a low affinity binding state for ligands; they shift to a high affinity state during activation (Moser et al. 2009). Integrins are localised in focal adhesions and interact with proteins of the extracellular matrix (ECM) through their extracellular domain and, via talin, with the actin cytoskeleton through their cytoplasmic tail (Zhang et al. 2008). Through these interactions integrins constitute a fundamental connection for bi-directional communication between the ECM and the intracellular environment. Talin, similarly to kindlins, bears a FERM domain composed of F0, F1, F2 and F3 subdomains. The F3 subdomain contains a PTB that is the major integrin binding site (Wegener et al. 2007). Both talin and kindlin are crucial for integrin activation by binding to the cytoplasmic tail of β integrins. The F3 subdomain of talin binds to

the membrane proximal NP*x*Y motif and induces separation of integrin tails, whereas kindlin binds to the membrane distal N*xx*Y motif (Moser et al. 2009).
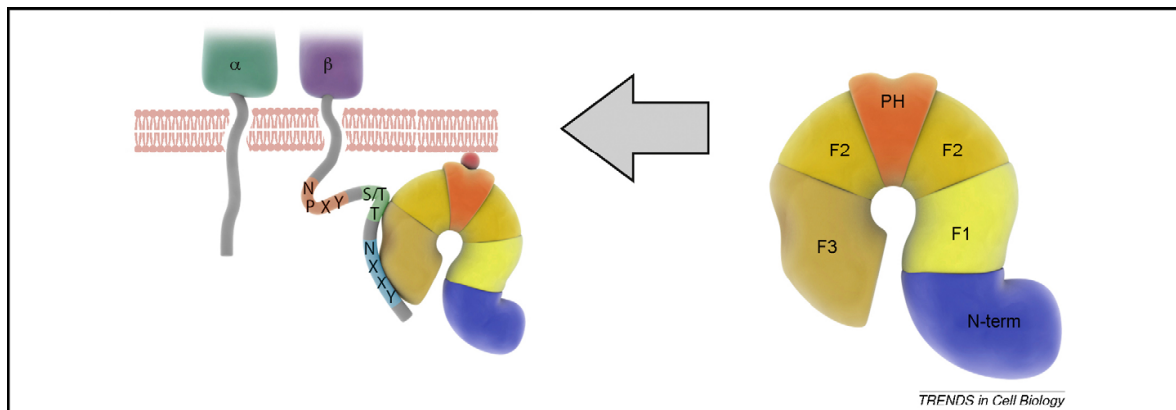
Figure 1.10: A model of kindlin binding to β integrin cytoplasmic tails. Kindlin prefers to interact with a membrane distal (T/S)T*xx*N*xx*Y amino acid sequence but interaction with the membrane proximal NP*x*Y motif has been also reported. The N-terminal region corresponds to the F0 subdomain Taken from Meves et al. (2009).

1.6.2 Expression and localisation of kindlins

Human kindlin genes show distinct differences in expression. Expression of kindlin-1 is restricted to the skin epithelial cells (keratinocytes) and intestinal epithelial cells (Lai-Cheong et al. 2008, Siegel et al. 2003, Ussar et al. 2006), while kindlin-2 is ubiquitously expressed with the exception of the hematopoietic cells, where kindlin-3 was found (Ussar et al. 2006). Kindlin-1 and kindlin-2 localise predominantly to focal adhesions in keratinocytes (Kloeker et al. 2004, Siegel et al. 2003, Tu et al. 2003, Ussar et al. 2006) but cytoplasmic localisation of kindlin-1 has also been reported, including the perinuclear area (Kloeker et al. 2004, Lai-Cheong et al. 2008, Siegel et al. 2003). Localisation of kindlin-2 to stress fibres has also been reported (Tu et al. 2003). Kindlin-2 is the only member of the kindlin family that contains a nuclear localisation signal (Ussar et al. 2006) and endogenous kindlin-2 was visualised in the nuclei of smooth muscle cells (Kato et al. 2004). Contrary to this, kindlin-1 but not kindlin-2 was found in the nucleus of normal human keratinocytes (Lai-Cheong et al. 2008). Mouse kindlin-3 localises to the podosomes of macrophages and dendritic cells that are integrin-dependent adhesion sites in hematopoietic cells (Ussar et al. 2006).

1.6.3 Kindlin in human diseases

All three kindlins have been implicated in human diseases and cancer. This family is named after dermatologist Theresa Kindler who described a patient with traumatic bulla formation, atrophy of the skin and congenital poikiloderma. Today this disease is named Kindler syndrome, an autosomal recessive genodermatosis caused by loss-of-function mutations in the *FERMT1* gene. These mutations are predicted to reduce expression and function of kindlin-1. It was reported that patients with Kindler syndrome have a predisposition to non-melanoma skin cancer and expression of kindlin-1 and kindlin-2 is altered in many cancer cell lines. Mutations in the *FERMT3* gene cause so called LAD-III syndrome (leukocyte adhesion deficiency), which is characterised by bleeding problems and life-threatening infections (Lai-Cheong et al. 2009).

1.7 Uev1a

Uev1a (ubiquitin-conjugating E2 enzyme variant, also called CROC1, CIR1, UBE2V) was originally identified as a signal transducing molecule able to activate the human *FOS* proto-oncogene promoter (Rothofsky and Lin 1997). Uev1a resembles ubiquitin-conjugating enzymes in sequence as well as structure, but lacks the ability to transfer ubiquitin to the substrate due to the absence of a catalytic cysteine residue (Sancho et al. 1998). Uev1 interacts with Ubc13 (Andersen et al. 2005), which is the only ubiquitin-conjugating enzyme identified so far that mediates the assembly of Lys63-linked polyubiquitination chains (Hofmann and Pickart 1999). For this process both of the proteins are required; neither Ubc13 nor Uev1a alone is able to promote Lys63 polyubiquitination chain formation (Hofmann and Pickart 1999, McKenna et al. 2001). The crystal structure of Uev1a has been solved recently. Based on this, a structural model of the Ub-Ubc13-Uev1a~Ub tetramer has been proposed that elucidates the mechanism how specificity in forming Lys63-linked polyubiquitin chains is achieved (Hau et al. 2006).

An increasing line of evidence supports the role of Ubc13-Uev1a complex in activation of NFκB (Deng et al. 2000, Shi and Kehrl 2003, Wang et al. 2001). One of the pathways that lead to the activation of NFκB is TNFα (tumour necrosis factor α) signalling. Briefly, the proinflammatory cytokine TNFα binds to the TNFR (TNFα receptor), which causes aggregation of the receptor and allows binding of TRADD (TNFR-associated death domain protein). TRADD recruits multiple adaptor proteins like TRAF (TNF-receptor-

associated factor) and RIP (receptor interacting protein 1) that subsequently recruit IκB kinase complex (IKK). IKK is composed of two kinase subunits IKKα and IKKβ and one regulatory subunit IKKγ (also called NEMO, NFκB essential modifier). Activated IKKβ phosphorylates IκBα (inhibitor of NFκB complex) that serves as a signal for SCF-ligases to ubiquitinate IκBα. Proteasomal degradation of IκBα frees the NFκB dimer, which translocates to the nucleus where it binds to the promoter or enhancer regions of target genes (Hayden and Ghosh 2004). It has been shown that the family of TRAF proteins, which contain a RING-domain, have ubiquitin-ligase activity and upon binding of the Ubc-Uev1a complex catalyse the synthesis of Lys63-linked polyubiquitin chains (Deng et al. 2000). This complex ubiquitinates RIP (Ea et al. 2006) as well as NEMO (Andersen et al. 2005), which leads to the activation of IKK (Figure 1.11).
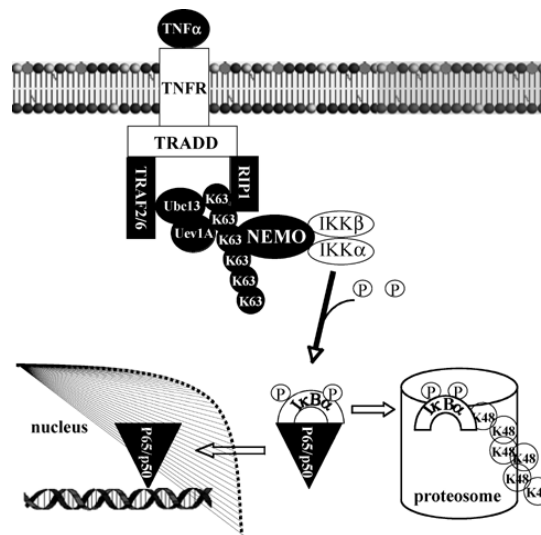
Figure 1.11: Model depicting the function of Ubc13-Uev1a ubiquitin conjugating enzyme in NFκB signalling pathway. TNFα binds to the TNFR that promotes the interaction between TRADD, RIP1 and TRAF2/6. Ubc13-Uev1a is involved in ubiqitination of NEMO and RIP by forming Lys63-linked polyubiquitin chains. Activated IKKβ phosphorylates IκBα. Phosphorylated IκBα is modified by Lys48-linked polyubiquitin chain that results in its degradation in proteasome. Activated NFκB dimer translocates to the nucleus. Taken from Syed (2006).

Activation of the NFκB signalling pathway leads to anti-apoptotic response (Kucharczak et al. 2003) and its constitutive activation is frequently observed in many cancer cells (Lin and Karin 2003). Uev1a has been proposed as a candidate proto-oncogene based on the observations that its expression is up-regulated in immortal cell lines in comparison to pre-immortal counterparts as well as in all cancer cell lines examined (Ma et al. 1998, Xiao et al. 1998). Consistent with this, Syed et al. (2006) have demonstrated that overexpression of Uev1a alone is capable of evoking NFκB signalling and protects cells from stress-

induced apoptosis. Thus, up-regulation of Uev1a seems to be sufficient to drive cells towards tumourigenesis.

1.8 Aims of the study

RhoBTB proteins constitute a subfamily of atypical Rho GTPases. They consist of a GTPase domain followed by a proline-rich region and two BTB domains. BTB domains are involved in the formation of Cul3-dependent ubiquitin ligase complexes, therefore the function of RhoBTB proteins seems to be distinct from that of the classical Rho GTPases. Since RhoBTB proteins have been described relatively recently, still little is known about their function and significance in cellular processes.

Connecting to previous research in our laboratory, we aim to further characterise the subcellular localisation of RhoBTB3, one of the RhoBTB isoforms, by counterstainig with various cellular markers. We will also explore the localisation of RhoBTB3 relative to the cytoskeleton. RhoBTB2 has been shown to act as an adaptor in multicomponent Cul3-dependent ligase complex and previous observations from our laboratory indicate that this feature might be shared also by RhoBTB3. Therefore the next aim of this study is to further characterise the function of RhoBTB3 in Cul3-dependent ligase complexes, namely its interaction with Cul3, heterodimerisation, ubiquitination and degradation. Potential binding partners (and therefore possible substrates of RhoBTB3-Cul3-dependent ligase complexes) have been identified previously in a two-hybrid screening. Another aim is to verify the interaction of RhoBTB3 with three of those candidate binding partners, MUF1, kindlin-2 and Uev1a. Because MUF1 is, like RhoBTB, involved in the formation of Cul-dependent ligase complexes, we will focus on the relationship between MUF1 and RhoBTB3. We will analyse the expression and subcellular localisation of MUF1, the latter one also with respect to RhoBTB3, and will address the interaction of both proteins by domain mapping. We will explore the significance of MUF1-RhoBTB interaction within Cul-ligase complexes and the mechanism of MUF1 degradation. We will also examine whether MUF1 is able to dimerise similarly to other LRR containing proteins. Finally, since MUF1 interacts with Cul5 and it has been described recently that cullins can form dimers, we will also explore a possible heterodimerisation of Cul3 and Cul5.

2 Material and Methods

2.1 Material

2.1.1 Cell lines and strains

Name	Origin/Source	Description
Mammalian cell lines		
COS7	*Cercopithecus aethiops*	African green monkey fibroblast-like cell line, isolated from kidney, contains large T antigen of SV40
293T HEK	*Homo sapiens*	Human embryonic kidney cells transformed with large T antigen of SV40
HeLa	*Homo sapiens*	Cervix carcinoma
Bacterial strains		
E. coli XL1-Blue		Bullock (1987)
Yeast strains		
Y190		Flick and Johnston (1990), Harper et al. (1993)

2.1.2 Vectors

Vector	Features	Source
pEGFP-C2 pEGFP-C3	4.7 kb; GFP N-terminal, kanamycin resistance, for transient expression in mammalian cells	Clontech
pCMV-Myc	3.8 kb; Myc N-terminal, ampicillin resistance, for transient expression in mammalian cells	Clontech
pcDNA3.1.(-)	5.4 kb; ampicillin resistance, for transient expression in mammalian cells	Invitrogen
pcDNA3-Myc3	5.4 kb; 3x Myc N-terminal, ampicilin resistance, for transient expression in mammalian cells	Ohta et al. (1999)
pRK5-Myc	5.4 kb; Myc N-terminal, ampicillin resistance, for transient expression in mammalian cells	Aspenström et al. (2004)
pGBKT7	7.3 kb; kanamycin resistance, for expression in yeast cells, GAL4-binding domain	Clontech

2.1.3 Oligonucleotides for siRNA

The oligonucleotides for Cul3 silencing along with ON-TARGETplus Non-targeting siRNA were obtained from ThermoScientific.

siCul3

Target sequence: NNGAAGGAAUGUUUAGGGAUA

Sense sequence: GAAGGAAUGUUUAGGGAUAUU

Antisense sequence: UAUCCCUAAACAUUCCUUCUU

2.1.4 Oligonucleotides for RT-PCR

MUF1/fwd/E5_E6	GAGAGCCTTACACTTTCCTACAATGGTC (Sigma)
MUF1/rev/ E9_E10	CTAATAGGCCAGCGTTCCCCA (Sigma)

Reaction Ready^{TM} Mouse GAPD Internal Normaliser - Primer set (Super Array Bioscience Corporation)

2.1.5 Oligonucleotides for PCR

The oligonucleotides listed below were obtained from Sigma. Engineered cloning sites are underlined.

Gene	Name	Sequence
Mm MUF1	MUF1/FL/fwd/EcoRI	GAATTCATGGAGGCCACGTCCCGGGA GGCGGCGCCAGCGAAGAGCTCGGCCT CGGGCCCCAGCGCTCCCCCCG
Mm MUF1	MUF1/mt/fwd	GAGCTCGGCCTCGGGCCCCAGCGCTC CCCCGCCCCGTTCGAGCTGTTCGGG CGG
Mm MUF1	MUF1/fwd/ΔSOCS/ EcoRI	GAATTCATGTATTACTTGGAGAGGAT TGAGGAAACTGCT
Mm MUF1	MUF1/fwd/LRR/ EcoRI	GAATTCATGGAGGCCACGTCCCGGGA GGCGGCGCCAGCGAAGAGCTCGGCCT CGGGCCCCAGCGCTCCCCCCG
Mm MUF1	MUF1/1110_1137/ rev/HindIII	AAGCTTAGACCCCTGACGGGTGCGGG GCCCTTTC
Mm MUF1	MUF1-FL/rev/Hind3	AAGCTTTCACATGGTGCTGACATAAT CTGCAAAGGC
Mm MUF1	MUF1-FL- flag/fwd/NheI	GCTAGCGCCGCCACCATGGACTACAA AGACGATGACGATAAAATGGAGGCC ACGTCCCGGGAG
Mm MUF1	MUF1/fwd/IPl/EcoRI	GAATTCGCCGCCACCATGGAAAACAG TACCACCACCATTTCTCGGGAGGAGC TTGAAGAGCTACAAGAAGCGGGATCC ATGGAGGC CACGTCCCGGGAG
Mm MUF1	MUF1/rev/IPl/HindIII	AAGCTTTCAGTCAGTCAGGATCCTCA CATGGTGCTGACATAATCTGCAAAGG C
Mm RhoBTB3	RBTB3-Rho- fwd/EcoRI	GAATTCTTATGTCCATCCACATCGTGG CGTTG
Mm RhoBTB3	RhoBTB3-H270L fwd	AGCCCTCAAGATCGTTCTCTGCTCTGT AAGCCATGTTTTC
Mm RhoBTB3	RhoBTB3-H270L rev	GAGCAGAGAACGATCTTGAGGGCTTC CACGACGCCCGTCAC
Mm RhoBTB3	B3-C/rev/EcoRI	GAATTCAGTCAGTCAAGCTTAGATCT CATGACTAAACAGCGACATTTCCGGG

2.1.6 Constructs

Construct	Insert extension	Backbone	Author
Constructs for expression in mammalian cells			
Mm Flag-MUF1	23-807	pcDNA3.1.(-)	This work
Mm Flag-MUF1ΔSOCS	82-807	pcDNA3.1.(-)	This work
Mm MUF1	25-807	pcDNA3-Myc3	This work
Mm MUF1/N	23-575	pcDNA3-Myc3	This work
Mm MUF1ΔSOCS	82-807	pcDNA3-Myc3	This work
Mm MUF1/C (587-786)	609-807	pcDNA3-Myc3	Marion Kopp
Mm MUF1/C (587-716)	609-735	pcDNA3-Myc3	Marion Kopp
Mm MUF1/C (702-786)	724-807	pcDNA3-Myc3	Marion Kopp
Mm MUF1-FL	25-807	pEGFP-C3	This work
Mm MUF1(L46P,C50F)	23-807	pEGFP-C3	This work
Mm MUF1ΔSOCS	82-807	pEGFP-C2	This work
Mm MUF1-LRR	403-807	pEGFP-C2	This work
Empty vector with I-Plastin tag I-Pl*	-	pcDNA3.1.(-)	This work
Mm I-Pl-MUF1-FL	23-807	pcDNA3.1.(-)	This work
Mm RhoBTB1-C	583-695	pEGFP-C1	Jessica Berthold
HsRhoBTB2-FL	1-728	pEGFP-C1	Berthold et al. (2008b)
Mm RhoBTB3-FL	1-611	pEGFP-C1	Berthold et al. (2008b)
Mm RhoBTB3(H270L)	1-611	pCMV-Myc	This work
Mm RhoBTB3-GTPase	1-204	pEGFP-C1	Berthold et al. (2008b)
Mm RhoBTB3-B1	236-402	pEGFP-C1	Berthold et al. (2008b)
Mm RhoBTB3-B2	396-592	pEGFP-C1	Berthold et al. (2008b)
Mm RhoBTB3-C	522-611	pEGFP-C1	Berthold et al. (2008b)
Mm RhoBTB3-PB1B2C	196-611	pEGFP-C1	Berthold et al. (2008b)
Mm RhoBTB3-B1B2C	236-611	pEGFP-C1	Berthold et al. (2008b)
Mm RhoBTB3-B2C	396-611	pEGFP-C1	Farshad Khademi
Hs RhoBTB3-FL	1-611	pRK5-Flag	Berthold et al. (2008b)
Hs RhoBTB2-FL	1-728	pRK5-Flag	Berthold et al. (2008b)
Hs RhoBTB1-FL	1-696	pRK5-Flag	Pontus Aspenström
Hs RhoBTB3	1-611	pRK5-Myc	Berthold et al. (2008b)
Hs RhoBTB2	1-728	pRK5-Myc	Aspenström et al. (2004)
Hs RhoBTB1	1-696	pRK5-Myc	Aspenström et al. (2004)
Mm RhoBTB3-GTPase	1-204	pRK5-Myc	Jessica Berthold
Hs Cullin 3 (Cul3)	1-768	pcDNA3-FlagJ	Ohta et al. (1999)
Hs Cullin 3 DN (Cul3 DN)	1-457	pcDNA3.1.-Flag	Pontus Aspenström
Hs Cullin 3 (Cul3)	1-768	pcDNA3-Myc3	Ohta et al. (1999)
Hs Cullin 5 (Cul5)	1-780	pcDNA3-Myc3	Ohta et al. (1999)
Hs Cullin 5 ΔNΔC (Cul5ΔNΔC)	100-541	pEGFP-C2	This work
Hs Roc1	1-108	pRK5-Myc	This work
Mm RBPMS1	1-606	pcDNA3-FlagJ	This work
Mm RBPMS3	1-675	pcDNA3-FlagJ	This work

Mm Uev1a	1-147	pcDNA3-Myc3	Jessica Berthold
Mm Uev1a	1-147	pEGFP-C2	Francisco Rivero
Mm kindlin-1	1-677	pEGFP-C	Reinhard Fässler
Mm kindlin-2	1-687	pEGFP-C	Reinhard Fässler
Mm kindlin-1	1-677	Flag	Reinhard Fässler
Mm kindlin-2	1-687	Flag	Reinhard Fässler
Hs kindlin-1 (258-677)	258-677	pcDNA-Flag	Lindsey Anderson
Hs kindlin-1 (1-495)	1-495	pcDNA-Flag	Lindsey Anderson
Mm kindlin-1/N (1-446)	1-446	pEGFP-C	Reinhard Fässler
Mm kindlin-1/C (471-677)	471-677	pEGFP-C	Reinhard Fässler
Rt MyoIXb	1-1980	pUHD-6xHis-Flag	Martin Bähler
Constructs for expression in *E. coli*			
Hs Rac1	1-192	pGEX-2TK	Berthold et al. (2008b)
Mm RhoBTB3-GTPase	1-204	pGEX-2T	Berthold et al. (2008b)
GST-Ub	2-76	pGEX-4T-1	Michael Gmachl
Constructs for yeast two-hybrid experiments			
Hs Cullin 3 (Cul3)	1-768	pGADT7	Berthold et al. (2008b)
Hs Cullin 5 (Cul5)	1-735	pGBKT7	This work

*AACAGTACCACCACCATTTCTCGGGAGGAGCTTGAAGAGCTACAAGAAGCG

2.1.7 Enzymes

- Calf intestine alkaline phosphatase (CIP) (Roche)

- Klenow fragment (DNA polymerase I) (Roche)

- Lysozyme (Sigma)

- M-MLV reverse transcriptase (Promega)

- Restriction enzymes (Amersham, Fermentas, Jena Biosciences, New England Biolabs)

- Ribonuclease A (RNase A) (Roche)

- Shrimp alkaline phosphatase (SAP) (Roche)

- T4 DNA ligase (Invitrogen)

- Taq DNA polymerase (Roche)

- Trypsin (Biochrom)

2.1.8 Antibodies and fluorescent dyes

2.1.8.1 Primary antibodies

Antibody		Source	WB	IF
β-Actin	mouse	Sigma	1:5000	-
Cullin 3	rabbit	Manabu Furukawa	1:1000	-
EEA1	mouse	Transduction Laboratories	-	1:100
Emerin	rabbit	ProSci	1 µg/ml	-
I-Plastin	rabbit	Grimm-Günter et al. (2009)	-	1:300
GAPDH	mouse	Sigma	8 µg/ml	-
GFP	mouse	Angelika A. Noegel	non-diluted	-
GM130	mouse	Markus Plomann	-	1:50
GST	rabbit	Angelika A. Noegel	1:5000-1:50,000	-
Myc	mouse	Angelika A. Noegel, Biomol	non-diluted	-
Flag (anti-ECS)	rabbit	Novus Biologicals	1:1000	1:200
Flag M2	mouse	Sigma	1:1000	-
α-Tubulin	mouse	Calbiochem	-	1:1000

2.1.8.2 Secondary antibodies

Antibody	Source	WB	IF
Goat anti-rabbit IgG, peroxidase-conjugated	Sigma	1:10,000	-
Goat anti-mouse IgG, peroxidase-conjugated	Sigma	1:10,000	-
Goat anti-mouse IgG, Alexa 488 conjugate	Molecular Probes, Invitrogen	-	1:1000
Goat anti-mouse IgG, Alexa 568 conjugate	Molecular Probes, Invitrogen	-	1:1000
Goat anti-mouse IgG, Alexa 568 conjugate	Molecular Probes, Invitrogen	-	1:1000
Anti-mouse Cy5 conjugated	Invitrogen	-	1:1000

2.1.8.3 Fluorescent dyes

- 4´, 6´- diamidino - 2 phenylindol (DAPI) (Sigma)
- MitoTracker® Red CMXRos (Molecular Probes)
- Hs Transferrin-Alexa Fluor 546 (Invitrogen)
- TRITC-Phalloidin (Sigma)

2.1.9 Inhibitors

- Benzamidine (Sigma)
- Colchicine (Sigma)
- Cycloheximide (Sigma)

- Latrunculin B – (Merck Biosciences (Calbiochem-Novabiochem)
- MG132 (Sigma)
- Phenylmethylsulfonyl fluoride (PMSF) Sigma
- Protease Inhibitor Cocktail (Sigma)
- RNasin RNase Inhibitor (Promega)
- Taxol (Biochemika)

2.1.10 Transfection reagents

- DharmaFECT®1 Transfection Reagent (ThermoScientific)
- Lipofectamine 2000 (Invitrogen)

2.1.11 Antibiotics

- Ampicillin (Sigma)
- Kanamycin monosulphate (Melford Laboratories)

2.1.12 Molecular weight markers

- PageRuler^{TM} Plus Prestained Protein Ladder SM1811 Mw 250/130/100/70/55/35/27/15/10 kDa (Fermentas)
- High molecular weight marker 250/150/100/75/50/37/25/20 kDa (Amersham Biosciences)
- EZ-Run^{TM} Prestained Rec Protein Ladder 130/95/72/55/43/34/26/17 kDa (Fisher Scientific)
- EZ-Run^{TM} Prestained Rec Protein Marker 118/85/47/36/26/20 kDa (Fisher Scientific)
- DNA Ladder 12216; 11198; 10180; 9162; 8144; 7126; 6108; 5090; 4072; 3054; 2036; 1636; 1018; 506; 396; 344; 298; 220; 201; 154; 134; 75 bp (Life Technologies)
- 1kb Full Scale DNA Ladder 10000, 8000, 6000, 4000, 3000, 2000, 1550, 1400, 1000, 750, 500, 400, 300, 200, 100, 50 bp (Fisher Scientific)
- 100 bp Scale DNA Ladder 2000, 1550, 1400, 1000, 750, 500, 400, 300, 200, 100, 50 bp (Fisher Scientific)

2.1.13 Chemicals

Laboratory reagents and materials were obtained from following suppliers: Amersham, Biomol, Fluka, Invitrogen, Melford Laboratories, Merck, National Diagnostic, Pharmacia, Promega, Sigma, Serva, Roche and Roth.

2.1.14 Kits

Pierce® BCA Protein Assay Kit	Pierce (ThermoScientific)
pGEM-T easy Cloning Kit	Promega
High Pure Plasmid Purification Kit	Roche
µMACS™ Epitope Tag Protein Isolating Kit	Miltenyi Biotec
Nucleobond AX 100	Macherey Nagel
NucleoSpin Extraction Kit	Macherey Nagel
ProFound™ Mammalian c-Myc Tag IP/CoIP Application Set	Pierce (ThermoScientific)
SuperSignal® West Pico	Pierce (ThermoScientific)

2.1.15 Laboratory material

3mm filter paper	Whatman
6-well plates	Nunc
24-well plates	Nunc
Cell scraper 25 cm	Sarstedt
Coverslips: 12/15/18 mm in diameter	Menzel-Gläser
Cryotubes 1 ml	Nunc
Eppendorf tubes: 0.5 ml, 1.5 ml, 2 ml	Eppendorf
Falcon tubes: 15 ml, 50 ml	Greiner Bio-one Cell Star
Filters: 0.20 µm, 0.45 µm	Millipore
Glass Pasteur pipettes	Brand
Glass slides	Menzel-Gläser
Hyperfilm ECL 18x24 cm	Amersham
Microscope slides 76x26 mm	Menzel-Gläser
Needles	BD Plastipak
Neubauer improved chamber depth: 0.100 mm; 0.0025 mm^2	Labor Optik
Nitrocellulose transfer membrane	Pall
Parafilm	Pechiney
PCR reaction tubes: 0.2 ml	VWR

Petri dishes: 60x15 mm, 100x20 mm, 140x20 mm	Nunc
Pipettes: 1-10 µl, 1-20 µl, 20-200 µl und 200-1000 µl	Gilson
Pipette tips	Greiner Bio-one Cell Star
PVDF transfer membrane	Pall
Serological pipettes: 5 ml, 10 ml, 25 ml	Sarstedt
Steritop bottle top filter 0.22 µm	Millipore
Syringes	BD Plastipak

2.2 Sterilisation

Media and buffers were sterilised by autoclaving at 120ºC. If sterilisation by autoclaving was not possible, 0.2 µm or 0.45 µm filter units were used.

2.3 Cell culture methods

Mammalian cells were cultivated at 37˚C in a humidified incubator supplied with 5% CO_2. The cells were grown in Dulbeccos´ Modified Eagle (DME) medium enriched with fetal bovine serum (FBS).

Culture medium for HeLa, COS7 and 239T HEK cells

DME medium ´high glucose´ (4.5 g/l) (Sigma)

10% heat inactivated FBS (Biochrom)

2 mM Glutamine (Sigma)

100 U/ml Penicillin, 100 µg/ml Streptomycin (PAA)

The medium for HeLa and 239T HEK cells contains additionally 1 mM sodium pyruvate (Sigma).

2.3.1 Defrosting of mammalian cell stocks

Mammalian cells were stored in medium containing DMSO (dimethylsulfoxide) (see section 2.3.7) in liquid nitrogen. To defreeze the cells, the vial was warmed in a 37˚C water bath and the cells were immediately resuspended in medium to dilute the DMSO. Cells were centrifuged ($1000 \times g$, 10 min, 4˚C), the medium was removed and the cells were resuspended in fresh medium and seeded on a 10 cm plate. Next day cells were split.

2.3.2 Passaging of mammalian cells

All mammalian cell lines were split in the same way. After aspirating of medium, cells were rinsed with PBS and incubated at 37°C with 0.05% trypsin and 0.53 mM EDTA in PBS until they were detached from the culture dish. The cells were resuspended in fresh medium and split. 293T HEK cells were split every 1-2 days when they reached 70-80% confluency at a ratio of 1:3 – 1:5. COS7 cells were split every 3 days when the plate was almost confluent at a ratio of 1:10. HeLa cells were split every 3-4 days at a ratio of 1:10.

2.3.3 Transfection of mammalian cells

Cells were split 24 h before transfection to the wells of a 6-well plate. The quantity of reagents used is calculated for one well of a 6-well plate. Transfection was performed with Lipofectamine 2000 as follows: 4 μg of DNA and 10 μl of lipofectamine were separately mixed with 250 μl of pre-warmed DME medium without FBS and after 5 min mixed together and incubated for 20 min at room temperature. Lipofectamine-DNA complexes were then added to the cells with 2 ml freshly changed DME medium (2 ml) containing 10% FBS.

If larger amounts of transfected cells were needed, cells were split to bigger plates and the amount of reagents was adjusted according to the size of the plate as recommended by manufacturer.

2.3.4 Drug treatment

Where indicated, cells were treated with the following drugs: taxol, colchicine or latrunculin B. Taxol and colchicine were added to the cells 20 h after transfection for 4 h (20 μM taxol, 25 μM colchicine). Latrunculin B was added to the cells 23.5 h after transfection for 30 min (final concentration 2.5 μM). Appropriate solvents were used as a control (DMSO/Ethanol).

2.3.5 Determination of protein stability (Wilkins et al. 2004)

6×10^6 293T HEK cells were seeded the day before transfection on a 10 cm Petri dish. Transfection of the appropriate plasmids was done with Lipofectamine 2000. 16 h after transfection cells were trypsinised and distributed into 4 wells of a 6-well plate. When the cells had re-attached (after 3-4 h), they were treated with 100 μM cycloheximide to arrest protein biosynthesis and either with 10 μM MG132 or DMSO. Cells were collected

at different time points and lysed (see section 2.7.1). Lysates were analysed by the SDS-PAGE electrophoresis (see section 2.7.3).

2.3.6 Gene silencing

To silence the expression of endogenous Cul3, ThermoScientific DharmaFECT®1 for transfection of oligonucleotides was used according to the manufacturers' protocol. Oligonucleotides targeting the Cul3 sequence were designed and used along with non-targeting siRNA as a negative control (see section 2.1.3).

293T HEK cells were cultivated during the duration of the whole experiment in antibiotics-free medium as these have large cytotoxic effects on the cells. 24 h prior to experiment, cells were trypsinised and 6.25×10^5 cells were seeded into one well of a 6-well plate. On the day of the experiment, 100 μl of 2 μM siRNA solution was mixed with 100 μl serum-free medium in one tube and 4 μl of DharmaFECT® solution was mixed with 196 μl serum-free medium in a second tube. After 5 min incubation, the content of both tubes was mixed together and incubated for another 20 min. During this time old medium was removed and 1600 μl of fresh medium was added to the cells. When incubation was completed, the silencing mixture was pipetted drop wise to the plate. Following controls were included in this experiment: 1. Untreated cells, 2. Mock-transfection (no siRNA), 3. Negative control siRNA

2.3.7 Cryostocks preparation

To prepare the cells for cryoconservation in liquid nitrogen, a confluent monolayer from a 10 cm plate was trypsinised and resuspended in cold DME medium and incubated for 30 min on ice. The cells were then centrifuged ($1000 \times g$, 10 min, 4˚C) and the pellet was resuspended in 1 ml freezing medium. Cryotubes were placed into a cryorack Nalgene® Mr. Frosty™ Cryo (with special filling soaked in isopropanol) and left in -80˚C overnight. The cryotubes were transferred to liquid nitrogen following day.

Freezing medium

70% DMEM
20% FCS
10% DMSO

2.4 Bacterial culture methods

2.4.1 Media for bacterial cells cultivation

The Luria Bertani (LB) media were prepared with deionised water and sterilised by autoclaving at 120˚C. After cooling down antibiotics were added to the final concentration of 100 mg/l (ampicillin) or 50 mg/l (kanamycin). The pH of the LB medium was set with 5 M NaOH. For the blue-white selection of *E. coli* transformants, 10 μl of 1 M IPTG solution (isopropyl β-D-1-thiogalactopyranoside) and 40 μl X-Gal solution (20 mg/ml solution of 5-bromo-4-chloro-3-indolyl-β-D-galactopyranoside dissolved in N,N´-dimethyl-formamide) were spread on agar plates. The SOC medium was sterilised through a 0.2 μm filter unit.

LB medium (pH 7.0 at 37˚C)
1% (w/v) Bacto-Trypton
0.5 % (w/v) Yeast Extract
0.5 % (w/v) NaCl

LB agar plates (pH 7.0 at 37˚C)
1 % (w/v) Bacto-Trypton
0.5 % (w/v) Yeast Extract
0.5 % (w/v) NaCl
1.5 % (w/v) Agar-Agar

SOC medium (pH 7 at 37˚C)
2 % (w/v) Bacto-Trypton
0.5 % (w/v) Yeast Extract
10 mM NaCl
2.5 mM KCl
20 mM Mg^{2+} (1:1 $MgCl_2·6H_2O$ and $MgSO_4·7H_2O$)
20 mM glucose

2.4.2 Preparation of *E. coli* XL-1 blue competent cells

A single bacterial colony was picked from an LB agar plate and pre-cultured overnight in 20 ml LB medium. 250 ml LB medium were inoculated with this overnight culture and allowed to grow to an optical density of OD_{600} = 0.4-0.5. The culture was then cooled down on ice for 20 min and centrifuged 10 min at 2500 × *g* at 4˚C. The pellet was resuspended in 80 ml ice cold TB buffer and again incubated on ice for 10 min. After centrifugation, the pellet was resuspended in 20 ml TB buffer and mixed with 1.6 ml DMSO. The cell suspension was aliquoted, frozen in liquid nitrogen and stored at -80˚C.

TB buffer

10 mM PIPES

15 mM CaCl$_2$

250 mM KCl

The pH 6.7 was set with KOH and then MnCl$_2$ was added to the final concentration of 55 mM.

2.4.3 Transformation of *E. coli* XL-1 blue competent cells

50 μl of competent cell suspension was thawed on ice for 10 min. Plasmid DNA or a ligation reaction was added to the bacterial cells and incubated for another 30 min on ice. A thermal shock of 42˚C was applied for 45 sec and the cells were subsequently cooled on ice for 1-2 min. After incubation in SOC medium without antibiotics (37˚C, 1 h), the cells were spreaded on agar plates with the appropriate antibiotic selection and incubated overnight at 37˚C.

2.4.4 Preparation of glycerol stocks

850 μl of an overnight culture were mixed with 150 μl of glycerol and stored at -80˚C.

2.5 Yeast two-hybrid system

2.5.1 Media for yeast cells cultivation

Media were sterilised by autoclaving, adenin solution and glucose by filtration.

YEPD-medium

2% (w/v) Difco Pepton

1% (w/v) Yeast extract

2% (w/v) Glucose

YEPD-agar plates

2% (w/v) Difco Pepton

1% (w/v) Yeast extract

2% (w/v) Glucose

1.8% (w/v) Agar-Agar

Selection plates

0.7% N base without amino acids

2% glucose

0.064% TL dropout (amino acid mix without tryptophan and leucine)

2% agar

0.003% (w/v) Adenin

2.5.2 Modified lithium acetate method for yeast transformation

Y190 yeast cells were cultivated in YEPD-medium at 30°C overnight. Cells were pelletted and following was added to the pellet:

- 20 μg Salmon sperm DNA
- 1 μg of Plasmid DNA
- 500 μl Plate mix
- 50 μl 1 M DTT

Next day yeast cells were incubated at 42°C for 10 min and spun down. The supernatant was removed and the cells were resuspended in a small amount of water and plated on the appropriate selection plates. Plates were incubated at 30°C for several days until colonies appeared.

Plate-mix

90 ml 50% PEG-4000

10 ml 1 M Lithium acetate

1 ml 1 M Tris-HCl, pH 7.5

0.2 ml 0.5 M EDTA, pH 8.0

2.5.3 Test of galactosidase activity

The yeast cells were blotted onto nitrocellulose membrane. The membrane was immersed in liquid nitrogen for 10 sec, then allowed to warm up to room temperature. The membrane was placed on filter paper pre-wetted with staining solution with cells facing up and incubated at 30°C for 12 h.

Z-buffer, pH 7.0

0.04 M $Na_2HPO_2 \cdot 7H_2O$

0.04 M $NaH_2PO_4 \cdot H_2O$

0.01 M KCl

0.01 M $MgSO_4 \cdot 7H_2O$

Staining solution:

100 ml Z-buffer

0.27 ml 2-β-Mercaptoethanol

1.67 ml X-Gal-solution (20 mg/ml

solution of 5-bromo-4-chloro-3-indolyl-

β-D-galactopyranoside N,N´-dimethyl-

formamide)

2.6 Immunohistochemistry

2.6.1 Fixation and permeabilisation of mammalian cells

Mammalian cells cultivated on coverslips were fixed with 4% paraformaldehyde in PBS for 20 min. After a washing step with PBS, cells were permeabilised with 0.2% Triton X-100 for 5 min and again washed with PBS.

Phosphate Buffered Saline (PBS), pH 7.4

1.37 M NaCl

27 mM KCl

100 mM Na_2HPO_4

18 mM KH_2PO_4

2.6.2 Immunodetection of proteins in the cells

To prevent unspecific antibody binding, cells were incubated in 5% FBS in PBG for 30 min. Primary and secondary antibodies were diluted in 1% FBS in PBG and cells were incubated with primary antibody for 1 h and with secondary antibody for 45 min. If DAPI staining was required, it was added to the diluted secondary antibody (final concentration 1 μg/ml). After incubation with each antibody, cells were washed several times with PBS. At the end, coverslips were mounted on glass slides with a drop of gelvatol.

PBG pH 7.4

0.5% (w/v) bovine serum albumin (BSA)

0.1 % (w/v) gelatine

in 1x PBS

Gelvatol

14.3% (v/v) Gelvatol (Polyvinylalcohol)

28.6% (v/v) Glycerine

2.5% (w/v) DABCO (1,4-diazabicyclo[2.2.2] octane) in PBS

2.6.3 Immunostaining of mitochondria

Cells were washed once with PBS, and then incubated for 45 min at room temperature with MitoTracker® Red CMXRos (final concentration 500 nM) in PBS. DMSO was used as a negative control. After incubation the staining solution was removed and cells were fixed and permeabilised as described above (see section 2.6.1).

2.6.4 Immunostaining of microtubules

Cells were washed with 1× BRB80 buffer and then fixed in 3% paraformaldehyde in 1× BRB80 buffer for 30 min. Permeabilisation and staining steps were done as described above.

<u>5× BRB80 buffer pH 6.8</u>
80 mM PIPES
1 mM $MgCl_2 \cdot 6H_2O$
1 mM EGTA

2.6.5 Immunostaining of actin filaments

Cells were fixed and permeabilised as described above (see section 2.6.1). To stain the actin cytoskeleton, TRITC-labelled phalloidin was used (for 30 min, final concentration 5 µg/ml).

2.6.6 Transferrin uptake

Cells were washed once with PBS and starved in DME medium without antibiotics, glutamine and FBS, only with 0.5% BSA for 1 hour. Cells were then incubated for 5 min in 200 µl complete medium (without BSA) with 10 µg/ml human transferrin labelled with Alexa Fluor 546 for 5 min. Non-internalised transferrin was removed by incubation of the cells with trypsin on ice for 5 min. After washing with PBS, cells were fixed with 4% paraformaldehyde, washed and incubated with 50 mM NH_4Cl for 10 min. Cells were permeabilised with 0.5% saponin in PBS for 10 min. For nuclei staining DAPI was diluted in 0.1% saponin in PBS and also all washing steps were done with 0.1% saponin in PBS.

2.6.7 Microscopy and image processing

Images were acquired with conventional fluorescence microscopes (Leica with DC 350 FX camera and Nikon with Photometrics CoolSnap[TM] ES camera) or with Leica SP2 confocal laser scanning microscope. Where indicated, images were deconvolved using AutoQuantX software. Images were overlaid and processed in Photoshop.

2.7 Biochemical methods

2.7.1 Lysis of mammalian cells

Cells were scraped into pre-cooled (4˚C) lysis buffer (200 µl for a well of a 6-well plate) and transferred to an eppendorf tube. After 30 min incubation on ice, cell debris was pelletted by centrifugation for 10 min at 10,000 × g at 4˚C and the supernatant was transferred to the fresh tubes.

Lysis buffer

150 mM NaCl

1% Triton® X-100

50 mM Tris-HCl, pH 8.0

2.7.2 Immunoprecipitation of proteins with Myc-epitope or GFP-epitope tag

Proteins containing Myc or GFP epitope were immunoprecipitated with kits obtained from Miltenyi Biotec (µMACS Epitope Tagged Protein Isolation Kit). These kits allow isolation of such tagged proteins by binding them to magnetic beads conjugated with anti-Myc or anti-GFP antibody.

170 µl of cell lysate was mixed with 8 µl anti-Myc or anti-GFP MicroBeads and incubated on ice for 30 min. µColumns were placed on a µMACS Separator and activated by applying lysis buffer. The lysate containing MicroBeads was then applied to the column. Magnetic beads remained retained in the column because of the strong magnetic field. Unbound proteins were washed out by stringent washing steps (4 times washing with wash buffer I, once washing with wash buffer II) and the tagged proteins were finally eluted by applying pre-heated (95˚C) elution buffer. First, 20 µl of elution buffer was applied to the column and incubated for 5 min. Elution was achieved by subsequent addition of 50 µl elution buffer. These eluates were analysed by SDS-PAGE electrophoresis. In case very weak interaction between two examined proteins was expected, low stringent conditions were used for lysis and washing steps. In that case this is mentioned at the corresponding experiments.

Wash buffer I

150 mM NaCl

1% NP-40

0.5% sodium deoxycholate

0.1% SDS

50 mM Tris-HCl, pH 8.0

Wash buffer II

20 mM Tris-HCl, pH 7.5

Elution buffer

50 mM Tris-HCl, pH 6.8

50 mM DTT

1% SDS

1 mM EDTA

0.005% bromophenol blue

10% glycerol

Low stringency lysis and washing buffer

1% NP-40

50 mM Tris-HCl, pH 8.0

2.7.3 SDS-polyacrylamide gel electrophoresis (SDS-PAGE)

In order to resolve proteins according to their molecular weight, denaturing SDS-PAGE was performed. Samples were mixed with 2× SDS-sample buffer in a 1:1 ratio and denatured at 95˚C for 5 min. For casting of the gels and for gel electrophoresis the SDS-PAGE system MiniPROTEAN® (Biorad) was used. Resolving gel was prepared by mixing components mentioned in the Table 2.1 and left to polymerise for 30 min. Isopropanol was applied on the top of the gel. After complete removal of isopropanol, stacking gel was loaded on top of the resolving gel and left to polymerise for 30 min. The gels were assembled and placed into the Biorad Mini-PROTEAN® Gel Chamber and 1× SDS running buffer was added. The samples were loaded onto the wells of the gel together with a molecular weight marker and were run at 80-120 V until the bromophenol blue dye of the samples reached the bottom of the gel.

1× SDS-running buffer, pH 8.3

25 mM Tris-base

192 mM Glycine

0.1% SDS

2× SDS-sample buffer

100 mM Tris-HCl, pH 6.8

4% SDS

20% glycerine

4% β-mercaptoethanol

0.005% (w/v) bromophenol blue

	Resolving gel			Stacking gel
	10%	15%	18%	5%
Acrylamide (30%) [ml]	20	30	36	4
1.5 M Tris-HCl, pH 8.8 [ml]	15.1	15.1	15.1	-
0.5 M Tris-HCl, pH 6.8 [ml]	-	-	-	2.4
10% SDS-solution [µl]	590	590	590	240
deionised H_2O [ml]	24.25	14.25	8.25	17.36
TEMED [µl] (for each 5 ml of gel)	15	15	15	10
10% APS [µl] (for each 5 ml of gel)	20	20	20	15

Table 2.1: Solution for preparation of polyacrylamide mini gels.

2.7.4 Staining of polyacrylamide gels with Coomassie-Brilliant-Blue R 250

Proteins separated on polyacrylamide gels were stained with Coomassie-Brilliant-Blue R 250 solution for 20 min at room temperature. The excess staining was removed with destaining solution. To dry the gel, it was incubated in Gel Dry Buffer for 5 min, then wrapped in permeable foil and left to dry overnight.

Staining solution

0.1% (w/v) Coomassie-Brilliant-Blue
    R 250

50% (v/v) Methanol

10% (v/v) Acetic acid

Destaining solution

10% (v/v) Ethanol

7% (v/v) Acetic acid

Gel dry solution

50% ethanol

5% glycerol

2.7.5 Transfer of proteins to membrane (Western blot)

Polyacrylamide gels were equilibrated in blotting buffer for 20-60 min. Polyvinylidene fluoride membrane (PVDF) was pre-wetted by placing in 100% methanol for 15 sec and then washed in distilled water for 1-2 min. Nitrocellulose membrane was used without any pre-wetting. The membrane was soaked in blotting buffer together with thick blotting papers for 5 min. Semi-dry transfer was carried out by using a Biorad Trans Blot SD Semidry Transfer Cell. The blotting sandwich was assembled as follows: anode, blotting

paper, membrane, gel, blotting paper and cathode. The transfer took 20-60 min at 10-15 V, depending on the size of the gel.

Blotting buffer
25 mM Tris base
193 mM Glycine
20% Methanol

2.7.6 Staining of proteins bound to the membranes

Transferred proteins were visualised with Ponceau S staining. This served as a control of protein transfer after the blotting and it also allowed marking the position of the molecular weight marker and individual samples. The staining was removed by TBS-T buffer in following washing steps.

Ponceau S	TBS-T buffer
0.1% Ponceau S	150 mM NaCl
1% Acetic acid	10 mM Tris-HCl, pH 8.0
	0.1% Tween 20

2.7.7 Immunodetection of proteins bound to the membrane

To prevent unspecific binding of proteins, the membrane was blocked by incubation with 10% skimmed milk in TBS-T for 30-60 min. Milk was shortly washed out and the membrane was incubated with primary antibody at the appropriate dilution in TBS-T for 2 h at room temperature or overnight at 4°C. The unbound primary antibody was washed out with 1× TBS-T buffer (3x 10 min) and the membrane was incubated for 1 h with the appropriate peroxidise-coupled secondary antibody (1:10,000 dilution). The secondary antibody was washed out similarly as the primary antibody. The chemiluminiscence reaction was done using SuperSignal® West Pico solutions. The membrane was exposed to X-ray film and developed by using developer and fixer solutions (Kodak).

2.7.8 Subcellular fractionation of mammalian cells

Cells were harvested by scraping in PBS with 1 mM DTT, 1 mM benzamidin, 1 mM EGTA and 1 mM PMSF (5 ml for a 10 cm dish). Cells were centrifuged for 5 min at $1000 \times g$ at 4°C. The pellet was dissolved in hypotonic lysis buffer and incubated on ice for

30 min. The suspension was then pressed through a syringe with a thin needle (0.4 mm in the diameter). Nuclei were sedimented at $1000 \times g$ for 15 min at 4˚C and the supernatant was subsequently ultracentrifuged for 30 min at 45,000 rpm at 4˚C. The cytosolic fraction is in the supernatant and the membranous fraction is in the pellet. The pellets were resuspended in 2× sample buffer and boiled at 95˚C for 10 min. The fractions were analysed by Western blotting. Anti-emerin antibody was used as a marker for the nuclear fraction and anti-GAPDH antibody as a marker for the cytosolic fraction.

Hypotonic lysis buffer
10 mM HEPES, pH 7.5
1.5 mM $MgCl_2$
1.5 mM KCl
Protease inhibitor cocktail
0.5 mM DTT

2.7.9 Ubiquitination assay

6×10^6 293T HEK cells were seeded the day before transfection on a 10 cm Petri dish. Transfection of the appropriate plasmids was done with Lipofectamine 2000. 10 h after transfection proteasomal inhibitor MG132 (5 μM) was added for 12 h. Cells were lysed and expressed proteins were co-immunoprecipitated using ProFound™ Mammalian c-Myc Tag IP/CoIP Application Set (Pierce). Briefly, the cell lysate was incubated with Myc-tagged agarose beads overnight at 4°C. Agarose beads were washed 8 times with washing buffer and native proteins were eluted with elution buffer. 0.5 μl of 1M Tris-HCl, pH 9.5 was added to each 10 μl of eluate to neutralise the pH. The ubiquitination reaction was setup as follows: 20 μl of purified protein complex was mixed with 500 ng yeast E1 (BostonBiochem), 850 ng human recombinant UbcH5a E2 (BostonBiochem), 2 μM human recombinant ubiquitin aldehyde (BostonBiochem), 0.29 nM GST-Ub (section 2.7.11), 1 mM ATP, 10 μM MG132, 5 mM $MgCl_2$, 0.5 mM DTT, 1 mM PMSF in 10 mM HEPES, pH 7.6. The reaction was incubated at 37˚C for 1 h, then SDS-sample buffer was added and samples were denatured (Wilkins et al. 2004).

2.7.10 Protein expression and purification

A single bacterial colony of *E. coli* XL1-blue was picked from an LB agar plate and pre-cultured overnight in 30 ml LB medium. 200 ml of fresh LB medium was inoculated with the overnight culture to an optical density of $OD_{600} = 0.1$ and allowed to grow to an optical density of $OD_{600} = 0.7$-0.8. The culture was then induced with 0.5 mM IPTG for 4 h. After induction, the culture was centrifuged for 10 min at $6000 \times g$ at 4˚C. The pellet was resuspended in lysis buffer and incubated for 30 min on ice. Lysis of bacterial cells was achieved with a French press. Cell debris was sedimented by centrifugation for 1 h at $17,300 \times g$ at 4˚C. The supernatant was supplemented with 0.1% Triton X-100 and was incubated with glutathione-agarose beads (Amersham, Buckinghamshire, UK) for 2 h at 4˚C. After incubation, the GST-agarose beads with bound protein were washed twice with washing buffer with 0.1% Triton X-100 and twice with washing buffer without Triton X-100. The purified protein was eluted with elution buffer.

Lysis buffer

50 mM Tris-HCl, pH 7.0

300 mM NaCl

5 mM EDTA

4 mM DTT

1 mM PMSF

1 mg/ml lysozyme

Washing buffer

50 mM Tris-HCl, pH 7.0

1 M NaCl

5 mM EDTA

4 mM DTT

0.1% Triton X-100

Elution buffer

1 M Tris-HCl, pH 8.0

100 mM NaCl

20 mM reduced glutathione

2.7.11 Expression and purification of GST-Ubiquitin (Ub)

GST-Ub (kind gift of Michael Gmachl, Innsbruck Medical University, Austria) was expressed and purified as described above (see section 2.7.10). Several eluates were recovered from glutathione-agarose beads that were tested on an SDS gel to determine the purity (Figure 2.1). The eluates were joined together and dialysed against 10 mM HEPES, pH 7.6. The dialysed protein was concentrated with Ultrafree-MC Centrifugal Filters Units (Millipore) and the protein concentration was measured (see section 2.7.12).
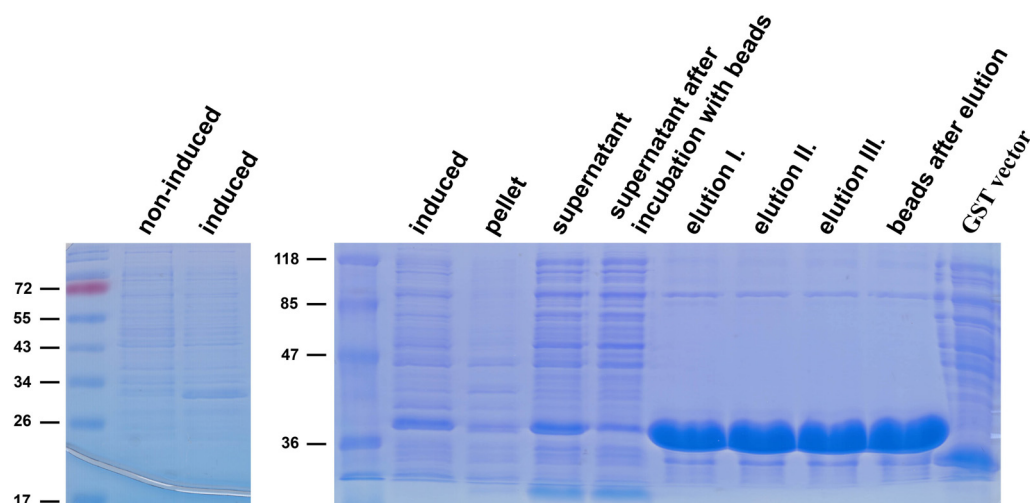
Figure 2.1: Expression and purification of GST-Ub. Ubiquitin was expressed as a GST fusion in *E. coli* XL1-blue. Bacterial cells were lysed and supernatant was incubated with glutathione agarose beads. After purification, lysates were resolved on 18% SDS gel and stained with Coomassie-Brilliant-Blue R 250 (see section 2.7.4).

2.7.12 BCA (bicinchoninic acid) protein assay

Concentration of proteins was measured with a Pierce® BCA Protein Assay Kit according to the manufacturers' recommendations. This method is based on reduction of Cu^{2+} to Cu^{1+} by protein in an alkaline environment. Two molecules of BCA form a complex with one cuprous ion and this complex exhibits absorbance at 562 nm. Briefly, BSA was diluted in the same buffer as the sample (concentration range between 2000 μg/ml and 2 μg/ml) and served as a standard of protein concentrations. Working reagent was prepared by mixing 50 parts of BCA reagent A (containing sodium carbonate, sodium bicarbonate, bicinchoninic acid and sodium tartrate) with 1 part of BCA reagent B (containing 4% cupric sulfate). 25 μl of diluted standard or sample was pipetted into a well in a 96-well plate and mixed with 200 μl of working reagent. Plate was incubated in the dark at 37°C for 30 min and absorbance was measured at 562 nm on a plate reader.

2.7.13 GTP binding assay

Hs Rac1 and the GTPase domain of RhoBTB3 were expressed as GST fusions in *E. coli* XL1-blue along with empty GST vector as a negative control (see section 2.7.10). After purification, lysates were resolved with SDS-PAGE electrophoresis and blotted onto nitrocellulose membrane. The membrane was rinsed twice with washing buffer followed by incubation in binding buffer for 2 h at room temperature. The membrane was then washed with washing buffer 4 times for 15 min each and subjected to autoradiography.

GTP-washing buffer

50 mM Tris-HCl, pH 7.4

0.3% Tween 20

10 μM MgCl$_2$

GTP-binding buffer

50 mM Tris-HCl, pH 7.4

0.3% Tween 20

10 μM MgCl$_2$

100 mM DTT

100 μM ATP

1 μCi/ml (α-^{32}P) GTP

2.8 Molecular biology methods

2.8.1 Isolation of plasmid DNA by the alkaline method (Birnboim and Doly 1979)

1.5 ml overnight culture was spun down (6000 × g, 5 min, 4˚C) and resuspended in 200 μl buffer P1. 200 μl of buffer P2 was added and samples were incubated 2-3 min at room temperature. After 200 μl of buffer P3 was added, samples were centrifuged (10 min, 12,000 × g, room temperature). The supernatant was transferred into a fresh tube and plasmid DNA was precipitated with 530 μl of isopropanol and subsequent centrifugation (20 min, 12,000 × g, 4˚C). The pelletted DNA was washed with 70% ethanol, dried and redissolved in the 5 mM Tris-HCl, pH 8.0 buffer. Contaminating RNA was removed from the sample during restriction by adding RNase A (final concentration 1 μg/μl).

Buffer P1, pH 8.0

50 mM Tris-HCl

10 mM EDTA

Buffer S2

200 mM NaOH

1% SDS

Buffer S3, pH 5.5

3 M Potassium acetate

2.8.2 Isolation of plasmid DNA for transfection of mammalian cells

To isolate high quality DNA the commercial kit „NucleoBond® AX 100" was used. 30 ml LB medium was inoculated with a single colony of *E. coli* picked from a plate. The culture was grown at 37˚C, 250 rpm overnight until an OD$_{600}$=3-6 was reached. Cells were then centrifuged at 6000 × g for 15 min at 4˚C. The bacterial pellet was resuspended in 4 ml of

buffer S1. Cells were lysed by addition of 4 ml of buffer S2 for 2-3 min and the lysate was afterwards neutralised with 4 ml of buffer S3 on ice for 5 min. The lysate was clarified by filtration and then applied to a column pre-equilibrated with buffer N2. Plasmid DNA remained bound to the silica-based anion-exchange resin while proteins, polysaccharides, tRNA and 5S RNA flew through the column. rRNA and mRNA were washed out with buffer N3 and plasmid DNA was subsequently eluted with 5 ml of elution buffer N5. DNA was afterwards precipitated with 3.5 ml of isopropanol and centrifuged at $\geq 15,000 \times g$ at 4°C for 30 min. The pellet was washed with 70% ethanol, dried and plasmid DNA was redissolved in 5 mM Tris-HCl, pH 8.0. The quality of the isolated plasmid was determined by spectrophotometry (see section 2.8.3).

Buffer S1, pH 8.0

50 mM Tris-HCl

10 mM EDTA

100 µg/ml RNase A

Buffer S2

200 mM NaOH

1% SDS

Buffer N3, pH 6.3 adjusted with H_3PO_4

100 mM Tris

15% ethanol

1.15 M KCl

Buffer S3, pH 5.1

2.8 M Potassium acetate

Buffer N2, pH 6.3 adjusted with H_3PO_4

100 mM Tris

15% ethanol

900 mM KCl

0.15% Triton X-100

Buffer N5, pH 8.5 adjusted with H_3PO_4

100 mM Tris

15% ethanol

1 M KCl

2.8.3 Determination of plasmid DNA concentration

DNA concentration was measured by spectrophotometry at wavelength $\lambda = 260$ nm (absorbance maximum of purine and pyrimidine bases). Optical density $OD_{260} = 1$ refers to the dsDNA concentration 50 µg/ml. The purity of the sample was determined by measuring the OD at wavelength $\lambda = 280$ nm (absorbance maximum of proteins). In case that A260/A280 is 1.6-2.0 (quotient lower than 1.6 indicates high contamination of DNA with proteins) DNA concentration can be calculated as follows:

$$\text{DNA concentration [µg/ml]} = OD_{260} \times 50 \times \text{factor of dilution}$$

2.8.4 DNA-agarose gel electrophoresis

Agarose gels were prepared by melting the appropriate amount of agarose in TAE or TBE buffer. After the agarose had cooled down, the gel was poured in a casting chamber and ethidium bromide was added (final concentration 0.1 μg/ml). The gel was placed in an electrophoresis chamber filled with appropriate buffer and after the samples and marker of molecular weight were loaded, electric current was applied that allowed separation of DNA fragments according to their molecular weight. The gel was examined under UV light and a picture was taken using a gel documentation system.

TAE buffer, pH 8.3

40 mM Tris base

20 mM Acetic acid

2 mM EDTA

TAE buffer, pH 8.0

89 mM Tris base

89 mM Boric acid

2 mM EDTA

DNA sample buffer (in TE buffer)

6% (v/v) Glycerine

0.05% (w/v) Bromophenol blue

TE buffer, pH 8.0

10 mM Tris base

1 mM EDTA

2.8.5 Polymerase chain reaction (PCR)

Standard polymerase chain reaction was performed in a thermocycler as follows:

~100 ng Plasmid-DNA as a template

10 μM oligonucleotide 5´-3´

10 μM oligonucleotide 3´-5´

500 μM dNTP-Mix

1× PCR-buffer (100 mM Tris-HCl, pH 8.3; 500 mM KCl; 20 mM $MgCl_2$)

3-4 U Taq-Polymerase

The usual volume of a PCR reaction was 25 μl. The programmes of the PCR reactions differ depending on the primers and template used.

2.8.6 Reverse transcription PCR (RT-PCR)

RT-PCR was performed using RNA isolated from mouse tissues (kind gift of Dr. W. Lu, Center for Biochemistry, Medical Faculty, University of Cologne, Germany) as template.

Reverse transcription was performed as follows: 3 µg RNA was mixed with 2 µl p(dN)6 random hexanucleotide primer and water in 20 µl reaction. The reaction was incubated for 5 min at 70˚C and then cooled for 2 min on ice. Following was added to the reaction:

5 µl M-MLV RT 5× buffer

1.25 µl 10mM dNTP

40 U rRNasin RNase Inhibitor

200 U M-MLV reverse transcriptase RNase H Minus

1.75 µl H_2O

The reaction was incubated for 1 h at 37˚C. Then PCR was preformed as follows:

5 µl RT-PCR reaction

1 µl 100 pmol/µl MUF1/fwd/E5-E6 primer

1 µl 100 pmol/µl MUF1/rev/E9-E10 primer

1 µl Reaction Ready^{TM} Mouse GAPD Internal Normaliser (436 bp)

1 µl 10 mM dNTP

1 µl 25 mM $MgCl_2$

1 µl Taq polymerase

7 µl H_2O

Conditions:

1. 95˚C 5 min   5. Step 2. – 4. repeated 30 times

2. 95˚C 1 min   6. 72˚C 10 sec

3. 55˚C 1 min   7. 4˚C for ever

4. 72˚C 50 sec

2.8.7 Elution of DNA-fragment from agarose gel

To isolate DNA form agarose gels the commercial kit NucleoSpin Extraction Kit was used. The DNA fragment of interest was cut out from a TAE agarose gel with a clean scalpel. The piece of gel was dissolved in buffer NT (100 mg of the gel was mixed with 200 µl of buffer NT) by heating at 50˚C. The sample was loaded into a column, which allows DNA binding and centrifuged. DNA bound into the column was washed with buffer NT3. Because this buffer contains ethanol that may inhibit subsequent reactions, the silica

membrane of the column was dried prior to elution with elution buffer. The quality of the eluted DNA was tested again on an agarose gel.

2.8.8 Restriction reaction

Plasmid DNA was cut with chosen restriction enzyme in a reaction mixture containing $1\times$ BSA and $1\times$ enzyme buffer suitable for restriction enzyme.

2.8.9 Dephosphorylation of DNA 5´- ends

The dephosphorylation reaction was prepared as follows: 1-2 µg of linearised plasmid was mixed with 1U of SAP (shrimp alkaline phosphatase), $1\times$ SAP buffer, and water to the final volume of reaction 20 µl. The reaction was incubated for 10 min at 37˚C and then stopped by 65˚C for 10 min.

$10\times$ SAP buffer

0.5 M Tris-HCl, pH 8.5

10 mM $MgCl_2$

2.8.10 Ligation of vector and DNA-fragment

A ligation reaction containing 1-3 µg total DNA was mixed in ratio 1:3 vector:insert with 1U T4-DNA-ligase. The final concentration of T4 ligase buffer was $1\times$. The reaction was incubated over night at 16˚C.

$10\times$ Ligase buffer

660 mM Tris-HCl, pH 7.5

50 mM $MgCl_2$

50 mM DTT

10 mM ATP

2.8.11 DNA-sequencing

All constructs were verified by sequencing with specific primers. Sequencing was performed by service laboratory of Centrum for Molecular Medicine Cologne (Germany), MWG (Germany) or Yorkshire Biolabs (United Kingdom).

3 Results

3.1 Characterisation of RhoBTB proteins

3.1.1 Subcellular localisation of RhoBTB3

Little is known about the precise localisation of RhoBTB proteins. Myc-tagged RhoBTB1 and RhoBTB2 were found localised in vesicles in the cytoplasm (Aspenström et al. 2004). Similarly, when GFP-RhoBTB3 is expressed at moderate levels, it localises to vesicles found in the perinuclear area and dispersed in the cytoplasm. RhoBTB3 also forms aggregates in the paranuclear area when overexpressed. These vesicles are in close proximity of the MTOC and partially co-localise with the early endosomal marker EEA1 and with the marker of the endoplasmic reticulum PDI (protein disulfide isomerase). RhoBTB3 positive vesicles were also observed in close proximity of microtubules and stress fibres (Berthold et al. 2008b). In order to examine the localisation of RhoBTB3 in more detail we performed counterstaining with additional cellular markers.

To prove that the pattern of subcellular localisation described above applies also to other cell lines, HeLa cells were transfected with GFP-RhoBTB3 (Figure 3.2 depicts different RhoBTB constructs used in this study). In HeLa cells GFP-RhoBTB3 localises to vesicles dispersed in the cytoplasm (Figure 3.1), similarly to what has been reported in other cell lines (Berthold 2006 dissertation thesis, Berthold et al. 2008b).
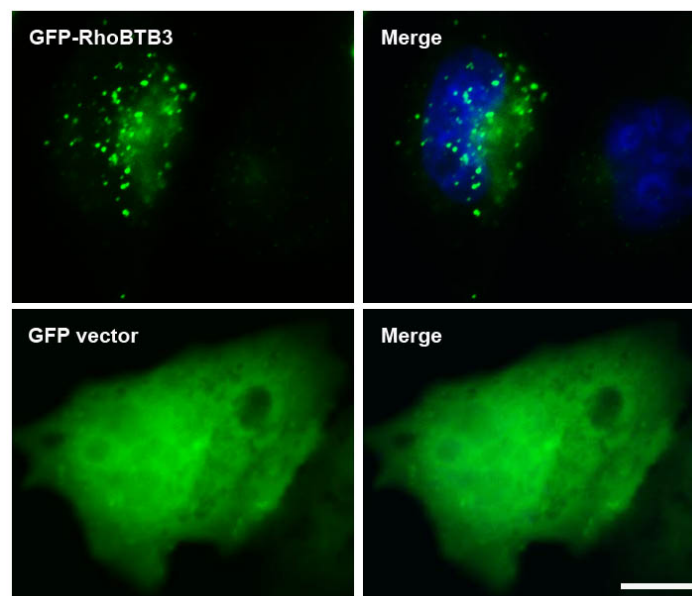
Figure 3.1: RhoBTB3 localises to vesicles dispersed through the cytoplasm in HeLa cells. Cells were transfected with GFP-tagged RhoBTB3 or with GFP empty vector. Cells were fixed and stained with DAPI (blue). Images were acquired with a fluorescence microscope and overlaid. Bar represents 10 μm.
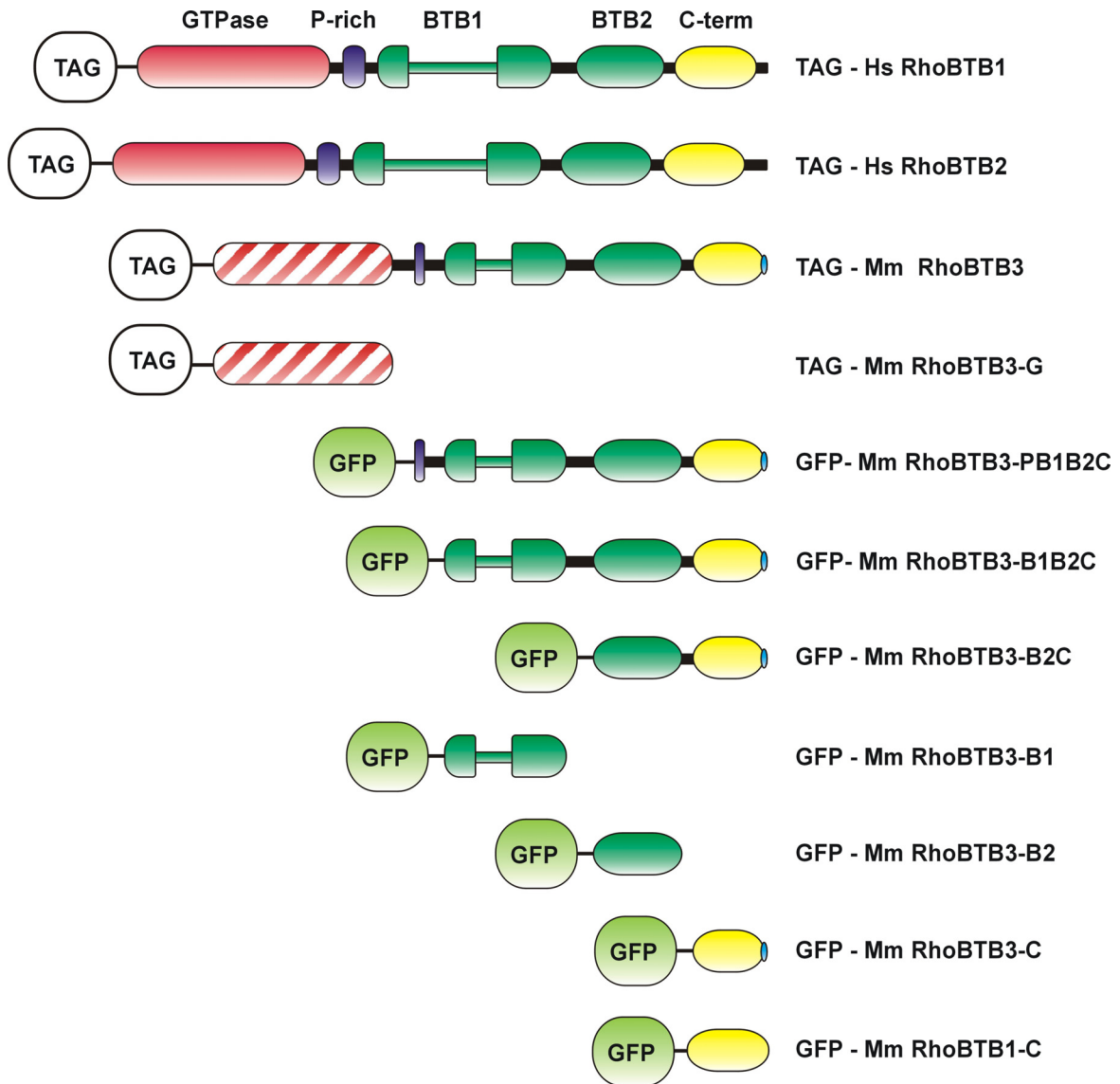
Figure 3.2: Domain architecture of RhoBTB and constructs used in this study. Where the tag is not specified, different tags were used (GFP, Flag, Myc, GST) and are indicated in the particular experiment. In RhoBTB3 the GTPase domain appears extensively erased, to the point that it is virtually unrecognisable as a GTPase. Only RhoBTB3 ends with a CAAX prenylation motif. G – GTPase; B1 – first BTB domain; B2 – second BTB domain; C – C-terminus;

3.1.1.1 RhoBTB3 partially localises at early endosomes through the C-terminal domain

As mentioned above, it was observed previously in our laboratory that GFP-RhoBTB3 partially co-localises with EEA1, a marker of early endosomes. It was also reported that it is the C-terminal domain with its CAAX motif at the very end that is responsible for the vesicular pattern of localisation of the protein (Berthold et al. 2008b). Therefore we hypothesised that only a shortened fused protein containing the C-terminus of RhoBTB3 will show co-localisation with the early endosomes. To verify this, COS7 cells were

transfected with GFP-RhoBTB3-B1, GFP-RhoBTB3-B2, GFP-RhoBTB3-C or GFP-RhoBTB3-B2C (Figure 3.2). Fixed cells were stained with anti-EEA1 antibody. In cells overexpressing GFP and GFP-tagged subdomains of RhoBTB3 EEA1 vesicles looked normal. A disrupted or weaker staining was observed only in a very low proportion of cells. GFP-RhoBTB3-B1 and GFP-RhoBTB3-B2 displayed diffused localisation and no co-localisation with EEA1 was observed. GFP-RhoBTB3-C and GFP-RhoBTB3-B2C localise at vesicles that, as expected, partially co-localise with the early endosome marker (Figure 3.3).

3.1.1.2 GFP-RhoBTB3 occasionally co-localises with transferrin

Another marker of early endosomes is transferrin. It binds to the transferrin receptor and is promptly internalised in clathrin-coated vesicles (Olusanya et al. 2001). HeLa cells were transfected with GFP-RhoBTB3. 24 h after transfection, cells were treated with AlexaFluor 546-labelled transferrin and subsequently fixed. GFP-RhoBTB3 vesicles did not significantly influence the localisation and distribution of transferrin containing vesicles. To examine whether GFP-RhoBTB3 and transferrin co-localise, confocal images were taken. As seen on figure 3.4, GFP-RhoBTB3 and transferrin only occasionally co-localised.
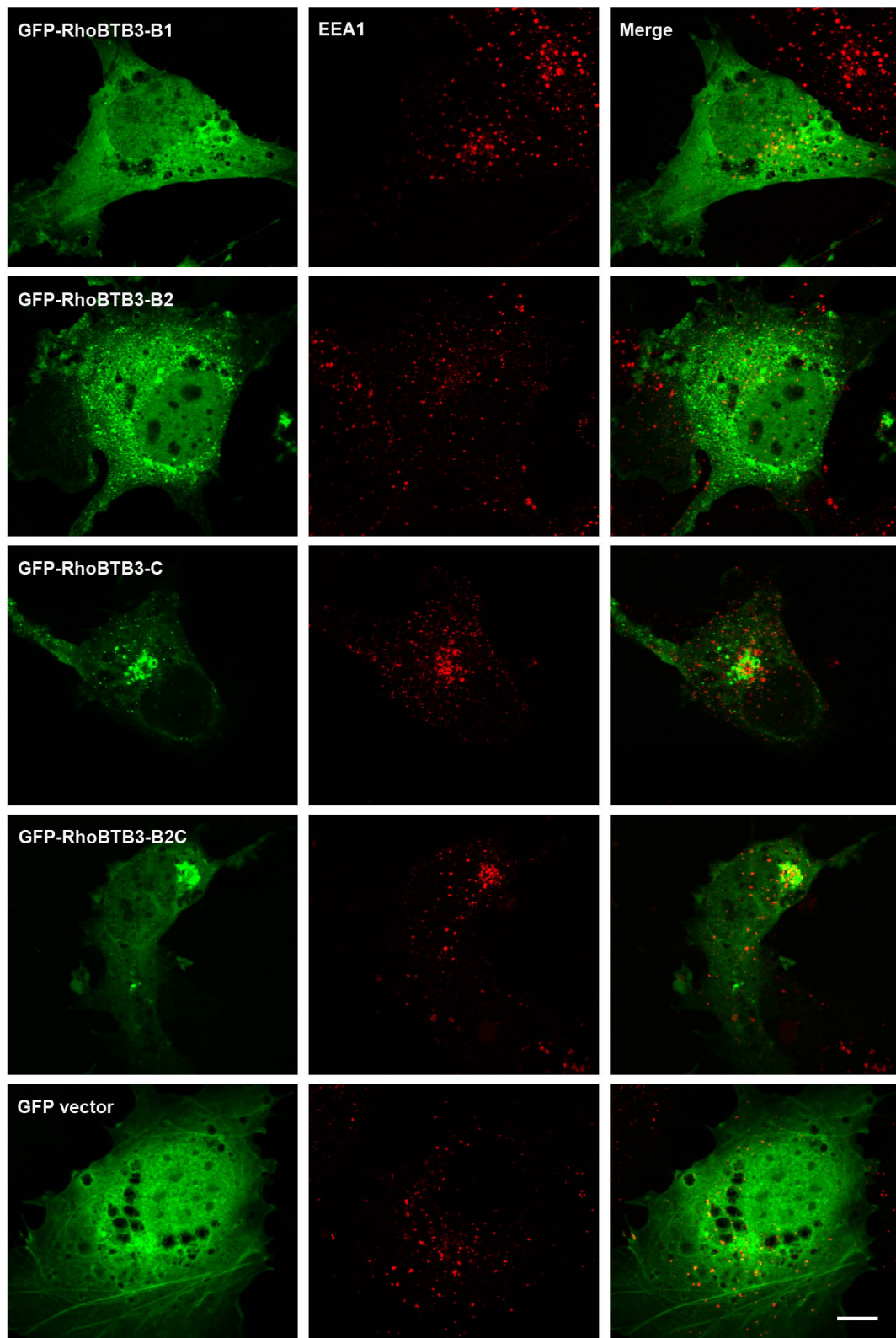
Figure 3.3: Co-localisation of RhoBTB3 domains with early endosomes. COS7 cells were transfected with the indicated GFP fusions or empty GFP vector as a control. To visualise early endosomes in fixed cells, primary antibody αEEA1 and secondary antibody Alexa Fluor 568 were used. Images were acquired with a confocal laser scanning microscope and overlaid. Bar represents 10 μm.
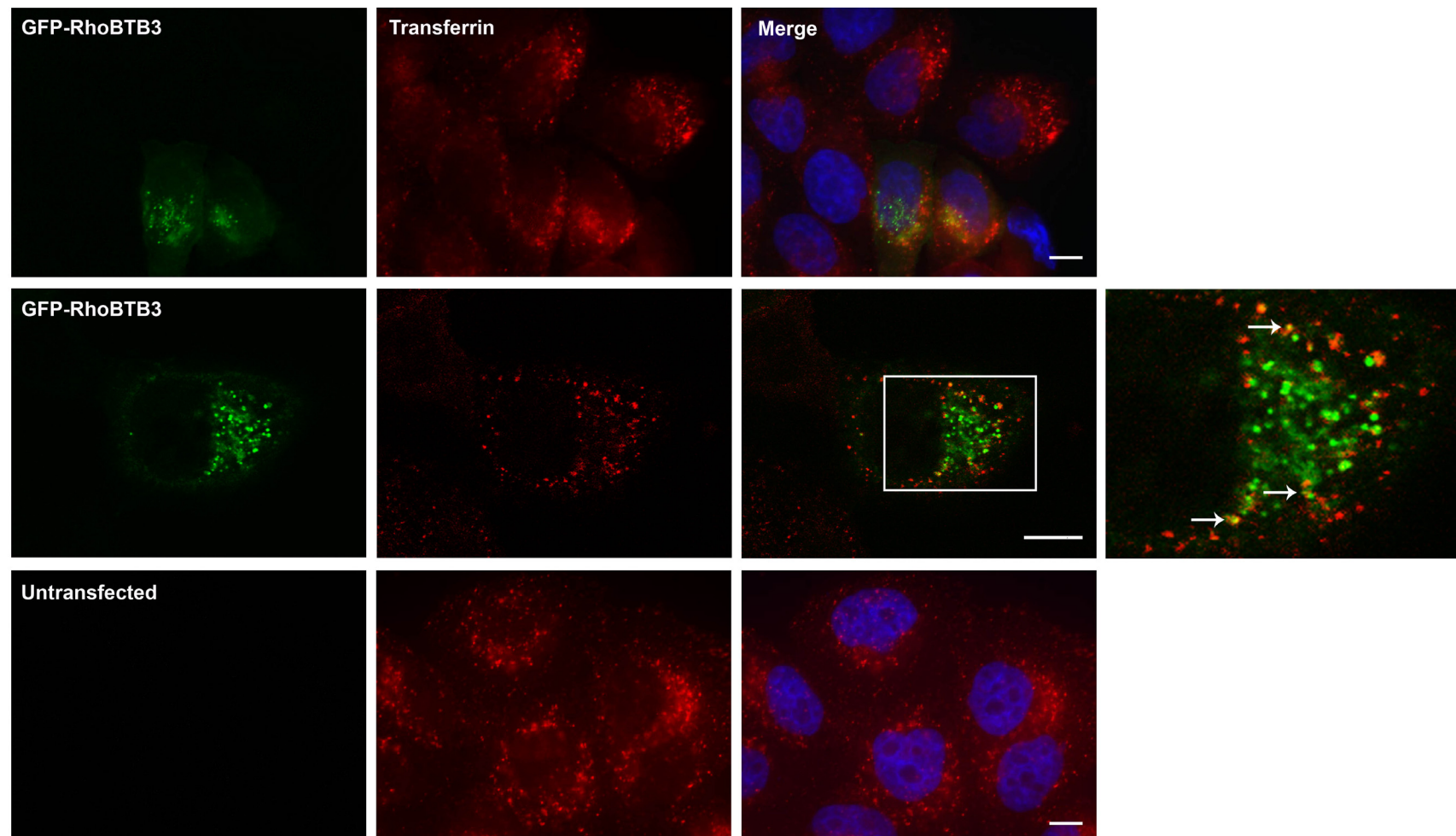
Figure 3.4: Co-localisation of RhoBTB3 with transferrin. HeLa cells were transfected with GFP-RhoBTB3 and 24 h after transfection incubated with Alexa Fluor 546-labelled human transferrin, fixed and permeabilised with 0.5% saponin. Images were acquired with a conventional fluorescence microscope (first and third row) or with a confocal laser scanning microscope (second row) and overlaid. Right hand panel is a magnification of the indicated area. Arrows point at RhoBTB vesicles that colocalise with transferrin. Bar represents 10 μm.

3.1.1.3 Overexpression of RhoBTB3 disrupts the Golgi apparatus

RhoBTB3 is the only RhoBTB protein that contains a CAAX prenylation motif at the C-terminus. It is known that proteins with prenylation motif are targeted to the Golgi apparatus (GA). Moreover, GFP-RhoBTB3 localises to vesicles in the perinuclear area that might be the GA. To examine whether RhoBTB co-localises with the GA, COS7 cells were transfected with one of the following constructs: GFP-RhoBTB3, Flag-RhoBTB3, GFP-RhoBTB2, Flag-RhoBTB2, GFP-RhoBTB3-B1, GFP-RhoBTB3-B2, GFP-RhoBTB3-C, GFP-RhoBTB3-B2C and GFP-RhoBTB1-C (Figure 3.2). Fixed cells were immunostained with anti-GM130 antibody that stains the GA. Expression of all RhoBTB constructs caused a significant disruption of the GA (Figure 3.5): staining of the GA was observed in vesicles dispersed through the cytoplasm, or in some cases the GA formed aggregates as opposed to cells expressing empty GFP where the GA formed stacks. GFP-RhoBTB3 only partially co-localised with the disrupted GA. To exclude the possibility that this partial co-localisation of GFP-RhoBTB3 is caused by the bulky GFP tag, the localisation of Flag-RhoBTB3 was also examined. Similarly, Flag-RhoBTB3 also partially co-localised with disrupted GA. GFP-RhoBTB3-C and GFP-RhoBTB3-B2C showed co-localisation with disrupted GA to a higher extent. Surprisingly, GFP-RhoBTB2 and Flag-RhoBTB2 also displayed partial co-localisation with the GA, although RhoBTB2 does not bear any prenylation motif. Those constructs with a GFP-tag were examined more closely and the ratio of cells with disrupted GA was determined. Expression of GFP-tagged RhoBTB proteins significantly disrupted GA, in all cases more than 52% of examined cells showed altered morphology of the GA in comparison to those expressing only GFP (19.9%) (Figure 3.6).
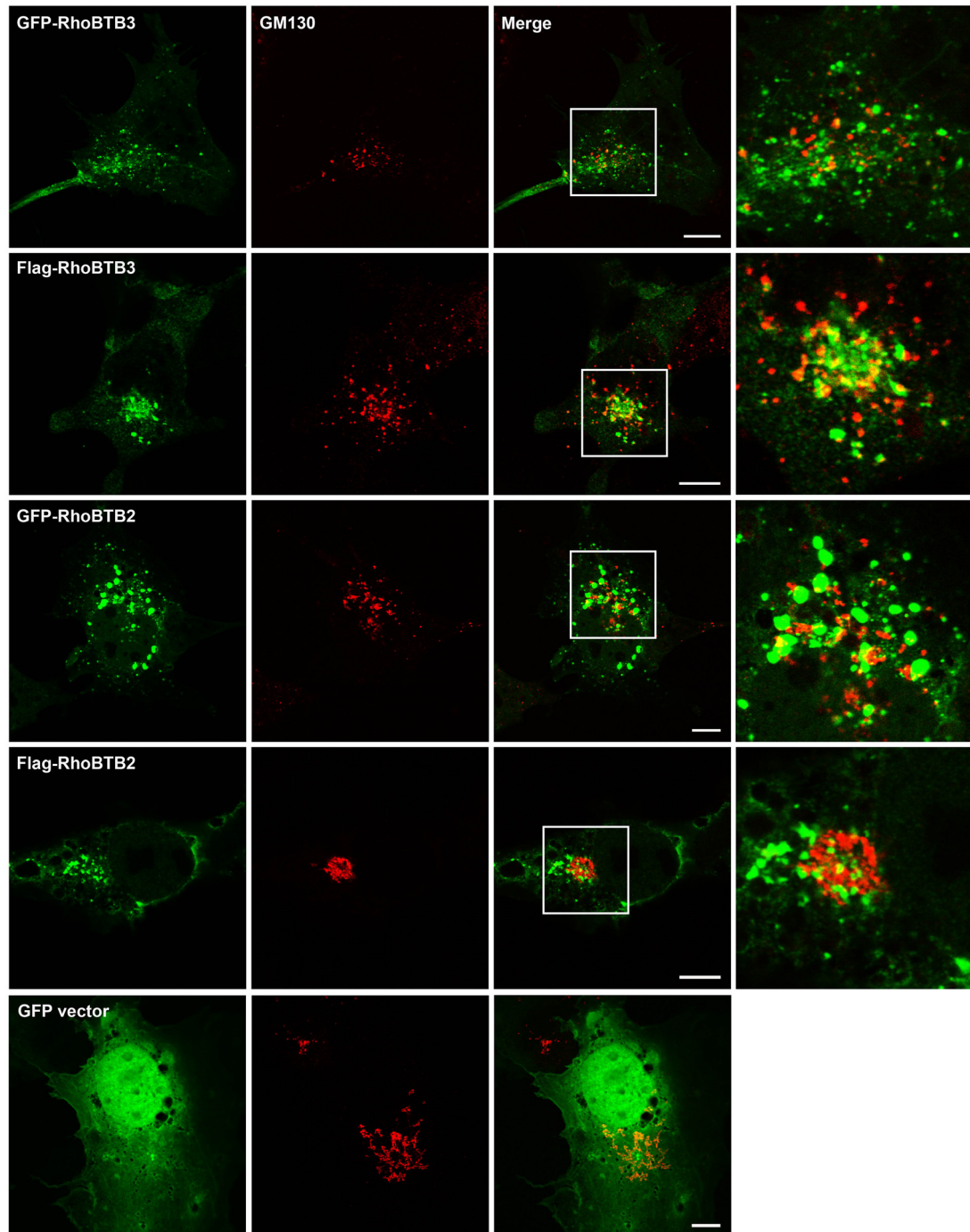
Figure 3.5: RhoBTB overexpression disrupts the Golgi apparatus. COS7 cells were transfected with the indicated GFP-tagged or Flag-tagged RhoBTB constructs or with empty GFP vector. Cells were fixed and immunostained with anti-GM130 antibody followed by Alexa Fluor 568-coupled secondary antibody. Flag-tagged proteins were visualised with anti-Flag (anti-ECS) antibody followed by staining with Alexa Fluor 488-coupled secondary antibody. Images were acquired with a confocal laser scanning microscope and overlaid. Right hand panels are magnifications of the indicated areas. Bar represents 10 μm. The figure continues on the next page.

GFP-RhoBTB3-B1   GM130   Merge

GFP-RhoBTB3-B2

GFP-RhoBTB3-C

GFP-RhoBTB3-B2C

GFP-RhoBTB1-C
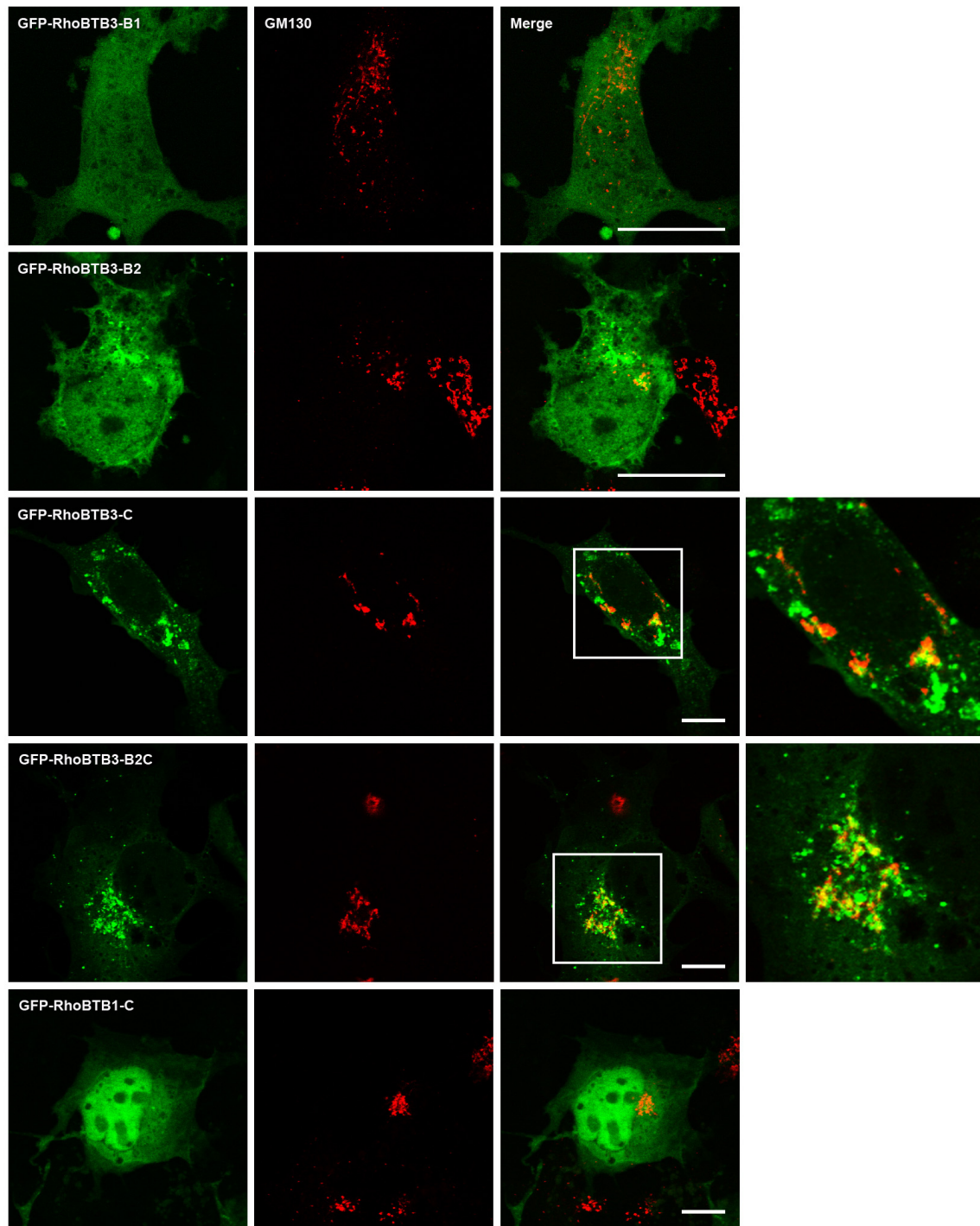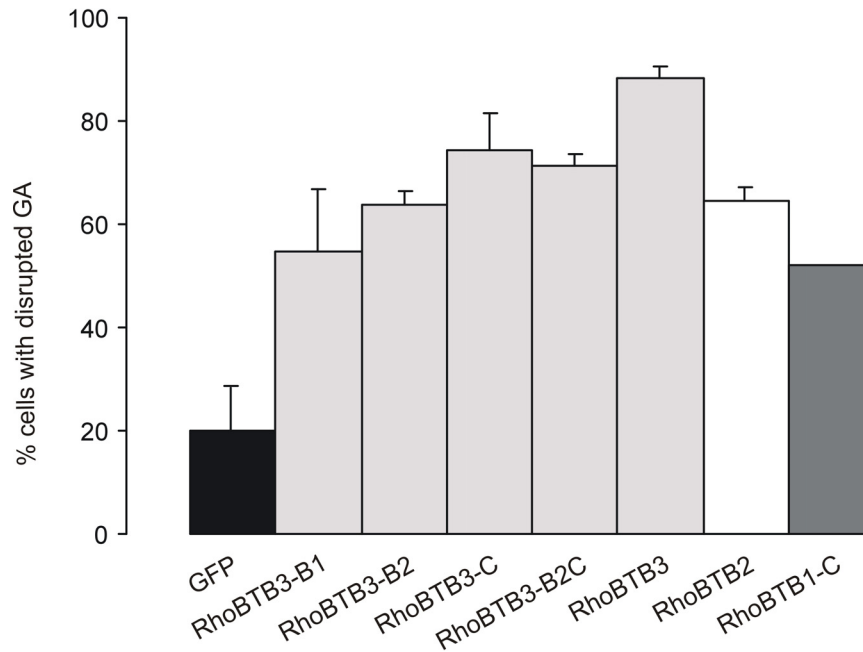
Figure 3.6: Disruption of Golgi apparatus by different RhoBTB proteins or domains. COS7 cells were transfected with the indicated GFP fusions. Fixed cells were immunostained with αGM130 to visualise the GA. The graph shows average and standard deviation of two independent experiments. Approximately 500 cells were scored for each sample.

3.1.1.4 RhoBTB3 does not localise to the mitochondria

In order to examine whether RhoBTB3 localises to one more membrane compartment, the mitochondria, COS7 cells were transfected with GFP-RhoBTB3. Prior to fixation cells were labelled with MitoTracker® Red CMXRos. This is a derivative of X-rosamine that passively diffuses across the plasma membrane and accumulates in active mitochondria where it reacts with thiols on proteins and peptides. From figure 3.7 it is apparent that GFP-RhoBTB3 vesicles showed no co-localisation with the mitochondrial network and overexpression of RhoBTB3 did not alter the mitochondrial staining.
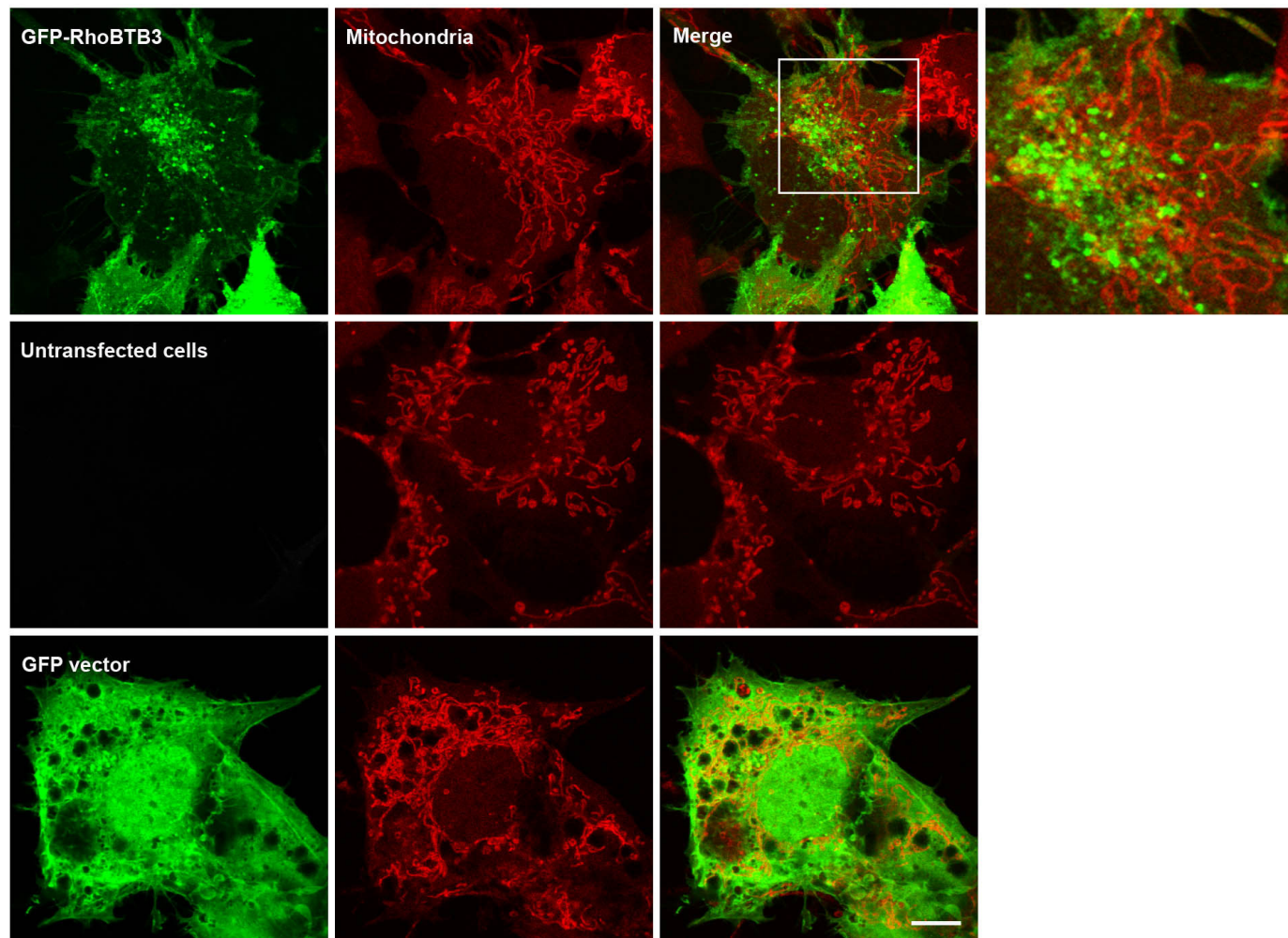
Figure 3.7: RhoBTB3 does not localise at mitochondria. COS7 cells were transfected with GFP-tagged Mm RhoBTB3 or with empty GFP vector as a control. Cells were incubated with 500nM MitoTracker® Red CMXRos prior to fixation. Images were acquired with a confocal laser scanning microscope and overlaid. Overexpression of RhoBTB3 does not alter mitochondrial staining. Bar represents 10 μm.

3.1.1.5 Interaction of RhoBTB3 with the cytoskeleton

3.1.1.5.1 Interaction of RhoBTB3 with microtubules

RhoBTB3 localises at vesicles that are found in the proximity of the microtubule organising centre (MTOC) and these vesicles were also identified in close proximity of microtubules (Berthold et al. 2008b).

To further examine the link between RhoBTB3 and the microtubule network, we used drugs that either stabilise (taxol) or disrupt (colchicine) the microtubule network. We would expect that if RhoBTB3 is not interacting (directly or indirectly) with the microtubule network, stabilisation or disruption of microtubules will have no effect on RhoBTB3 distribution. COS7 cells were transfected with GFP-RhoBTB3 (Figure 3.2). 20 h after transfection cells were treated with one of the drugs for 4 h (20 μM taxol or 25 μM colchicine) and fixed. Microtubules stabilised with taxol show clustered staining (Figure 3.8B, C). Stabilisation of microtubules might have some effect on GFP-RhoBTB3 localisation: it still displayed vesicular localisation but because there is no MTOC, the paranuclear localisation was altered and vesicles were more dispersed in the cytoplasm. GFP-RhoBTB3 did not co-localise with stabilised microtubules. Colchicine disrupted microtubules completely. Disruption of the microtubule network seemed to cause aggregation of GFP-RhoBTB3 (Figure 3.8D, E).

3.1.1.5.2 Co-localisation of RhoBTB2 and RhoBTB3 does not depend on an intact microtubule network

It was shown previously that RhoBTB proteins are able to build homo- and heterodimers and RhoBTB3 co-localises with RhoBTB2 (Berthold et al. 2008b). To rule out that this interaction is indirect through a possible microtubule binding, COS7 cells were transfected with GFP-MmRhoBTB3 and Flag-HsRhoBTB2 and treated with colchicine. Disruption of the microtubule network neither influenced localisation of RhoBTB2 and RhoBTB3 nor prevented their co-localisation (Figure 3.9).
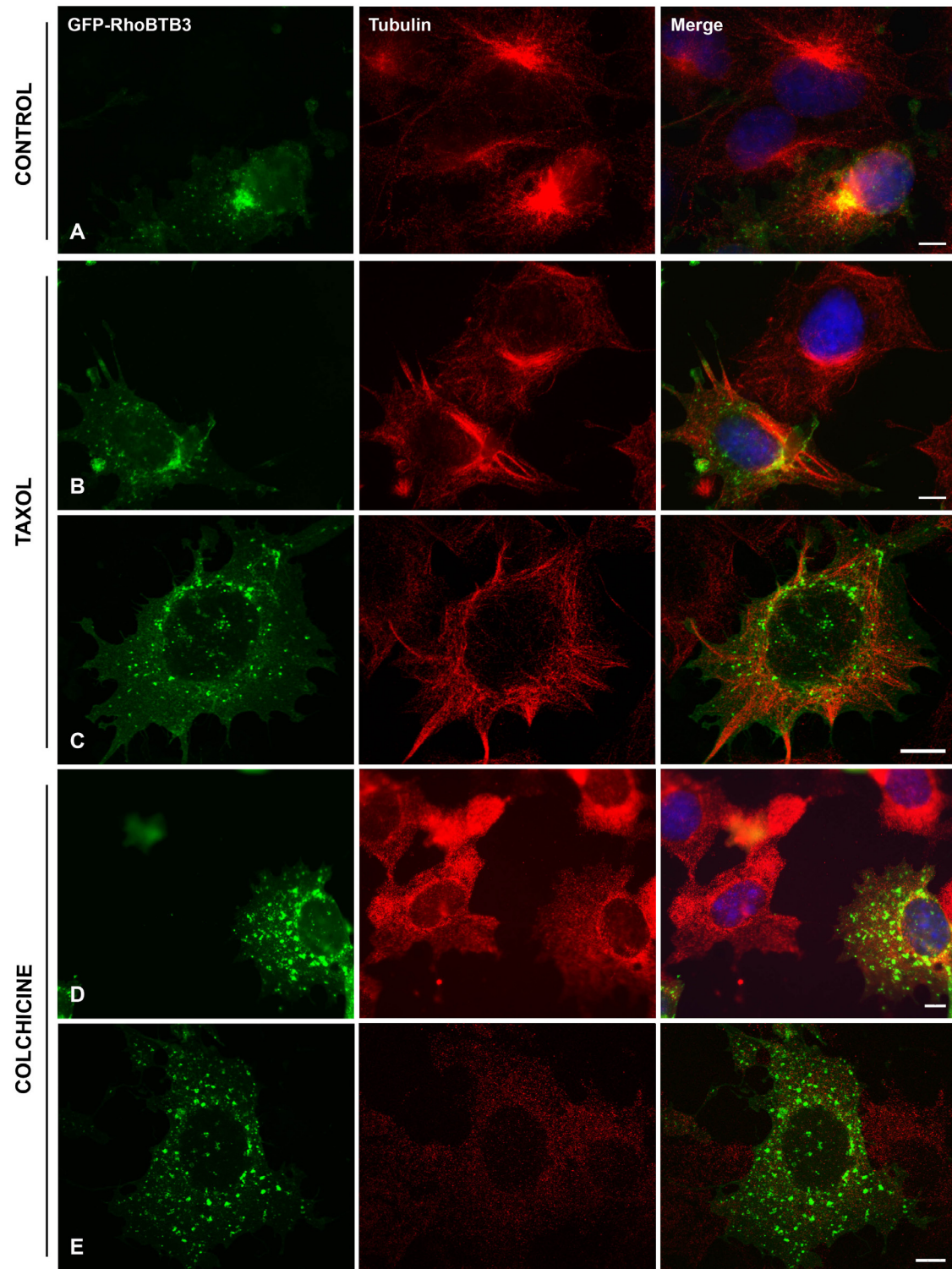
Figure 3.8: Microtubule-independent localisation of RhoBTB3. COS7 cells were transfected with GFP-RhoBTB3. Before fixation, cells were treated with the tubulin-stabilising agent taxol or with the tubulin-disrupting agent colchicine. Fixed cells were immunostained with anti-α-tubulin antibody followed by Alexa Fluor 568-coupled secondary antibody. Nuclei were visualised with DAPI. Images were acquired with a conventional fluorescence microscope (A, B, D) or with a confocal laser scanning microscope (C, E) and overlaid. A) Non-treated cells. B) and C) Cells treated with 20 μM taxol for 4 h. D) and E) Cells treated with 25 μM colchicine for 4 h. Bar represents 10 μm.
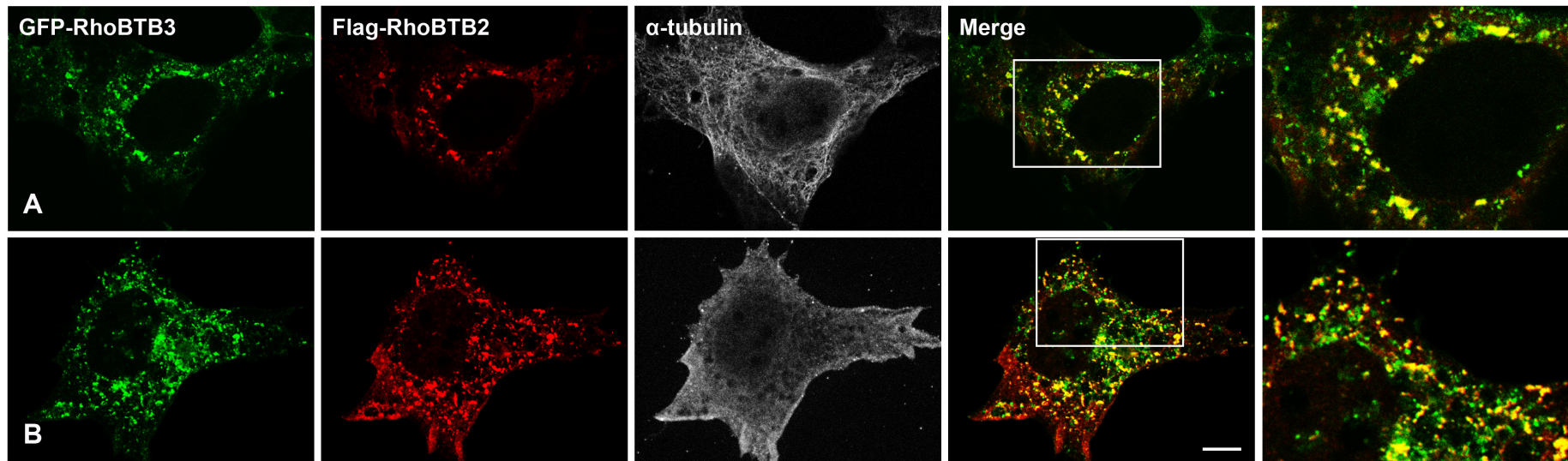
Figure 3.9: Microtubule independent co-localisation of RhoBTB3 and RhoBTB2. COS7 cells were transfected with GFP-RhoBTB3 and Flag-RhoBTB2. Before fixation, cells were treated with the tubulin-disrupting agent colchicine (25 µM) for 4h. Fixed cells were immunostained with anti-Flag (anti-ECS) antibody followed by Alexa Fluor 568-coupled secondary antibody and anti-α-tubulin antibody followed by Cy5-coupled secondary antibody. Images were acquired with a confocal laser scanning microscope and overlaid. A) Non-treated cells. B) Cells treated with colchicine. Right hand panels are magnifications of the indicated areas. Bar represents 10 µm.

3.1.1.5.3 Interaction of RhoBTB3 with the actin cytoskeleton

Ectopic expression of RhoBTB1 and RhoBTB2 has only a moderate influence on the organisation of the actin filament system (Aspenström et al. 2004). The influence of actin on RhoBTB distribution has not been examined before. To examine this, COS7 cells were transfected with GFP-RhoBTB3 (Figure 3.2). Cells were treated with latrunculin B and fixed. To visualise actin filaments, cells were stained with TRITC-phalloidin. After latrunculin B treatment, actin filaments were completely disrupted and the cell bodies appeared retracted. However, the paranuclear clustered distribution of RhoBTB3 was not altered (Figure 3.10).
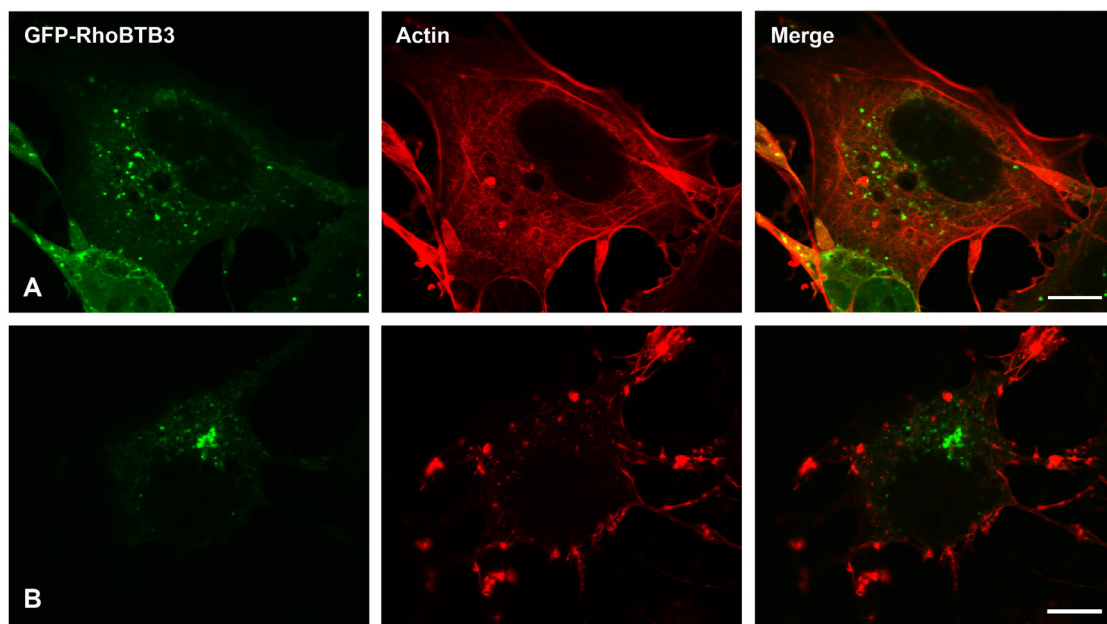
Figure 3.10: Actin-independent localisation of RhoBTB3. COS7 cells were transfected with GFP-tagged RhoBTB3. 30 min before fixation, cells were treated with the actin-disrupting agent latrunculin B (2.5 μM) or with ethanol as a control. Fixed cells were immunostained with TRITC-labelled phalloidin. Images were acquired with a confocal laser scanning microscope and overlaid. A) Non-treated cells. B) Cells treated with latrunculin B. Bar represents 10 μm.

3.1.2 The GTPase domain of RhoBTB3 does not bind GTP

It has been shown that RhoBTB2 does not bind GTP (Chang et al. 2006). The GTPase domain of RhoBTB3 is, in comparison to those of RhoBTB1 and RhoBTB2, broadly erased. Therefore it was of great interest to determine whether the GTPase domain of RhoBTB3 is still able to bind GTP.

The GTPase domain of RhoBTB3 (Figure 3.2) was expressed as a GST fusion protein in *E. coli*. The purified GST-tagged protein was resolved on two SDS gels. One gel was stained with Coomassie-Brilliant-Blue R 250 and one was blotted onto a nitrocellulose

membrane, incubated in buffer containing radioactive GTP and subjected to autoradiography. The gel stained with Coomassie-Brilliant-Blue R 250 shows the amount of recombinant protein. No binding of radioactive GTP to RhoBTB3 GTPase was observed, in contrast to GST-Rac1 that is known for GTP binding. No binding of radioactive GTP to GST was observed, which was used as a negative control (Figure 3.11).
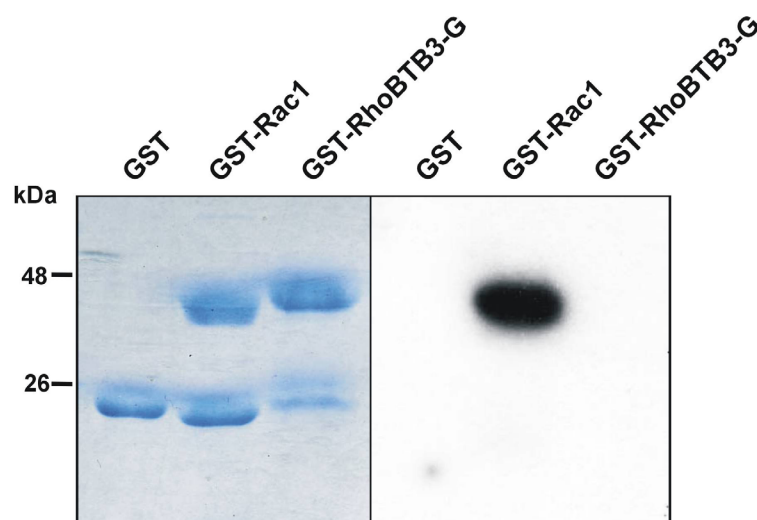
Figure 3.11: The GTPase domain of RhoBTB3 does not bind GTP *in vitro*. The GTPase domain of RhoBTB3 (RhoBTB3-G) was expressed as a GST fusion in *E. coli*, purified and resolved on 15% SDS-PAGE. One gel was stained with Coomassie-Brilliant-Blue R 250 and one was blotted onto nitrocellulose membrane. The membrane was incubated with (α-^{32}P) GTP. Human Rac1 was used as a positive control and GST as a negative control. This experiment was done in collaboration with Jessica Berthold.

3.1.3 Interaction of RhoBTB3 with Cul3

3.1.3.1 RhoBTB3 interacts with endogenous Cul3

It was shown previously that endogenous Cul3 co-immunoprecipitates RhoBTB2 (Wilkins et al. 2004). From previous experiments in our laboratory it was known that Myc-RhoBTB3 is able to co-immunoprecipitate Flag-Cul3. To confirm this data it was necessary to show that Myc-RhoBTB3 can co-immunoprecipitate also endogenous Cul3. 293T HEK cells were transfected with Myc-RhoBTB1, Myc-RhoBTB2 or Myc-RhoBTB3 (Figure 3.2). Directly after transfection, proteasomal inhibitor MG132 was added to the cells for 24 h. Protein complexes were immunoprecipitated with anti-Myc antibody coupled to magnetic beads. Figure 3.12 shows that all three RhoBTB proteins, when ectopically expressed, were able to co-immunoprecipitate endogenous Cul3. This result confirms previous observations that RhoBTB3 interacts with Cul3 *in vivo*. The reciprocal experiment was not possible, because of a lack of good antibodies recognising endogenous RhoBTB proteins.
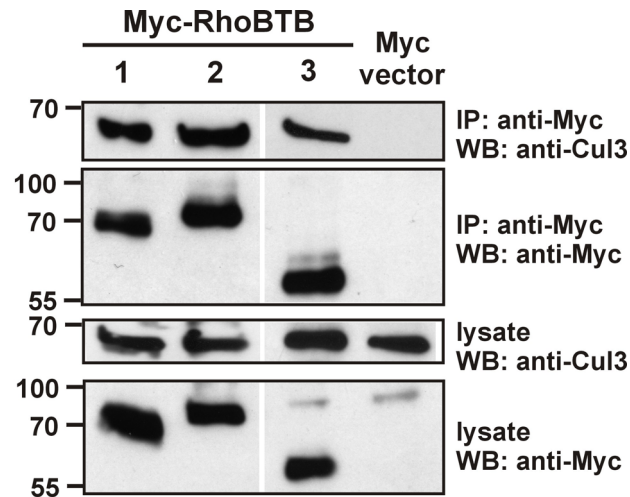
Figure 3.12: All three RhoBTB proteins interact with endogenous Cul3 *in vivo*. 293T HEK cells were transfected with the indicated Myc-RhoBTB or the empty Myc vector and treated with proteasomal inhibitor MG132 (5μM) for 24 hours. After lysis complexes were immunoprecipitated with anti-Myc antibody coupled to magnetic beads. Boiled lysates or immunoprecipitated samples were resolved on 10% SDS gel and blotted onto PVDF membrane. The membrane was incubated with the indicated primary antibodies and corresponding peroxidase-conjugated secondary antibodies followed by ECL detection.

3.1.3.2 Dimerisation of RhoBTB is Cul3-independent

Previous experiments performed in our laboratory showed that RhoBTB proteins are capable of assembling homodimers and heterodimers. Because all three RhoBTB proteins are able to bind Cul3 through the first BTB domain (Berthold et al. 2008b), it has to be ruled out that this dimerisation occurs through interaction with Cul3. To examine this, a gene silencing experiment was performed with the goal of downregulating the expression of endogenous Cul3. HEK 293T cells were first transfected with siRNA oligonucleotides to downregulate Cul3 and the following day with Myc-RhoBTB3 and Flag-RhoBTB2 (Figure 3.2). Protein complexes were immunoprecipitated with anti-Myc antibody coupled to magnetic beads. Immunoprecipitates and lysates were analysed for the presence of the tagged proteins by Western blotting. Figure 3.13 shows that although there was still some signal of Cul3 present after siRNA treatment, in comparison to the negative control Cul3 was significantly downregulated. Myc-RhoBTB3 was still able to co-immunoprecipitate Flag-RhoBTB2, which indicates that dimerisation of RhoBTB2 and RhoBTB3 is independent of Cul3.
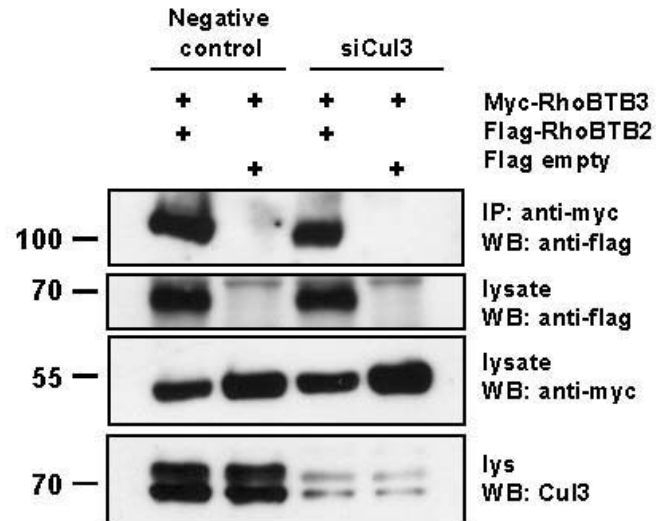
Figure 3.13: Downregulation of Cul3 does not abolish dimerisation of RhoBTB proteins. 293T HEK cells were transfected with Cul3 specific siRNA oligonucleotides or random oligonucleotides as a negative control. Following day cells were transfected with Myc-RhoBTB3 and either Flag-RhoBTB2 or empty flag vector. 24 h after transfection, cells were lysed and Myc-RhoBTB3 was precipitated with anti-Myc antibody coupled to magnetic beads. Samples were resolved on 10% SDS gel and blotted onto PVDF membrane. The membrane was incubated with the indicated primary antibodies and corresponding peroxidase-conjugated secondary antibodies followed by ECL detection. Cul3 is visible as two bands, the upper one corresponding to the neddylated form.

3.1.4 Proteasomal degradation of RhoBTB3 is prevented by intramolecular interaction

It was shown previously in our laboratory that the GTPase domain of RhoBTB is able to bind to the BTB tandem (Berthold et al. 2008b) and the hypothesis was put forward that the GTPase prevents binding of Cul3 to the first BTB domain and therefore blocks ubiquitination and subsequent degradation of RhoBTB in the proteasome. To test this hypothesis, a half life experiment was performed (see section 2.3.5). 293T HEK cells were transfected with GFP-RhoBTB3-B1B2C or GFP-RhoBTB3 and Myc-RhoBTB3-G (Figure 3.2). Lysates were collected at several time points and analysed for the presence of the tagged proteins by Western blotting. Figure 3.14 shows that when GFP-RhoBTB3-B1B2C was expressed alone, it was degraded very fast. Degradation was prevented by co-expression of Myc-RhoBTB3-GTPase. When proteasome inhibitor was added, very strong stabilisation of the GFP-RhoBTB3-B1B2C was apparent, as expected. Expression of full length GFP-RhoBTB3 was more stable and did not depend on the presence of the Myc-RhoBTB3-GTPase. This data indicates that an intramolecular interaction between the GTPase domain of RhoBTB3 and the B1B2C region prevents degradation of RhoBTB3.
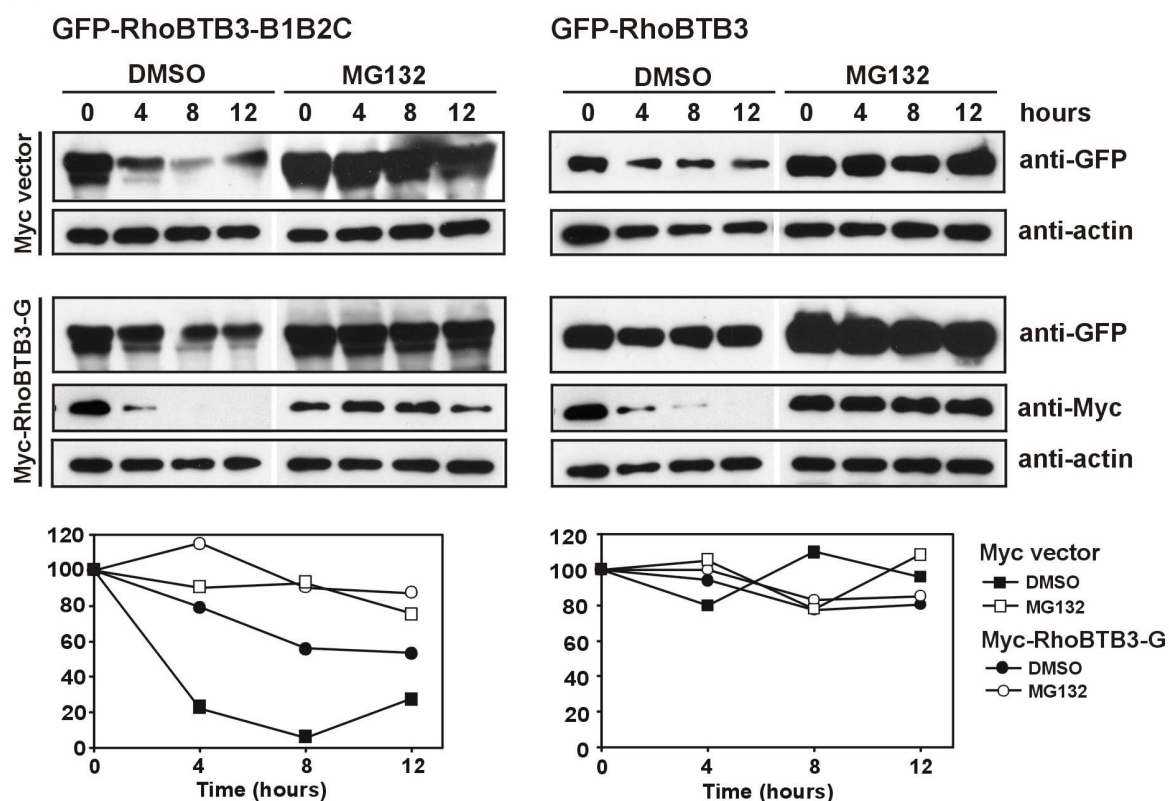
Figure 3.14: Intramolecular interaction between the GTPase and the BTB tandem prevents degradation of RhoBTB3. 293T HEK cells were transfected with GFP-RhoBTB3-B1B2C or GFP-RhoBTB3 and either Myc-RhoBTB3-GTPase or empty Myc vector. 16 h after transfection cells were split and treated with 100 μM cycloheximide and either with 10 μM MG132 or DMSO. At the time points 0, 4, 8 and 12h cells were collected and lysed. Lysates were tested on 10% SDS gel and blotted onto PVDF membrane. The membrane was probed with the indicated primary antibodies and corresponding peroxidase-conjugated secondary antibodies followed by ECL detection. Actin staining served as a loading control. The graphs show the amount of the GFP fusion protein normalised to the amount of actin and expressed as percentage relative to the 0 time point.

3.1.5 RhoBTB3 is ubiquitinated by a Cul3-dependent ligase

It was shown that RhoBTB2 is ubiquitinated in the presence of Cul3, Roc1, E1, E2 and ubiquitin (Wilkins et al. 2004). Because we showed that RhoBTB3 is degraded in the proteasome (see section 3.1.4), it was of great interest to test if RhoBTB3 is ubiquitinated. 293T HEK cells were transfected with GFP-RhoBTB3, Myc-Cul3 and Myc-Roc1. Co-immunoprecipitation was performed with anti-Myc antibody coupled to agarose beads. The ubiquitination assay was performed as described (see section 2.7.9). Samples were analysed for the presence of the indicated tagged proteins by Western blotting. GST-Ub was visualised with GST antibody. Figure 3.15 shows the high molecular weight smear of ubiquitinylated RhoBTB3 confirming that RhoBTB3 was ubiquitinated in the presence of Cul3, Roc1, E1, E2 and ubiquitin. Bands of smaller sizes (below 94 kDa) could also be

observed that might correspond to degraded protein. Cul3-dependent ubiquitination of RhoBTB3 was also shown by Berthold et al. (2008b).
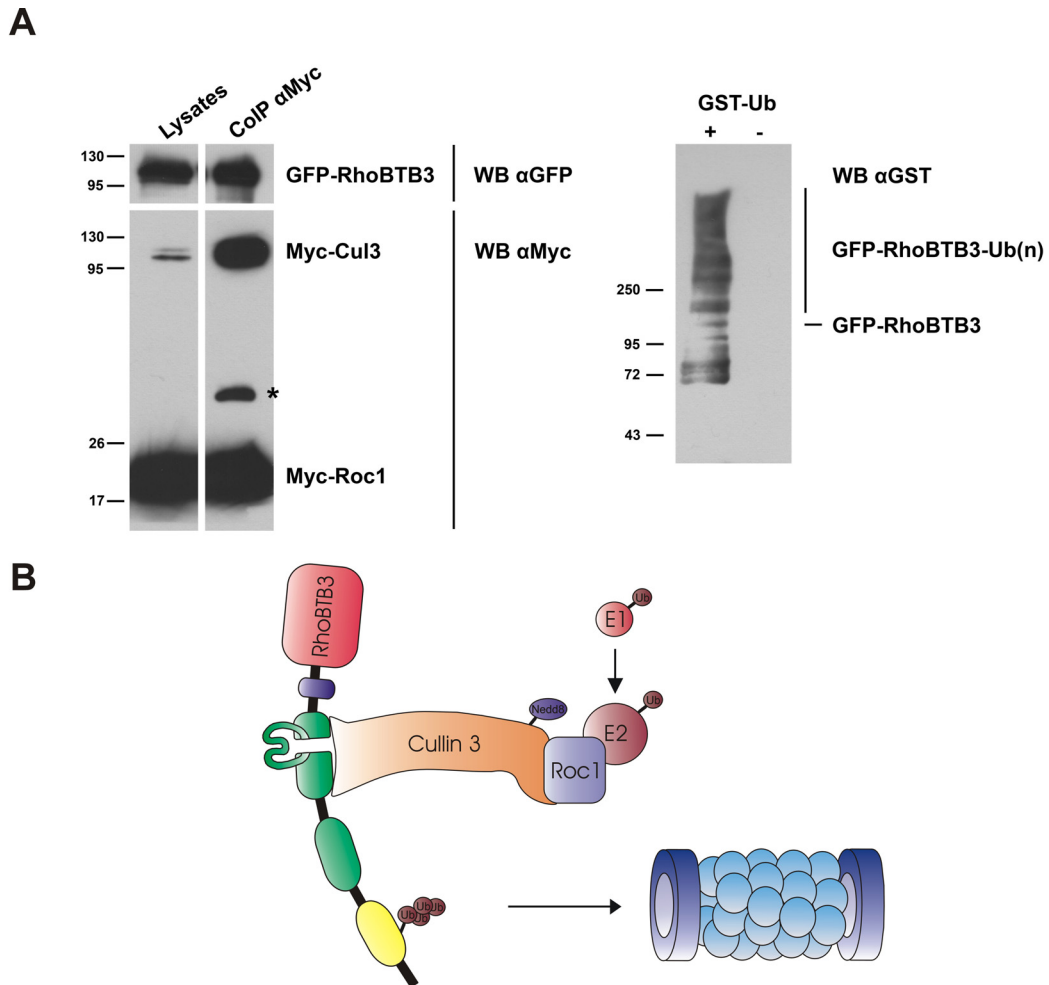
Figure 3.15: Ubiquitinylation of RhoBTB3. A) 293T HEK cells were co-transfected with GFP-RhoBTB3, Myc-Cul3 and Myc-Roc1. 10 h after transfection proteasomal inhibitor MG132 (5 µM) was added for 12 h. Protein complexes were immunoprecipitated with anti-Myc antibody coupled to agarose beads. Ubiquitination assay was performed with purified proteins in the presence of E1, E2 and purified GST-Ub. Boiled lysates, immunoprecipitated samples and samples from the ubiquitination assay were resolved on a 4-20% SDS gradient gel and blotted onto PVDF membrane. The membrane was incubated with the indicated primary antibodies and corresponding peroxidase-conjugated secondary antibodies followed by ECL detection. The asterisk marks non-specific binding of the antibody. B) Cartoon depicting the model of the ubiquitination and degradation of RhoBTB3.

3.2 Characterisation of MUF1/LRRC41, a binding partner of RhoBTB GTPases

To identify binding partners (and possible substrates) of RhoBTB3, a two hybrid screening on a mouse brain cDNA library was performed where RhoBTB3-B1B2C served as a bait. As a result, 1265 clones were reanalysed and 48 clones sequenced. One of the proteins identified in two hybrid screening was MUF1/LRRC41 (leucine rich repeat containing 41)

(S. Ramos, personal communication). MUF1, like RhoBTB proteins, is involved in processes linked to protein degradation (Kamura et al. 2001) therefore we decided to examine this protein more closely.

3.2.1 Computational characterisation of MUF1

In order to determine how MUF1 protein is conserved and widespread, similar proteins were identified by means of a BLAST search with mouse MUF1 protein sequence (GeneID 230654) as bait. 113 sequences were obtained and were individually examined. Each sequence was aligned with the bait MUF1 protein sequence using BLAST protein alignment programme. Many sequences were similar to the leucine-rich repeat region but the N-terminal part characteristic of MUF1 was missing. Shortened protein products, hypothetical proteins or MUF1-like proteins were excluded and figure 3.16 shows only these sequences that are complete. Full length protein sequences of MUF1 were obtained from following organisms: human (Hs), orang-utan (Pa), mouse (Mm), rat (Rn) and cow (Bt). As seen from figure 3.16., MUF1 is very highly conserved in mammals. Mm MUF1 is 97% identical and 98% similar to Rn MUF1. Mm MUF1 is 94% identical and 96% similar to Hs MUF1, Pa MUF1 and Bt MUF1. The blast search revealed also proteins similar to MUF1 that were predicted by automated computational analysis. These proteins shared significant similarity with Hs MUF1, but parts of the sequence were missing so they are not included in the alignment. Predicted proteins similar to MUF1 were found in following organisms: chimpanzee (*Pan troglodytes*), rhesus macaque (*Macaca mulatta*), dog (*Canis familiaris*), horse (*Equus cabalus*), opossum (*Monodelphis domestica*), platypus (*Ornithorhynchus anatinus*), chicken (*Gallus gallus*) and zebra finch (*Taeniopygia guttata*). Figure 3.16 also shows the position of the SOCS-box domain with the BC-box subdomain and the leucine-rich repeat region. To predict the subcellular localisation of MUF1, several programs were used. Two of them - SubLoc v1.0 and PSORT analysis identified MUF1 as a nuclear protein. With the latter one, three putative nuclear localisation signals (NLS) were identified at positions 287 (RRPR), 288 (RPRR) and 382 (PLKRFKR).

Figure 3.16 (next page): Alignment of MUF1 sequences. Protein sequences were aligned with ClustalX and edited with BioEdit. N terminally is the SOCS−box (A42-P71, marked in red frame) that contains the so-called BC-box (A45-V54, marked with a red arrow). Putative NLSs (nuclear localisation signals) were identified using PSORT programme at position 287 (RRPR), 288 (RPRR) and 382 (PLKRFKR) (marked in yellow). The leucine-rich repeat region is marked with a black arrow. Dashes indicate gaps introduced for optimal alignment. Identical residues are marked in grey, similar residues are marked in green. Hs: *Homo sapiens* GeneID 10489, Pa: *Pongo abelii* GeneID 100172869, Mm: *Mus musculus* GeneID 230654, Rn: *Rattus norvegicus* GeneID 362566, Bt*: Bos taurus* GeneID 337889.

```
                                                        ⟵        ⟶  BC-box (A45-V54)
HsMUF1  MAAPEAWRARSCWFCEVAAATTMEATSREAAPAKSSASGPNAPPALFELCGRAVSAHMGVLESGVWALPGPILQSILPLL  80
PaMUF1  MAAPEAWRARSCWFCEVAAATTMEATSREAAPAKSSASGPSAPPALFELCGRAVSAHMGVLESGVWALPGPILQSILPLL  80
MmMUF1  MAAPEAWRARSCWFCEVAAATTMEATSREAAPAKSSASGPSAPPALFELCGRAVSAHMGVLESGVWALPGPILQSILPLL  80
RnMUF1  MAAPEAWRARSCWFCEVAAATTMEATSREAAPAKSSASGPSAPPALFELCGRAVSAHMGVLESGVWALPGPILQSILPLL  80
BtMUF1  MAAPEAWRARSCWFCEVAAATTMEATSREAAPAKSSASGPSAPPALFELCGRAVSAHMGVLESGVWALPGPILQSILPLL  80


HsMUF1  NIYYLERIEETALKKGLSTQAIWRRLWDELMKTRPSSLESVTCWRAKFMEAFFSHVLRGTIDVSSDRRLCDQRFSPLLHS  160
PaMUF1  NIYYLERIEETALKKGLSTQAIWRRLWDELMKTRPSSLESVTCWRAKFMEAFFSHVLRGTIDVSSDRRLCDQRFSPLLHS  160
MmMUF1  NIYYLERIEETALKKGLSTQAIWRRLWDELMKTRPSSLESVTCWRAKFMEAFFSHVLRGTIDVSSDKRLCDQRFSPLLHS  160
RnMUF1  NIYYLERIEETALKKGLSTQAIWRRLWDELMKTRPSSLESVTCWRAKFMEAFFSHVLRGTIDVSSDKRLCDQRFSPLLHS  160
BtMUF1  NIYYLERIEETALKKGLSTQAIWRRLWDELMKTRPSSLESVTCWRAKFMEAFFSHVLRGTIDVSSDRRLCDQRFSPLLHS  160


HsMUF1  SRHVRQLTICNMLQGATELVAEPNRRVLETLASSLHTLKFRHLLFSDVAAQQSLRQLLHQLIHHGAVSQVSLYSWPVPES  240
PaMUF1  SRHVRQLTICNMLQGATELVAEPNRRVLETLASSLHTLKFRHLLFSDVAAQQSLRQLLHQLIHHGAVSQVSLYSWPVPES  240
MmMUF1  SRHVRQLTICNMLQGATELVAEPNRRVLETLASSLHTLKFRHLLFSDVAAQQSLRQLLHQLIHHGAVSQVSLYSWPVPES  240
RnMUF1  SRHVRQLTICNMLQGATELVAEPNRRVLETLASSLHTLKFRHLLFSDVAAQQSLRQLLHQLIHHGAVSQVSLYSWPVPES  240
BtMUF1  SRHVRQLTICNMLQGATELVAEPNRRVLETLASSLHTLKFRHLLFSDVAAQQSLRQLLHQLIHHGAVSQVSLYSWPVPES  240


HsMUF1  ALFILILTMSAGFWQPGPGGPPCRLCGEASRGRAPSRDEGSLLLGSRRPRRDAAERCAAALMASRRKSEAKQMPRAAPAT  320
PaMUF1  ALFILILTMSAGFWQPGPGGPPCRLCGEASRGRAPSRDEGSLLLGSRRPRRDAAERCAAALMASRRKSEAKQMPRAAPAA  320
MmMUF1  ALFILILTMSAGFWQPGPGSLPCRLCGEASRGRAPSRDEGSLLLGSRRPRRDAAERCAAALMATRRKSEVKQMPRAVPPT  320
RnMUF1  ALFILILTMSAGFWQPGPGSLPCRLCGEASRGRAPSRDEGSLLLGSRRPRRDAAERCAAALMATRRKSEVKQVPRALPTS  320
BtMUF1  ALFILILTMSAGFWQPGPGGPPCRLCGEASRGRAPSRDEGSLLLGSRRPRRDAAERCAAALMASRRKSEAKQTARAAPAT  320


HsMUF1  RVTRRSTQESLTAGGTDLKRELHPPATSHEAPGTKRSPSAPAATS--SASSSTSSYKRAPASSAPQPKPLKRFKRAAGKK  398
PaMUF1  RVTRRSTQESLTAGGTDLKRELHPPATSHEAPGTKRSPSAPAATS--SASSSTSSYKRAPASSAPQPKPLKRFKRAAGKK  398
MmMUF1  RVTRRSTQESLAIGGTDSK--LYLPATSYEASGTKQ-PSAPAA---ASA-SSSTSSKRAPASSASQPKPLKRFKRAAGKK  393
RnMUF1  RVTRRSTQESLTIGGTDSKRELYPPATSYEASGTKQ-PSS-APT--A-A-SSSTSSKRAPASSVSQPKPLKRFKRATGKK  394
BtMUF1  RVTRRSTQESLTAGGTDSKREPLPPATSHEAPGTKRPPSAPATTSSASASSSTSSKRAPASSAPQPKPLKRFKRAAGKK  400

                            LRR ⟵─────────────────────────────────────────────────⟶
HsMUF1  GARTRQGPGAESEDLYDFVFIVAGEKEDGEEMEIGEVACGALDGSDPSCLGLPALEASQRFRSISTLELFTVPLSTEAAL  478
PaMUF1  GARTRQGPGAESEDLYDFVFIVAGEKEDGEEMEIGEVACGALDGSDPSCLGLPALEASQRFRSISTLELFTVPLSTEAAL  478
MmMUF1  GPRTRQGSGAESEDLYDFVFIVAGEKEDGEEMEIGEVACGALDGSDPSCLGLPALEASQRFRSISTLELFTVPLSTEAAL  473
RnMUF1  GPRTRQGSGAESEDLYDFVFIVAGEKEDGEEMEIGEVACGALDGSDPSCLGLPALEASQRFRSISTLELFTVPLSTEAAL  474
BtMUF1  GARTRQGCGAESEDLYDFVFIVAGEKEDGEEMEIGEVACGALDGSDPSCLGLPALEASQRFRSISTLELFTVPLSTEAAL  480

        ⟵──────────────────────────────────────────────────────────────────────────⟶
HsMUF1  TLCHLLSSWVSLESLTLSYNGLGSNIFRLLDSLRALSGQAGCRLRALHLSDLFSPLPILELTRAIVRALPLLRVLSIRVD  558
PaMUF1  TLCRLLSSWVSLESLTLSFNGLGSNIFRLLDSLRALSGQAGCRLRALHLSDLFSPLPILELTRAIVRALPLLRVLSIRVD  558
MmMUF1  TLCHLLSSWVSLESLTLSYNGLGSNIFRLLDSLRALSGQAGCRLRALHLSDLFSPLPILELTRAIVRALPLLRVLSIRVD  553
RnMUF1  TLCHLLSSWVSLESLTLSYNGLGSNIFRLLDSLRVLSGQAGCRLRALHLSDLFSPLPILELTRAIVRALPLLRVLSIRVD  554
BtMUF1  TLCHLLSSWVSLESLTLSYNGLGSNIFRLLDSLRALSVQAGCRLRALHLSDLFSPLPILELTRAIVRALPLLRVLSIRVD  560

        ⟵──────────────────────────────────────────────────────────────────────────⟶
HsMUF1  HPSQRDNPGVPGNAGPPSHIIGDEEIPENCLEQLEMGFPRGAQPAPLLCSVLKASGSLQQLSLDSATFASPQDFGLVLQT  638
PaMUF1  HPSQRDNPGVPGNAGPPSHIIGDEEIPENCLEQLEMGFPRGAQPAPLLCSVLKASGSLQQLSLDSATFASPQDFGLVLQT  638
MmMUF1  HPSQRDNPAVPENAGPPGHIVGDEEIPENCLEQLEMGFPRGAQPAPLLCSVLKASGSLQQLSLDSATFASPQDFGLVLQT  633
RnMUF1  HPSQRDNPAVPENAGPPGHIIGDEEIPENCLEQLEMGFPRGAQPAPLLCSVLKASGSLQQLSLDSATFASPQDFGLVLQT  634
BtMUF1  HPSQRDNPAVPGNAGPPSNVIGDEEIPENCLEQLEMGFPRGAQPAPLLCSVLKASGSLQQLSLDSATFASPQDFGLVLQT  640

        ⟵──────────────────────────────────────────────────────────────────────────⟶
HsMUF1  LKEYNLALKRLSFHDMNLADCQSEVLFLLQNLTLQEITFSFCRLFEKRPAQFLPEMVAAMKGNSTLKGLRLPGNRLGNAG  718
PaMUF1  LKEYNLALKRLSFHDMNLADCQSEVLFLLQNLTLQEITFSFCRLFEKRPAQFLPEMVAAMKGNSTLKGLRLPGNRLGNAG  718
MmMUF1  LKEHNLSLKRLSFHDMNLADCQSEVLFLLKNLTLQEITFSFCRLFEKRPVQFLPEMVAAMKGNSTLKGLRLPGNRLGNAG  713
RnMUF1  LKEYNLSLKRLSFHDMNLADCQSEVLFLLKNLTLQEITFSFCRLFEKRPAQFLPEMVAAMKGNSTLKGLRLPGNRLGNAG  714
BtMUF1  LKEYNLTLKRLSFHDMNLADCQSEVLFLLQNLTLQEITFSFCRLFEKRPAQFLPEMVAAMKGNSTLKGLRLPGNRLGNAG  720

        ⟵──────────────────────────────────────────────────────────────────────────⟶
HsMUF1  LLALADVFSEDSSSSLCQLDISSNCIKPDGLLEFAKRLERWGRGAFGHLRLFQNWLDQDAVTAREAIRRLRATCHVVSDS  798
PaMUF1  LLALADVFSEDSSSSLCQLDISSNCIKPDGLLEFAKRLERWGRGAFGHLRLFQNWLDQDAVTAREAIRRLRATCHVVSDS  798
MmMUF1  LLALADVFSEDSSSSLCQLDISSNCIKPDGLLEFAKRLERWGRGAFGHLRLFQNWLDQDAVTAREAIRRLRATCHVVSDS  793
RnMUF1  LLALADVFSEDSSSSLCQLDISSNCIKPDGLLEFAKRLERWGRGAFGHLRLFQNWLDQDAVTAREAIRRLRATCHVVSDS  794
BtMUF1  LLALADVFSEDSSSSLCQLDISSNCIKPDGLLEFAKRLERWGRGAFGHLRLFQNWLDQDAVTAREAIRRLRATCHVVSDS  800

        ⟵───────────────⟶
HsMUF1  WDSSQAFADYVSTM  812
PaMUF1  WDSSQAFADYVSTM  812
MmMUF1  WDSTQAFADYVSTM  807
RnMUF1  WDSTQAFADYVSTM  808
BtMUF1  WDSSQAFADYVSTM  814
```

3.2.2 *Lrrc41* mRNA is ubiquitously expressed

To examine the expression profile of *Lrrc41* in mouse, RT-PCR was performed. As a template RNA isolated from various mouse tissues was used. The position of the *Lrrc41* primers for RT-PCR relative to the *Lrrc41* gene is shown in figure 3.17B. The primers were designed in a way that they amplified a 690 bp fragment only from cDNA and not from genomic DNA. Figure 3.17A shows that *Lrrc41* was expressed in all the tissues tested with the exception of skeletal muscle. The highest expression level was observed in testis. Other tissues expressing *Lrrc41* were brain, heart, liver and lung. This data support previous observations that human *LRRC41* is also ubiquitously expressed (Kopp 2006 diploma thesis).
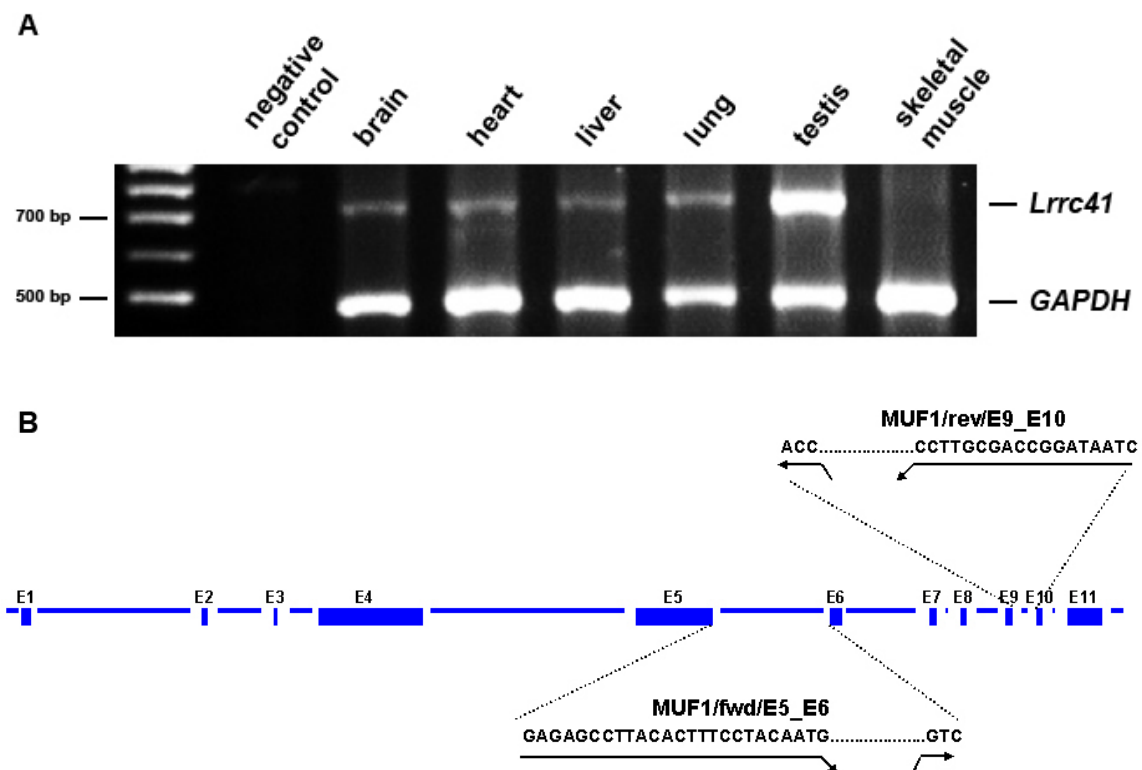
Figure 3.17: Expression of *Lrrc41*. A) RNA isolated from the indicated mouse tissues was reverse transcribed into cDNA and amplified with specific primers sitting on intron/exon boundaries. A 436 bp fragment of the housekeeping gene GAPDH was amplified simultaneously and was used as a positive control. Samples were tested on an agarose gel. B) Cartoon depicting the position of the primers.

3.2.3 Localisation of MUF1

To examine the subcellular localisation of MUF1, MUF1 GFP-fusion proteins (see figure 3.18) were expressed in COS7 cells and their localisation was examined using florescence microscopy. GFP-MUF1, GPF-MUF1(L46P,C50F) and GFP-MUF1ΔSOCS localised

almost solely to the nucleus (85.5% to 94.5% of cells), in some cases they could be found in both cytoplasm and nucleus (5% to 13.3%) and only a very small fraction of the transfected cells showed exclusively cytoplasmic localisation (1.2% and less). GFP-MUF1-LRR does not contain any putative NLS and in 86.6% of the cells this fusion protein localised in both cytoplasm and nucleus. 2.6% of the cells showed only nuclear localisation of GFP-MUF1-LRR and in 8.8% cells only cytoplasmic localisation (Figure 3.19).
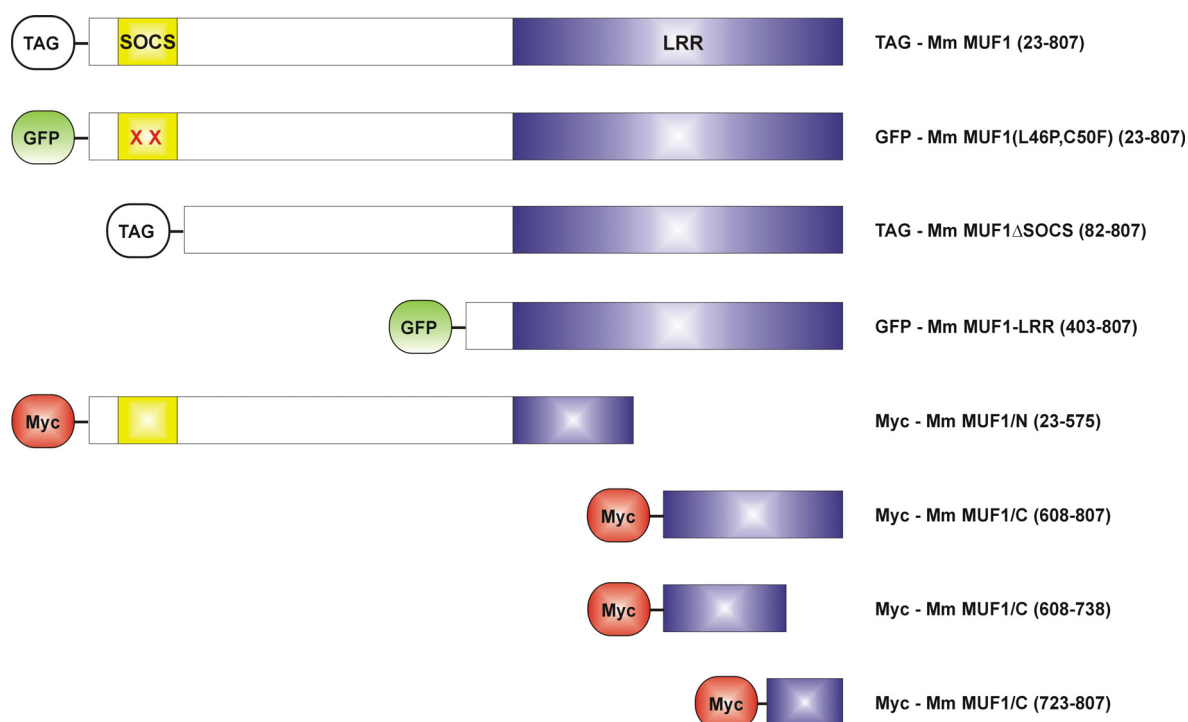
Figure 3.18: Domain architecture of MUF1 protein and constructs used in this study. Where the tag is not specified, different tags were used (GFP, Flag, Myc) as specified in the corresponding experiment. SOCS: SOCS (suppressor of cytokine signalling) box domain, LRR: leucine-rich repeat domain. GFP-MUF1(L46P,C50F) is full length protein containing two point mutations within SOCS-box that abolish interaction with Cul5. GFP-MUF1ΔSOCS has deleted the entire SOCS box.

Figure 3.19 (next page): GFP-MUF1 localises to the nucleus and requires the putative NLSs for nuclear targeting. COS7 cells were transfected with the indicated GFP-tagged MUF1 constructs. Transfected cells were fixed with paraformaldehyde and stained with the DNA dye DAPI. Images were acquired with a confocal microscope. Bar represents 10 μm. For statistic evaluation, approximately 1000 cells were scored for each sample. The graph shows average and standard deviation of two independent experiments.

GFP-MUF1

Merge

GFP-MUF1(L46P,C50F)

GFP-MUF1ΔSOCS

GFP-MUF1-LRR

GFP vector

Nuclear
Nuclear and cytoplasmic
Cytoplasmic

GFP-MUF1

GFP-MUF1(L46P,C50F)

GFP-MUF1ΔSOCS

GFP-MUF1-LRR

GFP

% cells
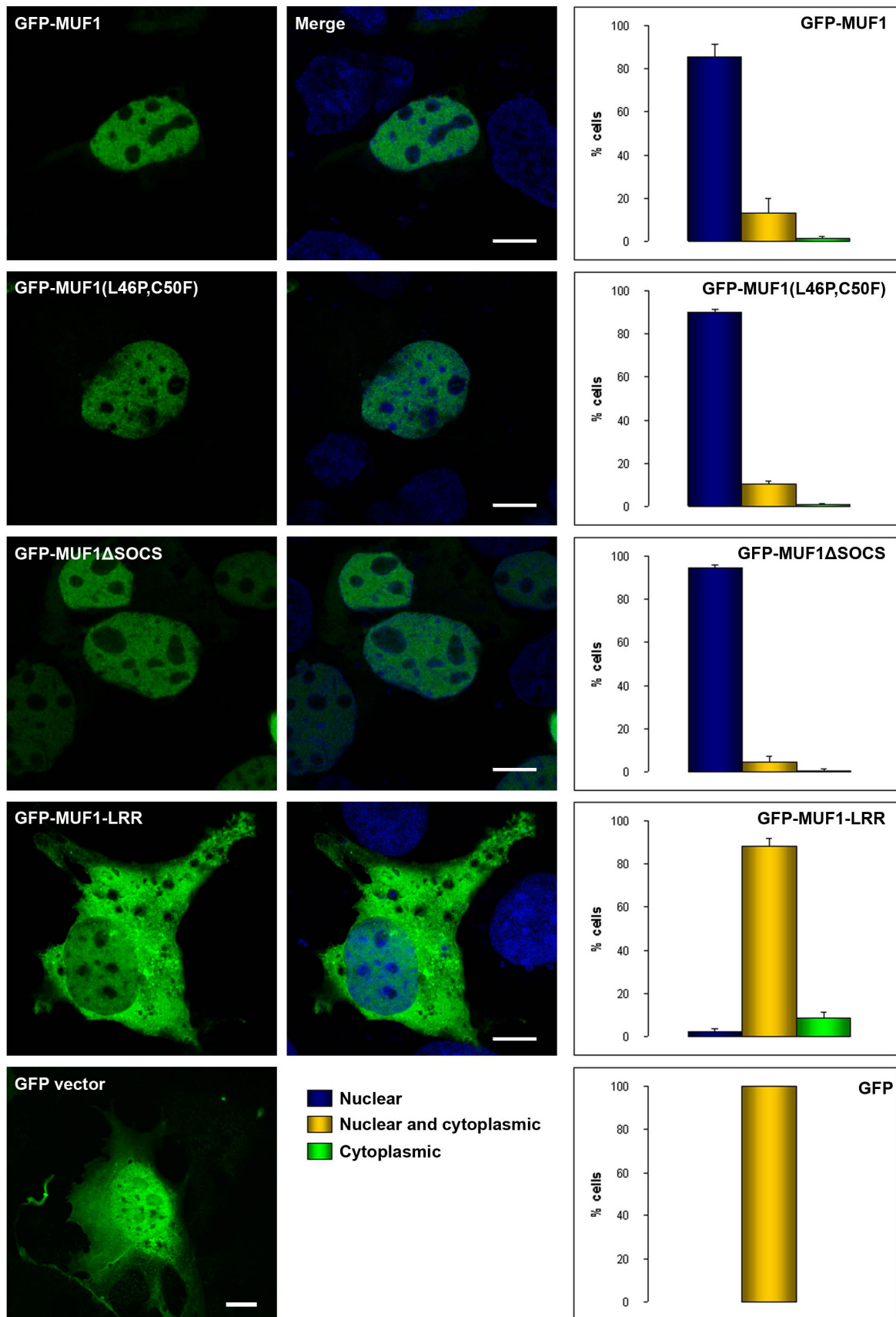
To support these results, subcellular fractionation was performed. As expected, GFP-MUF1-LRR was found in the nuclear and cytoplasmic fractions. GFP-MUF1, GPF-MUF1(L46P,C50F) and GFP-MUF1ΔSOCS were found in the nuclear fraction and surprisingly, also in a membranous fraction. The possible explanation for this phenomenon could be that because staining with anti-emerin antibody showed signal not only in nuclei fraction, but also in the membranous fraction, possibly there was some contamination of membranous fraction with nuclei (Figure 3.20).
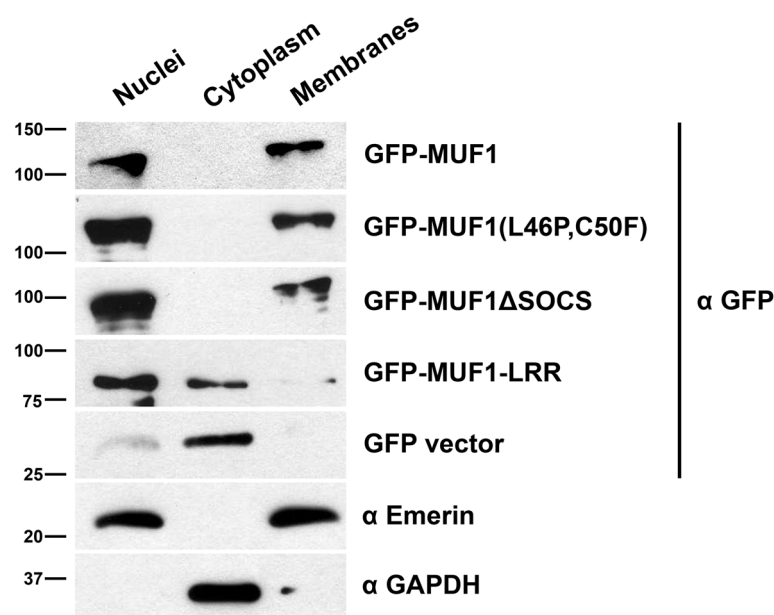
Figure 3.20: GFP-MUF1 localises to the nucleus and requires the putative NLSs for nuclear targeting. COS7 cells were transfected with indicated GFP-tagged MUF1 constructs. Cell lysates were separated into nuclear, cytosolic and membranous fractions by centrifugation and analysed by Western blotting. Blots were probed with anti-GFP antibody. Ratio of nuclear : cytoplasmic : membranous fraction is 1:0.5:2. MUF1, MUF1(L46P,C50F) and MUF1ΔSOCS were found in nuclear and membranous fractions. MUF1-LRR was found in nuclear and cytosolic fractions. An empty GFP vector was used as a control. Anti-emerin antibody was used as a marker for the nuclear fraction and anti-GAPDH antibody as a marker for the cytosolic fraction.

Because GFP is a bulky tag, it may be affecting the cellular localisation of GFP-MUF1. To confirm the subcellular localisation of MUF1 with another tag, we generated an expression vector with the I-Plastin (IPl) tag. This tag consists of the 18 N-terminal amino acids of I-Plastin (IPl) sequence, for which a polyclonal antibody is available in our laboratory. A MUF1 construct with an N-terminal IPl-tag was prepared and DNA was transfected into COS7 cells. Fixed cells were immunostained with anti-I-Plastin antibody. Consistent with previous results, IPl-MUF1 localised predominantly in the nucleus indicating that GFP did

not affect the distribution of the GFP fusions and that the endogenous protein is most probably predominantly nuclear (Figure 3.21).

Nuclear
Nuclear and cytoplasmic
Cytoplasmic

Figure 3.21: Subcellular localisation of MUF1. COS7 cells were transfected with IPl-tagged MUF1 or with empty vector with IPl-tag. Transfection with the empty plasmid served as a control to show that the I-Plastin antibody does not recognise any cellular structure. Transfected cells were fixed with paraformaldehyde and immunostained with I-Plastin antibody followed by Alexa Fluor 568-coupled secondary antibody. Nuclei were stained with the DNA dye DAPI. Images were acquired with a conventional fluorescence microscope. Bar represents 10 μm (B,D) and 100 μm (A,C). For statistic evaluation, approximately 1000 cells were scored. The graph shows average and standard deviation of two independent experiments.

3.2.4 MUF1 interacts with all three RhoBTB proteins *in vivo*

To confirm that MUF1 interacts with RhoBTB3 *in vivo*, a series of co-immunoprecipitation experiments were performed. 293T HEK cells were transfected with MUF1 and RhoBTB1, 2 or 3. Co-immunoprecipitation was performed with anti-Myc antibody coupled to magnetic beads. Immunoprecipitates and lysates were analysed for the presence of the indicated tagged proteins by Western blotting. In a first experiment Myc-

MUF1 and Flag-RhoBTB1, 2 and 3 were used. Figure 3.22A shows that Myc-MUF1 specifically co-immunoprecipitated all three RhoBTB proteins. To confirm this result, the experiment was repeated with swapped tags. Myc-RhoBTB2 and Myc-RhoBTB3 co-immunoprecipitated Flag-MUF1. Interestingly, Myc-RhoBTB1 did not co-immunoprecipitate Flag-MUF1 (Figure 3.22B). It is possible that RhoBTB1 binds to MUF1 with lower affinity than RhoBTB2 and RhoBTB3. We performed a co-immunoprecipitation experiment using low stringency lysis and washing conditions. However, unspecific binding of Flag-MUF1 was observed (Figure 3.22C). The observation that Myc-RhoBTB1 did not co-immunoprecipitate Flag-MUF1 was very surprising and contradictory to the observation that Myc-MUF1 co-immunoprecipitated Flag-RhoBTB1. A possible explanation for this is that there might be some alterations in protein folding due to the tag that abolish protein interactions. In conclusion, these results demonstrate that all three RhoBTB proteins interact with MUF1 *in vivo*.

Because RhoBTB3 is a cytoplasmic protein (Berthold et al. 2008b) and MUF1 localises predominantly to the nucleus (see section 3.2.3), it was of great interest to examine their mutual localisation in mammalian cells. COS7 cells were co-transfected with Flag-RhoBTB3 and GFP-MUF1 constructs. Interestingly, when GFP-tagged MUF1 proteins and Flag-RhoBTB3 were co-expressed, GFP-tagged MUF1 proteins retained partially in the cytoplasm where they co-localise with Flag-RhoBTB3 in a paranuclear cluster (Figure 3.23). Figure 3.23 shows only co-localisation of GFP-MUF1 and GFP-MUF1-LRR with Flag-RhoBTB3. GFP-MUF1(L46P,C50F) and GFP-MUF1ΔSOCS behaved similarly to GFP-MUF1 (only statistic data are shown).

Figure 3.22: Interaction of MUF1 with RhoBTB proteins. 293T HEK cells were transfected with the indicated MUF1 and either RhoBTB1, RhoBTB2 or RhoBTB3. Empty Myc or Flag vectors were used as controls. Protein complexes were immunoprecipitated with anti-Myc antibody coupled to magnetic beads. Boiled lysates or immunoprecipitated samples were resolved on 10% SDS gels and blotted onto PVDF membrane. The membrane was incubated with the indicated primary antibodies and corresponding peroxidase-conjugated secondary antibodies followed by ECL detection. A) Interaction of Myc-MUF1 and Flag-RhoBTB1/2/3, high stringency lysis and washing conditions. B) Interaction of Flag-MUF1 and Myc-RhoBTB1/2/3, high stringency lysis and washing conditions. C) Interaction of Flag-MUF1 and Myc-RhoBTB1/2/3, low stringency lysis and washing conditions. Asterisk marks non-specific binding of the antibody.

Figure 3.23: MUF1 retains in the cytoplasm in a RhoBTB3-dependent manner. COS7 cells were transfected with GFP-tagged MUF1 constructs and Myc-RhoBTB3, fixed and immunostained with anti-Flag (anti-ECS) antibody. Nuclei were visualised with DAPI. Images were acquired with a confocal laser scanning microscope and overlaid. RhoBTB3 caused MUF1 to be partially retained in the cytoplasm in a paranuclear pattern where they co-localised. Only MUF1 and MUF1-LRR are shown here as an example. The graphs show average and standard deviation of two independent experiments. Scale represents 10 μm. For statistic evaluation, approximately 1000 cells were scored in two independent experiments. Compare with the localisation of the same constructs in the absence of RhoBTB3 (Figure 3.19). Note that the effect of RhoBTB3 does not require the presence of the SOCS-box.

3.2.5 RhoBTB3 has probably multiple binding sites on MUF1

To identify the binding site of RhoBTB3 within MUF1 protein, different shortened MUF1 constructs were used (Figure 3.18). 293T HEK cells were co-transfected with Flag-RhoBTB3-FL and one of the Myc-MUF1 C-terminal constructs. Myc-MUF1/C (609-807AA) contains the MUF1 sequence that was identified in the two-hybrid screening. Myc-MUF1/C (609-735) and Myc-MUF1/C (724-807) constructs were used to narrow down the interaction. Co-immunoprecipitation was performed with anti-Myc antibody coupled to magnetic beads. Immunoprecipitates and lysates were analysed for the presence of the indicated tagged proteins by Western blotting. Figure 3.24A shows that all three C-terminal Myc-tagged proteins co-immunoprecipitated Flag-RhoBTB3. Apparently, binding to RhoBTB3 occurs through multiple binding sites.

To examine if also the N-terminal part of MUF1 can bind to RhoBTB3, 293T HEK cells were co-transfected with Flag-RhoBTB3 and Myc-MUF1/N. Co-immunoprecipitation was performed with anti-Myc antibody coupled to magnetic beads. Immunoprecipitates and lysates were analysed for the presence of the indicated tagged proteins by Western blotting. Surprisingly, the N-terminal part of MUF1 also co-immunoprecipitated Flag-RhoBTB3 (Figure 3.24B). This observation can be explained by the fact that this N-terminal fusion protein contains also part of the leucine-rich repeat region (131 amino acids) that is a well known motif for mediating protein-protein interactions (Bella et al. 2008).
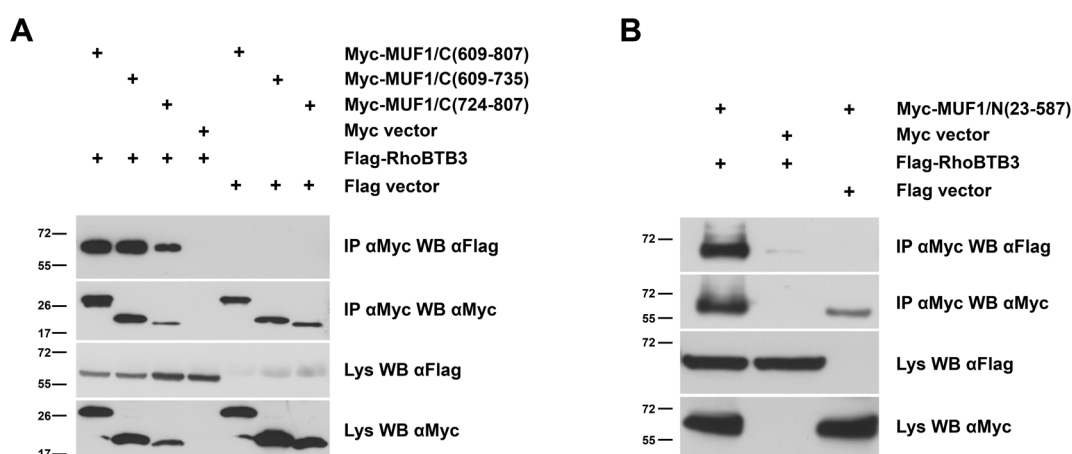
Figure 3.24: Myc-MUF1/N and Myc-MUF1/C co-immunoprecipitate RhoBTB3. 293T HEK cells were transfected with Flag-RhoBTB3 or empty Flag vector and the indicated Myc-tagged MUF1 constructs or empty Myc vector as a control. Protein complexes were immunoprecipitated with anti-Myc antibody coupled to magnetic beads. Boiled lysates or immunoprecipitated samples were resolved on 10% SDS gel and blotted onto PVDF membrane. The membrane was incubated with the indicated primary antibodies and corresponding peroxidase-conjugated secondary antibodies followed by ECL detection. A) Interaction of C-terminal fragments of MUF1 and RhoBTB3. B) Interaction of N-terminal fragment of MUF1 and RhoBTB3.

3.2.6 MUF1 has probably multiple binding sites on RhoBTB3

To map the binding of MUF1 on RhoBTB3, co-immunoprecipitation experiments were performed using different GFP-tagged RhoBTB3 constructs (Figure 3.2). 293T HEK cells were co-transfected with Myc-MUF1 and GFP-tagged RhoBTB3 deletion constructs. Co-immunoprecipitation was performed with anti-GFP antibody coupled to magnetic beads. Immunoprecipitates and lysates were analysed for the presence of the indicated tagged proteins by Western blotting.

In the first experiment, 293T HEK cells were co-transfected with Myc-MUF1 and GFP-RhoBTB3-GTPase or GFP-RhoBTB3-PB1B2C. Figure 3.25A shows that both GFP-RhoBTB3-GTPase and GFP-RhoBTB3-PB1B2C co-immunoprecipitated Myc-MUF1, although the interaction between RhoBTB3-PB1B2C and MUF1 seemed to be stronger.

To further map the binding of MUF1 on RhoBTB3-PB1B2C, 293T HEK cells were co-transfected with Myc-MUF1 and GFP-RhoBTB3-B1, GFP-RhoBTB3-B2 or GFP-RhoBTB3-C. Figure 3.25B shows that all three GFP-tagged RhoBTB3 proteins co-immunoprecipitated Myc-MUF1. This result indicates that MUF1 might have multiple binding sites on RhoBTB3.
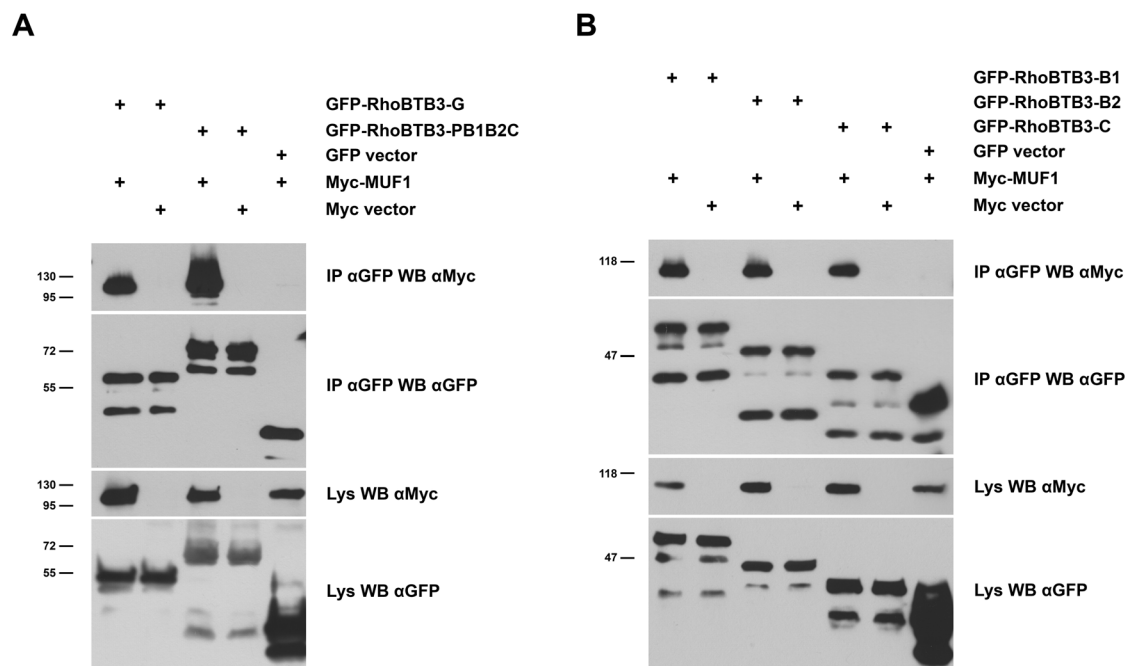
Figure 3.25: Interaction of MUF1 with different domains of RhoBTB3. 293T HEK cells were transfected with Myc-MUF1 or empty Myc vector and indicated GFP-tagged RhoBTB3 constructs or empty GFP vector as a control. Protein complexes were immunoprecipitated with anti-GFP antibody coupled to magnetic beads. Boiled lysates or immunoprecipitated samples were resolved on 10% SDS gel and blotted onto PVDF membrane. The membrane was incubated with the indicated primary antibodies and corresponding peroxidase-conjugated secondary antibodies followed by ECL detection. A) Interaction of MUF1 with RhoBTB3-GTPase and RhoBTB3-PB1B2C. B) Interaction of MUF1 with RhoBTB3-B1, RhoBTB3-B2 and RhoBTB3-C.

3.2.7 MUF1 interacts with RhoBTB3 in a Cul3 and Cul5 independent manner

As already mentioned in the introduction (see section 1.4.3), the first BTB domain of RhoBTB3 interacts with Cul3 (Berthold et al. 2008b) and MUF1 binds Cul5 through the SOCS box domain (Kamura et al. 2001). To rule out that RhoBTB3 binds MUF1 indirectly through possible heterodimerisation of Cul3 and Cul5 (see section 3.2.11), a RhoBTB3 mutant that does not bind Cul3 and a MUF1 mutant that does not bind Cul5 were prepared and their interaction was examined.

First, a RhoBTB3 mutated in one residue (histidine 270) within first BTB domain was prepared (H270L). This histidine residue was chosen because it is necessary for interaction of the BTB/POZ domain protein Btb3p with *S. pombe* Cul3 (Pcu3p) (Geyer et al. 2003) and is also present in the first BTB domain of RhoBTB3. To test whether this point mutation is sufficient to abolish Cul3 interaction with RhoBTB3, 293T HEK cells were transfected with Flag-Cul3 and either Myc-RhoBTB3 or Myc-RhoBTB3(H270L). Co-immunoprecipitation was performed with anti-Myc antibody coupled to magnetic beads. Immunoprecipitates and lysates were analysed for the presence of the indicated tagged proteins by Western blotting. Figure 3.26 shows that while Myc-RhoBTB3 still co-immunoprecipitated Flag-Cul3, Myc-RhoBTB3(H270L) did not. The single point mutation H270L localised in the first BTB domain is therefore sufficient to abolish interaction of RhoBTB3 with Cul3.
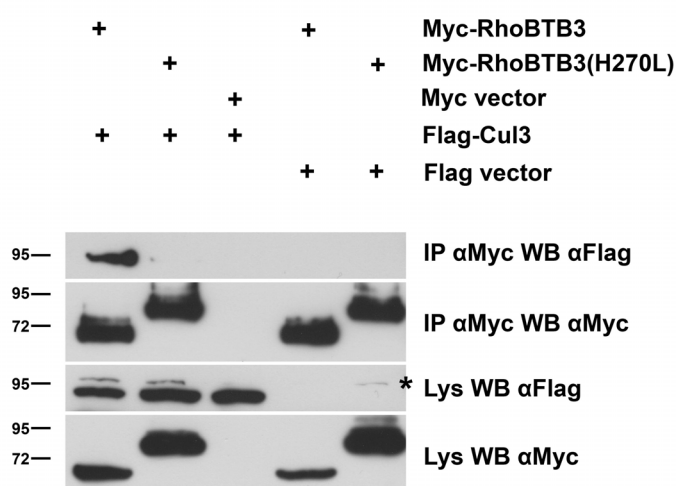
Figure 3.26: RhoBTB3(H270L) mutant does not bind Cul3. HEK 293T cells were transfected with Flag-Cul3 or empty Flag vector and either Myc-RhoBTB3, Myc-RhoBTB3-H270L or empty Myc vector. Protein complexes were immunoprecipitated with anti-Myc antibody coupled to magnetic beads. Boiled lysates or immunoprecipitated samples were resolved on 10% SDS gel and blotted onto PVDF membrane. The membrane was incubated with the indicated primary antibodies and corresponding peroxidase-conjugated secondary antibodies followed by ECL detection. Asterisk marks non-specific binding of the antibody.

Second, a MUF1 construct with deleted SOCS box domain was prepared to prevent binding of MUF1 to Cul5. 293T HEK cells were transfected with Flag-MUF1ΔSOCS and Myc-RhoBTB3(H270L). As a positive control, cells were transfected with Flag-MUF1 and Myc-RhoBTB3. Co-immunoprecipitation was performed with anti-Myc antibody coupled to magnetic beads. Immunoprecipitates and lysates were analysed for the presence of the indicated tagged proteins by Western blotting. Myc-RhoBTB3(H270L) was still able to co-immunoprecipitate Flag-MUF1ΔSOCS (Figure 3.27). This result shows that the interaction of RhoBTB3 and MUF1 is not mediated by a possible dimerisation of Cul3 and Cul5, which is addressed below (see section 3.2.11).
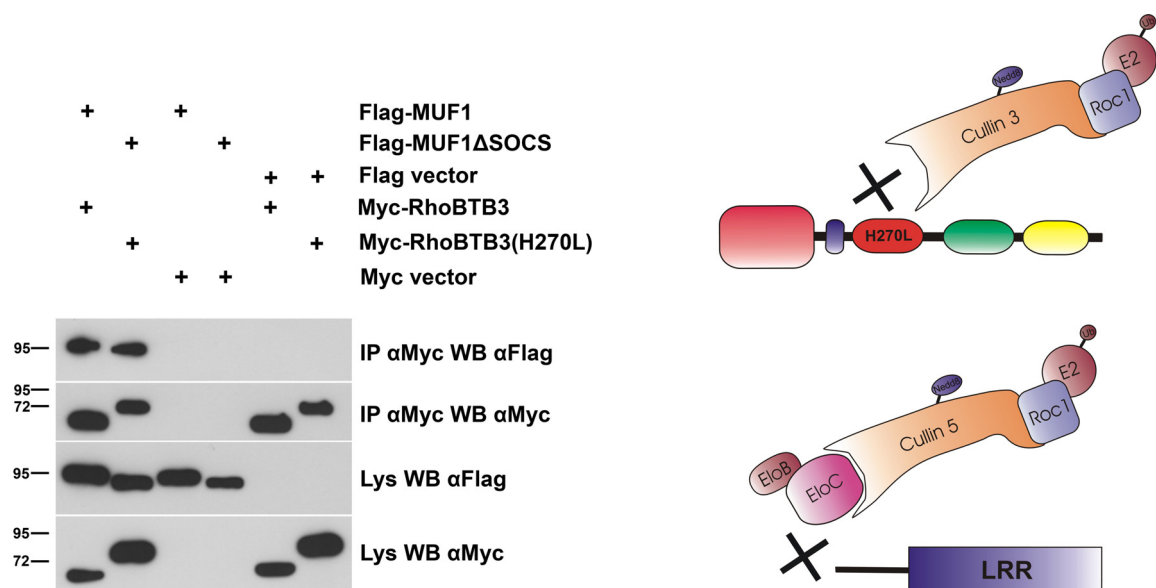
Figure 3.27: MUF1 interacts with RhoBTB3 in a Cul3 and Cul5 independent manner. HEK 293T cells were transfected with Myc-RhoBTB3(H270L) or empty Myc vector and Flag-MUF1-ΔSOCS or empty Flag vector. As positive control, cells were co-transfected with Myc-RhoBTB3 and Flag-MUF1. Protein complexes were immunoprecipitated with anti-Myc antibody coupled to magnetic beads. Boiled lysates or immunoprecipitated samples were resolved on 10% SDS gel and blotted onto PVDF membrane. The membrane was incubated with the indicated primary antibodies and corresponding peroxidase-conjugated secondary antibodies followed by ECL detection. The cartoon on the right hand side represents RhoBTB3-H270L and MUF1ΔSOCS that are not able to bind to their corresponding cullins.

3.2.8 MUF1 is degraded in the proteasome in a Cul5 independent manner

The observation that MUF1 interacts with RhoBTB proteins raised the question of the relationship between these two proteins in cullin-multiprotein complexes. We envisioned two possible models: a) MUF1 is ubiquitinated by a Cul3 complex dependent on RhoBTB, which acts as the substrate specific adaptor; b) RhoBTB is ubiquitinated by a Cul5 complex dependent on MUF1, which acts as the substrate specific adaptor. To test

this hypothesis, a half life experiment was performed (see section 2.3.5). 293T HEK cells were transfected with Myc-MUF1ΔSOCS and GFP-RhoBTB3 or Myc-RhoBTB3(H270L) and GFP-MUF1. Lysates were collected at several time points and analysed for the presence of the tagged proteins by Western blotting. Figure 3.28A shows that Myc-MUF1ΔSOCS was very fast degraded in the presence of GFP-RhoBTB3. Addition of the proteasomal inhibitor MG132 stabilised MUF1ΔSOCS, confirming that degradation is proteasomal specific. When co-expressed with GFP, no significant degradation of MUF1ΔSOCS was observed. MUF1ΔSOCS lacks the SOCS-box that mediates interaction with Cul5 therefore this degradation is Cul5-independent and occurs probably through Cul3 by binding to RhoBTB3. To mediate this effect, the C-terminal part of RhoBTB3 (B1B2C) is sufficient (data not shown). As shown above (see section 3.2.7), Myc-RhoBTB3(H270L) did not bind Cul3. Figure 3.28B shows that although RhoBTB3(H270L) was also degraded, this effect was clearly less dramatic as it was for MUF1ΔSOCS. Degradation of RhoBTB3(H270L) is not enhanced in the presence of MUF1. To conclude, these experiments provide evidence that MUF1 is degraded in the proteasome in a Cul5 independent manner probably by Cul3-RhoBTB3 ligase complex.
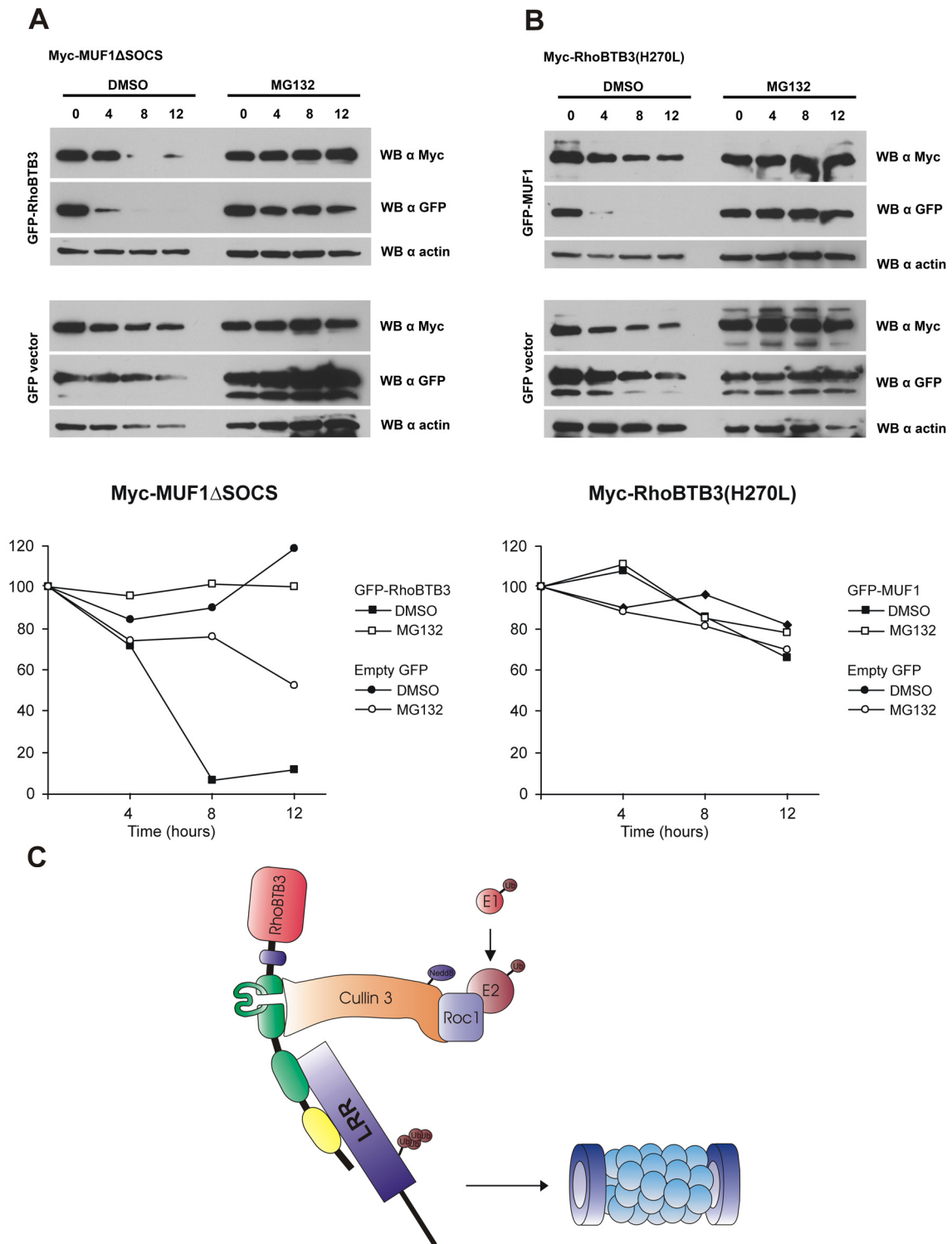
Figure 3.28: MUF1 is degraded in the proteasome by Cul3-RhoBTB3 ligase complex. 293T HEK cells were transfected with indicated plasmids. 16 h after transfection cells were split and treated with 100 μM cycloheximide and either with 10 μM MG132 or DMSO. At the time points 0, 4, 8 and 12h cells were collected and lysed. Lysates were tested on 10% SDS gel and blotted onto PVDF membrane. The membrane was probed with indicated primary antibodies and corresponding peroxidase-conjugated secondary antibodies followed by ECL detection. Actin staining served as a loading control. The graphs show the amount of the GFP fusion protein normalised to the amount of actin and expressed as percentage relative to the 0 time point. A) Cells were co-transfected with Myc-MUF1ΔSOCS and either GFP-RhoBTB3 or empty GFP vector as a control. B) Cells were co-transfected with Myc-RhoBTB3(H270L) and either GFP-MUF1 or empty GFP vector. C) Cartoon depicting possible relationship between MUF1 and RhoBTB3 in Cul3-dependent complex. RhoBTB3 is a substrate specific adaptor that targets MUF1 for proteasomal degradation.

3.2.9 MUF1 is able to homodimerise

Proteins containing a leucine-rich repeats form very often homo- and heterodimers or even larger assemblies like tetramers (Bella et al. 2008). To examine if MUF1 is also able to build homodimers, Flag-MUF1 and Myc-MUF1 were co-transfected into 293T HEK cells. Co-immunoprecipitation was performed with anti-Myc antibody coupled to magnetic beads. Immunoprecipitates and lysates were analysed for the presence of the indicated tagged proteins by Western blotting. Figure 3.29 shows that Myc-MUF1 co-immunoprecipitated Flag-MUF1. To prove that this homodimerisation was not mediated by interaction with Cul5, Flag-MUF1ΔSOCS was also used. This shorter protein did not bind Cul5 (Kamura et al. 2001). Figure 3.29 shows that Myc-MUF1 also co-immunoprecipitated Flag-MUF1ΔSOCS, therefore homodimerisation of MUF1 is not mediated by Cul5.
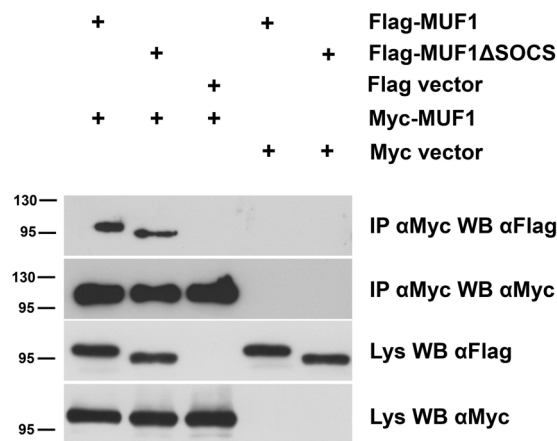
Figure 3.29: Homodimerisation of MUF1. HEK 293T cells were transfected with Myc-MUF1 and either Flag-MUF1 or Flag-MUF1ΔSOCS. Empty Myc or Flag vectors were used as a control. Protein complexes were immunoprecipitated with anti-Myc antibodies coupled to magnetic beads. Boiled lysates or immunoprecipitated samples were resolved on 10% SDS gel and blotted onto PVDF membrane. The membrane was incubated with the indicated primary antibodies and corresponding peroxidase-conjugated secondary antibodies followed by ECL detection.

3.2.10 Characterisation of MUF1 interaction with potential binding partners

To understand the function of MUF1 protein, it is of a great interest to identify possible interaction partners. Large scale screenings that reveal a list of protein-protein interactions constitute a great help to study this issue. Stelzl et al. (2005) performed large scale yeast two-hybrid screening and identified MyoIXb as an interaction partner of MUF1 with a score medium confidence of interaction. Another large scale screenings revealed RBPMS protein as a potential binding partner of MUF1 (Rual et al. 2005).

3.2.10.1 MyoIXb as a potential binding partner of MUF1

Myosins are molecular motors that convert chemical energy stored in ATP into direct mechanical force along actin filaments. Human myosin IXb is an unconventional myosin that comprises a RhoGAP (RhoGTPase-activating protein) domain (Reinhard et al. 1995). MyoIXb exhibits increased GAP activity for Rho proteins (Müller et al. 1997) and is recruited to the extending lamellipodia, ruffles and filopodia where it acts as a motorised RhoGAP molecule (van den Boom et al. 2007).

To verify the possible interaction between MUF1 and MyoIXb, co-immunoprecipitation analysis was performed. 293T HEK cells were transfected with MyoIXb-Flag and Myc-MUF1. One sample transfected with Flag-MUF1 and Myc-RhoBTB3 was used as a positive co-immunoprecipitation control. Co-immunoprecipitation was performed with anti-Myc antibody coupled to magnetic beads. Immunoprecipitates and lysates were analysed for the presence of the indicated tagged proteins by Western blotting. No interaction of MyoIXb and MUF1 was observed despite the fact that co-immunoprecipitation of MUF1 with RhoBTB3 was successful (Figure 3.30).
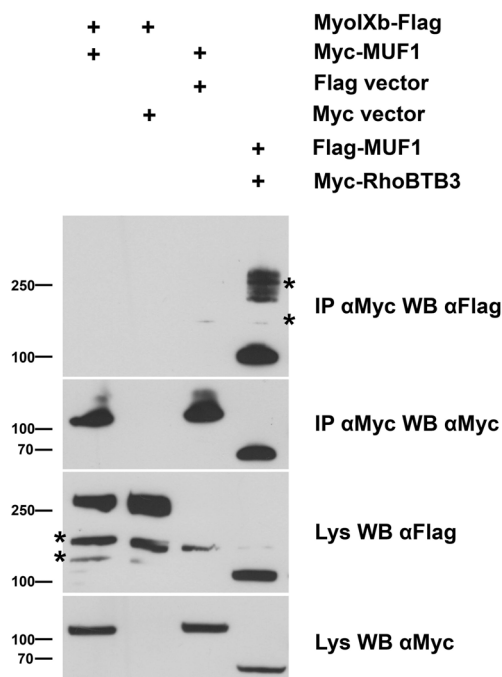
Figure 3.30: MUF1 does not co-immunoprecipitate MyoIXb. 293T HEK cells were transfected with MyoIXb-Flag and Myc-MUF1 or with the corresponding empty vectors as a negative control. Flag-MUF1 and Myc-RhoBTB3 co-transfection was used as a positive control. Protein complexes were immunoprecipitated with anti-Myc antibody coupled to magnetic beads. Boiled lysates or immunoprecipitated samples were resolved on 4-20% SDS gradient gel and blotted onto PVDF membrane. The membrane was incubated with the indicated primary antibodies and corresponding peroxidase-conjugated secondary antibodies followed by ECL detection. Asterisks mark non-specific binding of the antibody.

Because binding of MyoIXb and MUF1 might be weak and the lysis buffer commonly used may disrupt this interaction, a low stringency buffer was used for the cell lysis and washing steps in a new experiment (see section 2.7.2). However, despite the mild lysis and washing conditions, an interaction between MyoIXb and MUF1 was not observed (not shown).

3.2.10.2 RBPMS as a potential binding partner of MUF1

RBPMS (RNA Binding Protein with Multiple Splicing) proteins belong to the large family of RNA-binding proteins. Alternative splicing of the single copy of the *RBPMS* gene gives rise to at least twelve transcripts, nine of them encoding an RNA-recognition motif at the N-terminus (Shimamoto et al. 1996). RBPMS is involved in transforming growth factor-β (TGF-β) signalling by increasing Smad-mediated transcriptional activity (Sun et al. 2006).

Most of the RBPMS transcripts encode the same N-terminus containing the RNA-binding motif, but differ in their C-terminus. For testing the interaction between RBPMS and MUF1, we have chosen mouse variant 1 (NP_062707.1), which is the most frequently occurring transcript and variant 3 (NP_001036140.1), which has a distinct C-terminus compared to isoform 1 and we subcloned their cDNAs to the expression vectors. 293T HEK cells were transfected with Flag-RBPMS1 or Flag-RBPMS3 and Myc-MUF1. One sample transfected with Flag-MUF1 and Myc-RhoBTB3 was used as a positive co-immunoprecipitation control. Co-immunoprecipitation was performed with anti-Myc antibody coupled to magnetic beads. Immunoprecipitates and lysates were analysed for the presence of the indicated tagged proteins by Western blotting. As figure 3.31A shows, Myc-MUF1 did not co-immunoprecipitate neither Flag-RBPMS1 nor Flag-RBPMS3.

To confirm this, another co-immunoprecipitation was performed this time with anti-GFP antibody coupled to magnetic beads. 293T HEK cells were transfected with Flag-RBPMS1 or Flag-RBPMS3 and GFP-MUF1-LRR. One sample transfected with GFP-RhoBTB3 and Flag-RhoBTB2 was used as a positive co-immunoprecipitation control. Immunoprecipitates and lysates were analysed for the presence of the indicated tagged proteins by Western blotting. As figure 3.31B shows, GFP-MUF1-LRR did not co-immunoprecipitate neither Flag-RBPMS1 nor Flag-RBPMS3. Low stringency buffer was used for the cell lysis and washing steps in both experiments.

A

Flag-RBPMS1 +   +
Flag-RBPMS3   +   +
Flag vector   +
Flag-RhoBTB3   +
Myc-MUF1 + + +   +
Myc vector   + +

55 —
34 —
IP αMyc WB αFlag

95 —
IP αMyc WB αMyc

55 —
34 —
Lys WB αFlag

95 —
Lys WB αMyc

B

Flag-RBPMS1 +   +
Flag-RBPMS3   +   +
Flag vector   +
Flag-RhoBTB2   +
GFP-MUF1-LRR + + +
GFP vector   + +
GFP-RhoBTB3   +

55 —
34 —
IP αGFP WB αFlag

95 —
72 —
34 —
IP αGFP WB αGFP

55 —
34 —
Lys WB αFlag

95 —
72 —
34 —
Lys WB αGFP
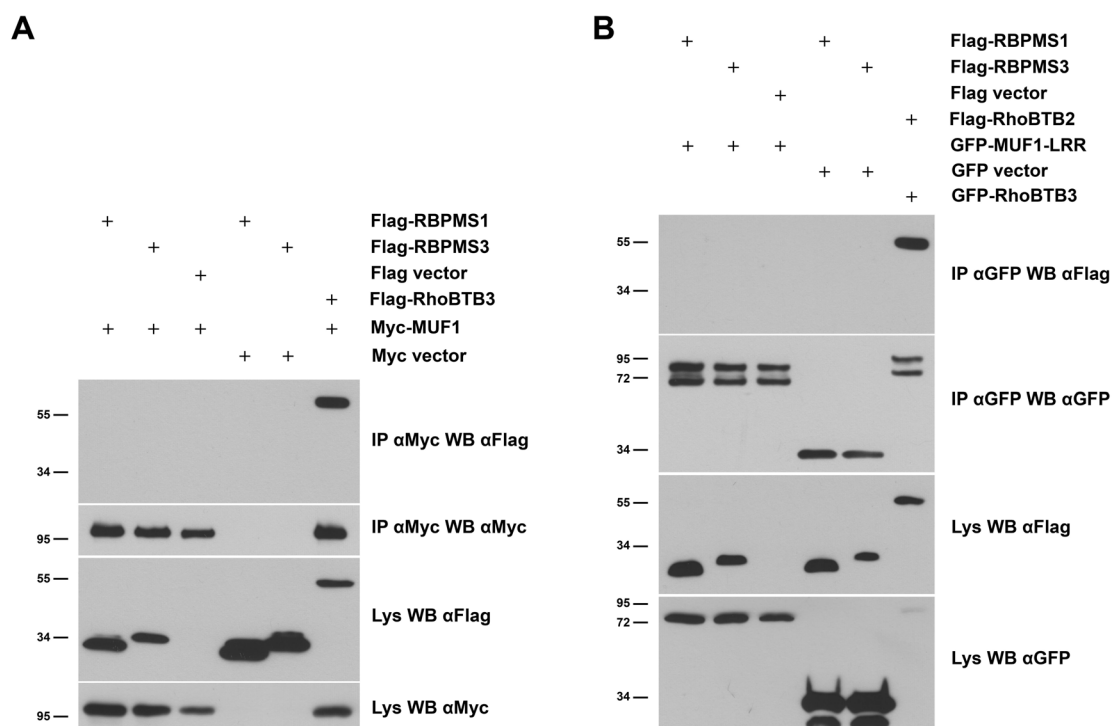
Figure 3.31: MUF1 does not co-immunoprecipitate RBPMS1 or RBPMS3. 293T HEK cells were transfected with the indicated plasmids. Protein complexes were immunoprecipitated and boiled lysates or immunoprecipitated samples were resolved on 10% SDS gel and blotted onto PVDF membrane. The membrane was incubated with the indicated primary antibodies and corresponding peroxidase-conjugated secondary antibodies followed by ECL detection. A) Myc-MUF1 did not co-immunoprecipitate Flag-RBPMS1 or Flag-RBPMS3. Protein complexes were immunoprecipitated with anti-Myc antibody coupled to magnetic beads. B) GFP-MUF1-LRR did not co-immunoprecipitate Flag-RBPMS1 or Flag-RBPMS3. Protein complexes were immunoprecipitated with anti-GFP antibody coupled to magnetic beads.

3.2.11 Dimerisation of cullins

As already mentioned in the introduction (see section 1.4.3), RhoBTB3 is an adaptor of cullin 3-based ligases (Berthold et al. 2008b) and MUF1 is an adaptor of cullin 5-based ligases (Kamura et al. 2001). This raises the question whether MUF1 and RhoBTB3 are together involved in multiprotein complexes containing Cul3 and Cul5 simultaneously. That would indicate that there is cross-talk among cullin-dependent ubiquitin ligases. It was shown recently that several cullins can make homodimers, e.g. Cul1 (Chew et al. 2007), Cul3 (Chew et al. 2007, Wimuttisuk and Singer 2007), Cul4A (Chew et al. 2007) and Cul7 (Skaar et al. 2005), although homodimersation of Cul2 and Cul5 was not observed (Chew et al. 2007). Cul3 can also heterodimerise with Cul1 (Wimuttisuk and Singer 2007). To examine whether Cul3 can also heterodimerse with Cul5, two different approaches were used – yeast two-hybrid and co-immunoprecipitation.

Cul3-pGADT7 and Cul5-pGBKT7 were transformed into yeast cells in order to perform yeast two-hybrid experiments. These experiments were performed several times but brought inconsistent and irreproducible results.

As a second approach, co-immunoprecipitation studies in mammalian cells were performed. 293T HEK cells were transfected with Myc-Cul3 or Myc-Cul5 and Flag-Cul3. Co-immunoprecipitation was performed with anti-Myc antibody coupled to magnetic beads. Immunoprecipitates and lysates were analysed for the presence of the indicated tagged proteins by Western blotting. Figure 3.32A shows that both Myc-Cul3 as well as Myc-Cul5 co-immunoprecipitated Flag-Cul3, therefore Cul3 is able to make homodimers as well as heterodimers with Cul5.

Wimuttisuk and Singer (2007) claimed that dimerisation of Cul3 is mediated by a single Nedd8 molecule in a way that one neddylated Cul3 and one non-neddylated Cul3 form a dimer. To examine whether this is also the case for heterodimerisation of Cul3 and Cul5, 293T HEK cells were transfected with Myc-Cul3 or Myc-Cul5 and a dominant negative mutant of Cul3 (Cul3-DN-Flag). Cul3-DN-Flag lacks the C-terminus, therefore is unable to bind Roc1. This mutant also lacks the lysine residue that is neddylated (K719). Co-immunoprecipitation was performed with anti-Myc antibody coupled to magnetic beads. Immunoprecipitates and lysates were analysed for the presence of the indicated tagged proteins by Western blotting. Figure 3.32B shows that both Myc-Cul3 as well as Myc-Cul5 co-immunoprecipitated Cul3-DN-Flag. These data imply that the dimerisation of the examined cullins does not depend on the C-terminal part of Cul3.

Apart from cullin dimerisation, there is increasing evidence that substrate specific adaptors can form homo- and heterodimers and this interaction is crucial for substrate ubiquitination. This was shown for example for yeast F-box proteins Pop1p and Pop2p (Seibert et al. 2002, Wolf et al. 1999) or the BTB domain containing protein Kelch (McMahon et al. 2006). To examine whether Cul3 and Cul5 heterodimerise through substrate specific adaptors, Cul5ΔNΔC mutant was prepared. This mutant lacks the N-terminal part of Cul5 necessary for interaction with substrates (Xu et al. 2003), and also the C-terminal part that is neddylated (Wimuttisuk and Singer 2007). 293T HEK cells were transfected with Myc-Cul3 and GFP-Cul5ΔNΔC. Co-immunoprecipitation was performed with anti-GFP antibody coupled to magnetic beads. Immunoprecipitates and lysates were analysed for the presence of the indicated tagged proteins by Western blotting. Figure 3.32C shows that GFP-Cul5ΔNΔC co-immunoprecipitated Myc-Cul3 therefore heterodimerisation of Cul3 and Cul5 is not mediated through substrate specific adaptors.

Figure 3.32: Dimerisation of Cul3 and Cul5. 293T HEK were transfected with the indicated constructs or empty Flag and Myc vectors as controls. Protein complexes were immunoprecipitated with anti-Myc antibody coupled to magnetic beads. Boiled lysates or immunoprecipitated samples were resolved on 10% SDS gel and blotted onto PVDF membrane. The membrane was incubated with the indicated primary antibodies and corresponding peroxidase-conjugated secondary antibodies followed by ECL detection. Asterisks mark non-specific binding of the antibody. A) Interaction of Myc-Cul3 and Myc-Cul5 with Flag-Cul3. B) Interaction of Myc-Cul3 and Myc-Cul5 with Cul3-DN-Flag. C) Interaction of GFP-Cul5ΔNΔC with Myc-Cul3. D) Cartoon depicting the possible mechanism of binding of Cul3 and Cul5.

3.3 Kindlin, an interaction partner of RhoBTB3

Kindlin-2/Mig-2 is one of several proteins identified previously in our laboratory during attempts to identify binding partners (and possible substrates) of RhoBTB3 (S. Ramos, personal communication). It was the C-terminus of kindlin-2 that was identified (554-680AA). To confirm this interaction, several co-immunoprecipitation studies were performed in mammalian cells. Figure 3.33 depicts the constructs used in the following studies.

Figure 3.33: Domain architecture of kindlin-1 and kindlin-2 and constructs used in this study. Kindlins are composed of FERM (4.1, ezrin, radixin, moesin) domain, which is subdivided into four subdomains named F0, F1, F2 and F3. The F2 subdomain is interrupted by a pleckstrin homology domain (PH). NLS represents nuclear localisation signal.

3.3.1 RhoBTB2 and RhoBTB3 interact with kindlin-1 and kindlin-2

293T HEK cells were transfected with kindlin-1-Flag or kindlin-2-Flag and either Myc-RhoBTB3 or Myc-RhoBTB2. Co-immunoprecipitation was performed with anti-Myc antibody coupled to magnetic beads. Immunoprecipitates and lysates were analysed for the presence of the indicated tagged proteins by Western blotting. Figure 3.34A shows that Myc-RhoBTB3 co-immunoprecipitated kindlin-2-Flag thus confirming observations from the two-hybrid screening that RhoBTB3 interacts with kindlin-2. Moreover, Myc-RhoBTB3 co-immunoprecipitated also kindlin-1-Flag (Figure 3.34A) and similarly, Myc-RhoBTB2 also co-immunoprecipitated both kindlin-1-Flag and kindlin-2-Flag (Figure 3.34B).

Figure 3.34: RhoBTB2 and RhoBTB3 co-immunoprecipitate kindlin-1 and kindlin-2. 293T HEK cells were transfected with kindlin-1-Flag, kindlin-2-Flag or empty Flag vector and Myc-RhoBTB2, Myc-RhoBTB3 or empty Myc vector. Protein complexes were immunoprecipitated with anti-Myc antibody coupled to magnetic beads. Boiled lysates or immunoprecipitated samples were resolved on 10% SDS gels and blotted onto PVDF membrane. The membrane was incubated with the indicated primary antibodies and corresponding peroxidase-conjugated secondary antibodies followed by ECL detection. A) Interaction of Myc-RhoBTB3 with kindlin-1-Flag and kindlin-2-Flag. B) Interaction of Myc-RhoBTB2 with kindlin-1-Flag and kindlin-2-Flag.

3.3.2 RhoBTB3 has probably multiple binding sites on kindlin-1

We obtained two splicing variants of human kindlin-1, one of them is missing the C-terminal part – kindlin-1 (1-495) and another one is missing the N-terminal part – kindlin-1 (258-677) (Figure 3.33). To test which splicing variant binds to RhoBTB3, co-immunoprecipitation was performed. 293T HEK cells were transfected with Flag-kindlin-1 (1-495) or Flag-kindlin-1 (258-677) and Myc-RhoBTB3. Co-immunoprecipitation was performed with anti-Myc antibody coupled to magnetic beads. Immunoprecipitates and lysates were analysed for the presence of the indicated tagged proteins by Western blotting. Both Flag-kindlin-1 (1-495) and Flag-kindlin-1 (258-677) were co-immunoprecipitated with Myc-RhoBTB3 (Figure 3.35). Interestingly, it was the C-terminal part of kindlin-2 (residues 554-680) that was identified in the two-hybrid screening. This region corresponds to the region 551-677 AA in kindlin-1. This indicates that RhoBTB3 may have multiple binding sites on kindlins. To confirm this, two additional constructs were used – GFP fusions of the N-terminal part and the C-terminal part of kindlin-1 (Figure 3.33). 293T HEK cells were transfected with GFP-kindlin-1/N or GFP-kindlin-1/C and Myc-RhoBTB3. Co-immunoprecipitation was performed with anti-GFP antibody coupled to magnetic beads. Immunoprecipitates and lysates were analysed for the presence of the indicated tagged proteins by Western blotting. Both, GFP-kindlin-1/N and GFP-

kindlin-1/C, co-immunoprecipitated Myc-RhoBTB3 supporting the hypothesis that RhoBTB3 may have multiple binding sites on kindlins (Figure 3.36).

Figure 3.35: RhoBTB3 co-immunoprecipitates kindlin-1 (1-495) and kindlin-1 (258-677). 293T HEK cells were transfected with Flag-kindlin-1 (1-4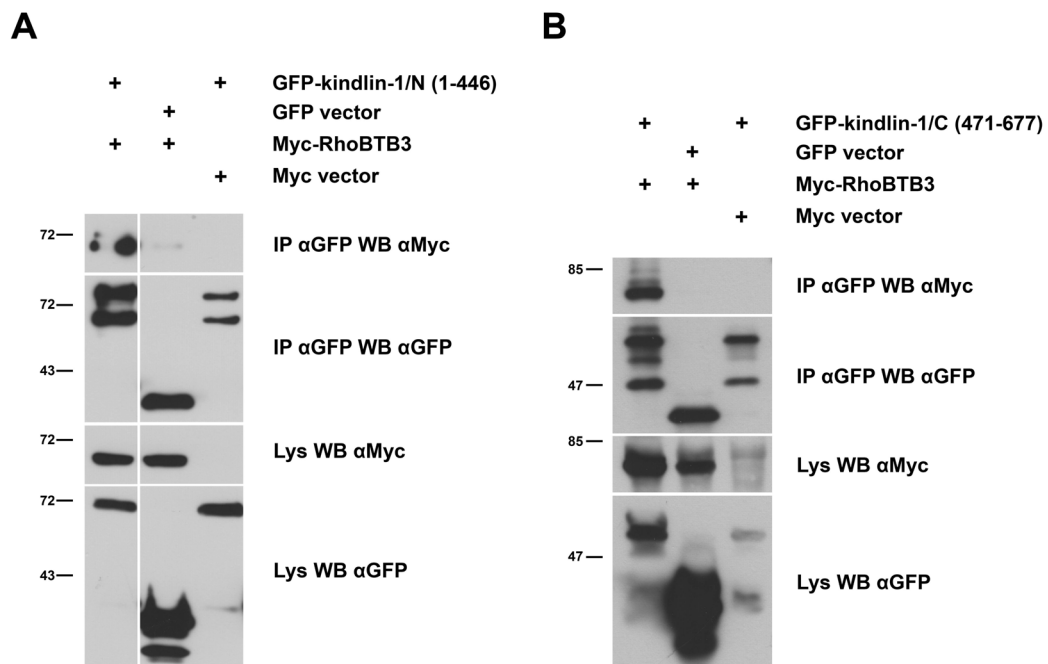95) or Flag-kindlin-1 (258-677) or empty Flag vector and Myc-RhoBTB3 or empty Myc vector. Protein complexes were immunoprecipitated with anti-Myc antibody coupled to magnetic beads. Boiled lysates or immunoprecipitated samples were resolved on 10% SDS gel and blotted onto PVDF membrane. The membrane was incubated with the indicated primary antibodies and corresponding peroxidase-conjugated secondary antibodies followed by ECL detection.

Figure 3.36: Kindlin-1/N and kindlin-1/C co-immunoprecipitate RhoBTB3. 293T HEK cells were transfected with GFP-kindlin-1/N or GFP-kindlin-1/C or empty GFP vector and Myc-RhoBTB3 or empty Myc vector. Protein complexes were immunoprecipitated with anti-Myc antibody coupled to magnetic beads. Boiled lysates or immunoprecipitated samples were resolved on 10% SDS gels and blotted onto PVDF membrane. The membrane was incubated with the indicated primary antibodies and corresponding peroxidase-conjugated secondary antibodies followed by ECL detection. A) Interaction of GFP-kindlin-1/N with Myc-RhoBTB3. B) Interaction of GFP-kindlin-1/C with Myc-RhoBTB3. This part of the experiment was done in collaboration with Julia Lutz.

3.3.3 RhoBTB3 partially co-localises with kindlin-1 and kindlin-2

To examine if kindlin also co-localises with RhoBTB3, COS7 cells were co-transfected with either GFP-kindlin-1 or GFP-kindlin-2 and Flag-RhoBTB3. Fixed cells were immunostained with anti-Flag (anti-ECS) antibody. In COS7 cells GFP-kindlin-1 and GFP-kindlin-2 localised in the cytoplasm and stronger signal was observed in the paranuclear area where it partially co-localises with RhoBTB3 (Figure 3.37).
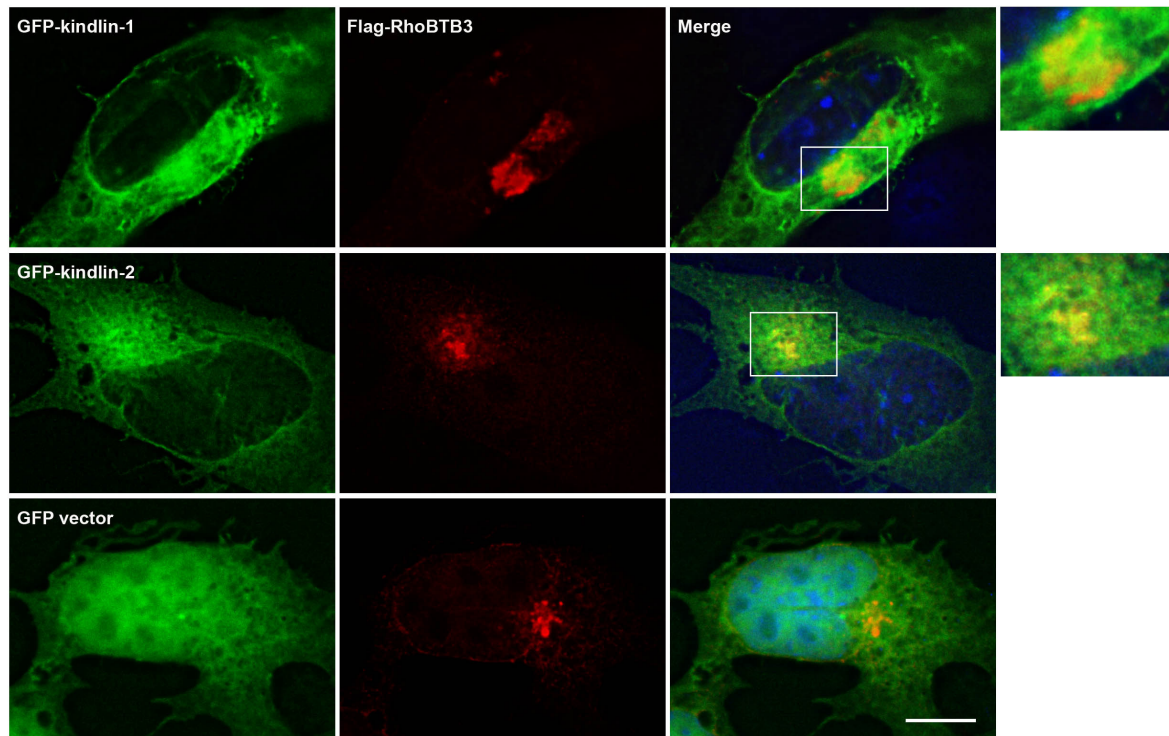
Figure 3.37: Kindlin-1 and kindlin-2 partially co-localise with RhoBTB3. COS7 cells were transfected with Flag-RhoBTB3 and either GFP-kindlin-1, GFP-kindlin-2 and or with empty GFP vector. Cells were fixed and immunostained with anti-Flag (anti-ECS) antibody followed by staining with Alexa Fluor 568-coupled secondary antibody. Images were acquired with a conventional fluorescence microscope, deconvolved and overlaid. Right hand panels are magnifications of the indicated areas. Bar represents 10 μm.

3.4 Uev1a, an interaction partner of RhoBTB3

Uev1a (ubiquitin-conjugating E2 enzyme variant) is another potential binding partner of RhoBTB3 identified in a two hybrid screening (S. Ramos, personal communication). Interaction between Uev1a and RhoBTB2-B1B2C and RhoBTB3-B1B2C has been confirmed by yeast two-hybrid analysis (Berthold 2006 dissertation thesis). However, it has not been confirmed that RhoBTB3 binds Uev1a *in vivo*. To examine this, 293T HEK cells were transfected with Myc-Uev1a and GFP-RhoBTB3. Co-immunoprecipitation was performed with anti-GFP antibody coupled to magnetic beads. Immunoprecipitates and lysates were analysed for the presence of the indicated tagged proteins by Western blotting. Figure 3.38 shows that GFP-RhoBTB3 co-immunoprecipitated Myc-Uev1a therefore confirming the interaction between Uev1a and RhoBTB3.
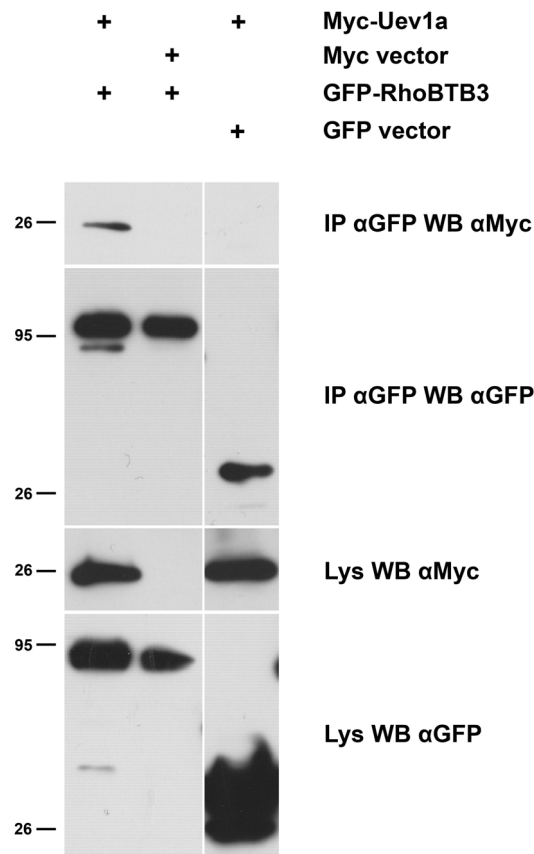
Figure 3.38: RhoBTB3 co-immunoprecipitates Uev1a. 293T HEK cells were transfected with GFP-RhoBTB3 or empty GFP vector and Myc-Uev1a or empty Myc vector. Protein complexes were immunoprecipitated with anti-GFP antibody coupled to magnetic beads. Boiled lysates or immunoprecipitated samples were resolved on 10% SDS gels and blotted onto PVDF membrane. The membrane was incubated with the indicated primary antibodies and corresponding peroxidase-conjugated secondary antibodies followed by ECL detection.

To examine if Uev1a also co-localises with RhoBTB3, COS7 cells were co-transfected with GFP-Uev1a and Flag-RhoBTB3. Fixed cells were immunostained with anti-Flag (anti-ECS) antibody. GFP-Uev1a localised in the nucleus and the cytoplasm. Additionally, GFP-Uev1a positive vesicles were observed in the paranuclear area, where they partially co-localise with RhoBTB3 (Figure 3.39).

Figure 3.39: Uev1a partially co-localises with RhoBTB3. COS7 cells were transfected with GFP-Uev1a and Flag-RhoBTB3 or with empty GFP or Flag vectors. Cells were fixed and immunostained with anti-Flag (anti-ECS) antibody followed by staining with Alexa Fluor 568-coupled secondary antibody. Images were acquired with a conventional fluorescence microscope, deconvolved and overlaid. Right hand panel is magnification of the indicated area. Bar represents 10 μm.

4 Discussion
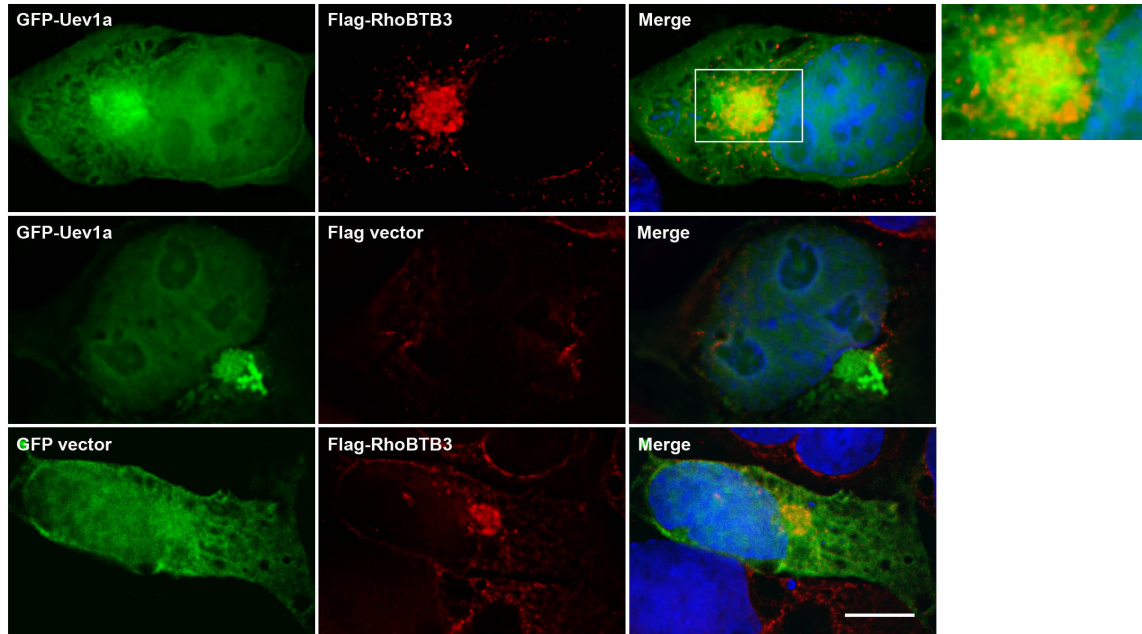
4.1 Subcellular localisation of RhoBTB3

The major obstacle that hampers the study of the subcellular localisation of RhoBTB3 is a lack of good antibodies recognising the endogenous protein. Although the available antibodies recognise endogenous RhoBTB3 on Western blot under certain conditions, probably low cellular levels of RhoBTB3 is the major cause that it cannot be detected using immunofluorescence techniques. We have therefore resorted to the use of tagged proteins in our studies.

RhoBTB3 localises to vesicles dispersed in the cytoplasm and accumulation of the vesicles is observed in the paranuclear area around the MTOC in COS7 and PAE (porcine aortic endothelial) cells (Berthold 2006 dissertation thesis, Berthold et al. 2008b). In this study, we extended this observation also to HeLa cells. RhoBTB3 is the only RhoBTB protein containing a prenylation motif at the C-terminus. Prenylation is a post-translational modification that targets the protein to membranous structures. It was shown that the C-terminus of RhoBTB3 is necessary and sufficient for the vesicular localisation of RhoBTB3 (Berthold et al. 2008b).

To identify the nature of these vesicles various stainings of RhoBTB3-transfected cells were performed. Counterstaining with different cellular markers revealed that RhoBTB3 (at least partially) co-localises with the markers of the endocytic pathway. RhoBTB3 positive vesicles occasionally co-localise with the early endosomal marker transferrin and with the early endosomal marker EEA1. It is the C-terminus that is responsible for RhoBTB3 localisation to early endosomes. The co-localisation with GM130 (GA marker) is more extensive and here again, the C-terminus is responsible for this localisation. These data are consistent with previous observations from our laboratory showing that RhoBTB3 co-localises with another GA marker, namely mannosidase II (Berhold 2006 dissertation thesis). Surprisingly, RhoBTB2 also showed a vesicular localisation and partial co-localisation to the GA. A vesicular localisation of RhoBTB2 was also reported before (Chang et al. 2006). However, because RhoBTB2 lacks a prenylation motif, it is possible that RhoBTB2 is associated with vesicular structures by interaction with other yet unidentified protein(s).

Overexpression of all RhoBTB proteins or only single RhoBTB domains altered the structure of the GA causing formation of aggregates or vesicles dispersed in the cytoplasm. Based on our co-localisation observations, it is possible that most of

the RhoBTB proteins localise primarily to the GA within the cell and overexpression of large amount of exogenous proteins just cause GA disruption. The localisation of RhoBTB3 and the dramatic effect of RhoBTB3 overexpression on GA morphology suggest that this protein might participate in vesicle transport, a role already proposed for RhoBTB2. In the study performed by Chang et al. (2006), knockdown of endogenous RhoBTB2 hindered the ER to GA transport and resulted in altered distribution of the vesicular stomatitis virus glycoprotein. While this thesis was in progress, Espinosa et al. (2009) reported the localisation of RhoBTB3 in the GA by counterstainig with two different GA markers, TGN46 and GCC185, which is in agreement with our own results. In support of a function of RhoBTB3 in vesicular transport, it was shown that this protein interacts with Rab9 through B2C domains. Espinosa et al. (2009) also showed that RhoBTB3 is required for recycling of MPRs to the GA and proposed that Rab9 activates RhoBTB3 on GA, which removes the cargo selection protein TIP47 from the vesicles and permits membrane fusion of vesicles with the GA. These authors also suggest that binding of Rab9 to the C-terminus of RhoBTB3 frees the GTPase domain that is then able to hydrolyse ATP.

GFP-RhoBTB3 vesicles were also observed in close proximity of microtubules and, as mentioned above, around the MTOC (Berthold et al. 2008b). We performed taxol or colchicine treatment that promoted microtubule stabilisation or disruption, respectively. Although RhoBTB3 vesicles were still dispersed in the cytoplasm, the MTOC localisation was not observed anymore. Furthermore, disruption of the microtubule network caused aggregation of RhoBTB3. Thus it seems that an intact microtubule network is necessary for proper RhoBTB3 localisation and possibly also function. Consistent with this observation, RhoBTB2 vesicles appeared also adjacent to microtubules and an intact microtubule network seemed required for the mobility of RhoBTB2 positive vesicles (Chang et al. 2006). GFP-RhoBTB3 vesicles were also observed adjacent to actin filaments (Berthold et al. 2008b). However, disruption of the actin cytoskeleton did not significantly influence the localisation of RhoBTB3 positive vesicles, as these were still observed dispersed in the cytoplasm and in the paranuclear area. Although the precise function of RhoBTB3 needs to be examined in more details, the evidence gathered so far indicates that RhoBTB proteins are involved in vesicular trafficking.

4.2 RhoBTB3 is an adaptor of Cul3-dependent ligase complexes

RhoBTB proteins are very atypical members of the Rho family of small GTPases. Unlike in most Rho GTPases, the GTPase domain does not function as a switch, at least for GTP. This was first documented for RhoBTB2 by Chang et al. (2006) who observed that the GTPase domain of RhoBTB2 does not bind GTP using a blot overlay approach. We show in this work that this feature is also shared by RhoBTB3, as its GTPase domain did not bind (α-^{32}P) GTP. Interestingly, it was shown recently, that RhoBTB3 can bind and hydrolyse ATP (Espinosa et al. 2009).

In comparison to the classical Rho GTPases, RhoBTB proteins also possess additional domains beyond the GTPase domain and these domains can mediate interaction with other cellular proteins. The BTB-domain, which has been found in about 200 proteins in humans, binds to Cul3. The BTB-Cul3 complex resembles the structure of the well characterised SCF and ECV/ECS complexes (Krek 2003) that link the substrate to the catalytical core of the ubiquitin ligase and facilitate ubiquitination and degradation of the substrate protein. In fact, this has been shown for several BTB-containing proteins (Furukawa et al. 2003, Geyer et al. 2003, Pintard et al. 2003, Xu et al. 2003), including RhoBTB2 (Wilkins et al. 2004). RhoBTB3, similarly to RhoBTB2, binds Cul3 through its first BTB domain (Berthold et al. 2008b) and in this work we confirmed the interaction of all three RhoBTB proteins with endogenous Cul3 by co-immunoprecipitation. Our laboratory has shown that RhoBTB3 is, similarly to RhoBTB2, ubiquitinated in the presence of Cul3 and degraded in the proteasome (Berthold et al. 2008b).

The BTB domains of RhoBTB proteins contain each an N-terminal extension that in other BTB domains folds into one α-helix and one β-strand and mediates the formation of oligomers (Stogios et al. 2005). It was shown experimentally that RhoBTB proteins exist as homo- and heterodimers, and both BTB domains participate in dimerisation (Berthold et al. 2008b). Since both, RhoBTB2 and RhoBTB3, can interact with Cul3 (which itself dimerises), one might suspect that Cul3 mediates RhoBTB dimerisation. However, we were able to show by co-immunoprecipitation analysis that almost complete abrogation of Cul3 expression by siRNA does not have any effect on heterodimerisation of RhoBTB2 and RhoBTB3. This observation is supported by many examples of proteins that dimerise through the BTB domain (Aravind and Koonin 1999, Stogios et al. 2005), and several are recognised Cul3 adaptor proteins, like the promyelocytic leukaemia zinc finger (PLZF) protein (Furukawa et al. 2003) and Keap1 (Zhang et al. 2004). Based on these and other

studies, dimerisation has been proposed as a general feature of Cul3 substrate adaptors (McMahon et al. 2006).

We show here that the GTPase domain, which is able to bind to the C-terminal region of the protein that comprises the BTB tandem (Berthold et al. 2008b), could be responsible for an intramolecular interaction that either blocks the formation of a Cul3-dependent complex or otherwise hinders its ubiquitination activity. An experiment determining the stability of RhoBTB3 showed that the C-terminal region of RhoBTB3 (B1B2C) is degraded very fast in the proteasome and this degradation is prevented by simultaneous co-expression of the GTPase domain. Consistent with this observation, full length RhoBTB3 is more stable than its C-terminal region (B1B2C) expressed alone.

Autoinhibition of RhoBTB3 has been reported recently by Espinosa et al. (2009). Authors of this study have observed that the GTPase domain, which has an ATPase activity, displays approximately the double rate of ATP hydrolysis when expressed alone in comparison to the full length RhoBTB3. Binding of Rab9 to the C-terminal (B2C) part of RhoBTB3 relieves the autoinhibition of the GTPase domain and restores ATP hydrolysis. Therefore it is possible that the interaction of cellular proteins with other domains than the GTPase also mediates the activation of RhoBTB3. It needs to be established whether this particular interaction exposes also the Cul3 binding site or if this process is a part of a different pathway.

Our results strongly support the hypothesis that RhoBTB3 serves as an adaptor in Cul3-dependent ligase complexes. Based on this observations, we proposed a model (Figure 4.1) in which interaction of the GTPase domain with unknown proteins would relieve the autoinhibitory mechanism. The GTPase and other domains, as well as the insertion of the first BTB domain could function as substrate recognition domains. In this process RhoBTB proteins become ubiquitinated and degraded.
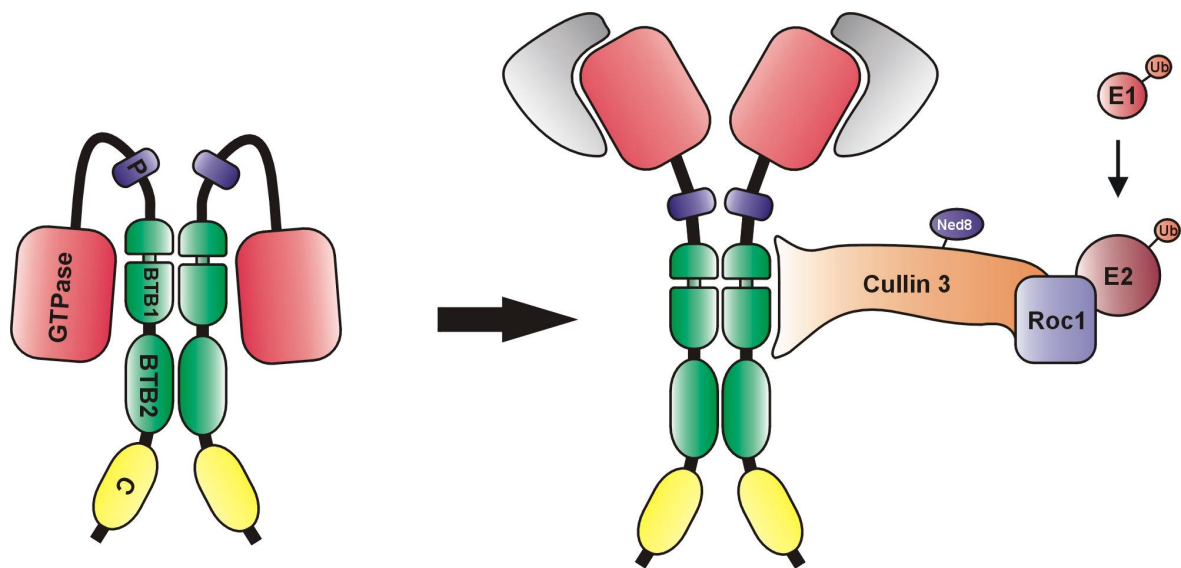
Figure 4.1: Model of the mechanism of action of RhoBTB proteins. RhoBTB proteins recruit Cul3 (regulated by attachment of Nedd8), Roc1 and the E2 (ubiquitin-conjugating enzyme), components of the ubiquitination pathway to constitute an ubiquitin ligase. E1 is the ubiquitin-activating enzyme. RhoBTB proteins probably exist as homo- and heterodimers. RhoBTB is depicted as a parallel dimer, but it remains to be established whether the dimer is parallel or antiparallel. An intramolecular interaction between the GTPase domain and the BTB region would maintain the dimer in an inactive state. Although we have depicted the GTPase interacting with the BTB tandem of the same molecule, an interaction with the tandem of the partner molecule is equally possible. Interaction of the GTPase domain with unknown proteins would relieve the autoinhibition, allowing recruitment of the Cul3 scaffold to the first BTB domain. The GTPase and other domains, as well as the insertion of the first BTB domain could function as substrate recognition domains. The proline-rich region is a potential SH3 domain-binding domain. RhoBTB proteins also become ubiquitinated. Taken from Berthold et al. (2008b).

4.3 Characterisation of MUF1

Using BLAST search analysis, complete MUF1 proteins from different organisms (human, orang-utan, mouse, rat and cow) were identified and aligned. All five MUF1 proteins show a very high degree of similarity. This indicates a conserved function of MUF1. The SOCS-box localised in the N-terminal part of the protein was in all aligned sequences identical, implying its importance for interaction with Cul5 (Kamura et al. 2001). Putative nuclear localisation signals predicted by the PSORT analysis programme were also identical in all five examined sequences. Our findings therefore indicate that MUF1 is very well conserved in *Mammalia* class. Using BLAST search, we also identified predicted proteins similar to MUF1 in number of other organisms. Interestingly, all MUF1 proteins obtained from BLAST search are from *Mammalia* class, except from two representatives belonging to the *Aves* class.

In conclusion, MUF1 is present apparently only in some vertebrate classes where it may have a specific function. Due to the presence of two widely spread domains, we speculate that the gene encoding MUF1 protein arose by a fusion of a gene encoding the LRR region with some gene encoding a protein bearing a SOCS-box domain.

4.4 Expression and subcellular localisation of MUF1

Murine MUF1 is encoded by the *Lrrc41* gene. In this study we demonstrate that the *Lrrc41* gene is ubiquitously expressed. RT-PCR performed on mRNA isolated from different mouse tissues revealed that *Lrrc41* is present in almost all samples tested with exception of skeletal muscle. *Lrrc41* was detected in brain, heart, liver, lung and the highest expression was observed in testis. This result is in agreement with previous observations from our laboratory. Using a *Human Multiple Tissue Expression Array* it was shown that human *LRRC41* is ubiquitously expressed (Kopp 2006 diploma thesis). This was very important to determine in order to confirm that MUF1 and RhoBTB proteins do actually 'meet' in the same tissue.

Both in humans and mice, all three *RHOBTB* genes are rather ubiquitously expressed, although with notable differences in the pattern of tissue levels among the three genes (Nagase et al. 1998a, Nagase et al. 1998b, Ramos et al. 2002).

In human, expression of *Lrrc41* overlaps with expression of *RHOBTB1* in testis, of *RHOBTB2* in brain and heart and of *RHOBTB3* in testis, brain and heart. Expression of

Lrrc41 overlaps with expression of mouse *Rhobtb1* in heart, testis, liver and lung, of *Rhobtb2* in brain and of *Rhobtb3* in brain and heart.

Immunofluorescence studies showed that MUF1 localises predominantly in the nucleus, independently of the used tag (GFP, I-Plastin tag). This effect is not mediated by the SOCS-box of MUF1, as proteins with mutation in the SOCS-box or with the SOCS-box deletion are still predominantly localised in the nucleus. Predicted putative nuclear localisation signals might be responsible for MUF1 targeting to this compartment. GFP-tagged MUF1 containing only leucine-rich repeat region shows both nuclear and cytoplasmic localisation. These observations were also confirmed by subcellular fractionation. Our attempt to verify the subcellular localisation of MUF1 by detecting endogenous protein failed, as a polyclonal antibody raised against a peptide encompassing residues 771-784 was very unspecific both on the fixed cells as well as on Western blot.

Since MUF1 is predominantly a nuclear protein, it was of a great interest to examine the mutual localisation of RhoBTB3 and MUF1 in the cell. There is no experimental evidence that RhoBTB proteins localise in the nucleus. Chang et al. (2006) claim, that endogenous RhoBTB2 can be seen in the nucleus in some cells, but this is presented as not shown. To date, only cytoplasmic localisation of RhoBTB proteins has been documented. We observed that upon co-expression of MUF1 and RhoBTB3, MUF1 still localises mainly in the nucleus, but interestingly, part of the protein is retained in the cytoplasm, where it co-localises with RhoBTB3 in the paranuclear area. The LRR region of MUF1 is sufficient for mediating this effect. The possible relevance of MUF1 re-localisation to the cytoplasm in dependence of RhoBTB3 will be discussed below.

4.5 MUF1 as an adaptor for Cul5 ubiquitin ligases

Adaptor specific subunits of cullin-dependent ubiquitin ligases are very often capable of forming dimers. F-box proteins, substrate-specific adaptors in SCF complexes, dimerise through the D-domain just N-terminally from the F-box (Tang et al. 2007). Dimerisation was shown for example for the yeast F-box proteins Pop1p and Pop2p (Seibert et al. 2002, Wolf et al. 1999), βTRCP1 (Suzuki et al. 2000) and a number of other F-box proteins. Dimerisation was also observed in case of the von Hippel-Lindau (VHL) tumour suppressor gene, a substrate-specific adaptor in ECV complexes (Chung et al. 2006). As already mentioned, BTB-domain containing proteins dimerise through the BTB domain (Stogios et al. 2005). Given that a large number of substrate-binding adaptors are dimeric

and the fact that proteins with LRR domains exist as dimers (Bella et al. 2008), we tested the ability of MUF1 to form homodimers. We confirmed that MUF1 homodimerises and proved that this homodimerisation is not mediated by Cul5. Dimerisation is most probably achieved through interaction of LRRs. Because MUF1 shows predominantly nuclear localisation and nuclear localisation has been reported for Cul5 as well (Furukawa et al. 2000), we favour the hypothesis that Cul5-MUF1 complex is involved in ubiquitination and degradation of nuclear proteins. MUF1 might recognise these substrates by the LRR, as this is a common protein-protein interaction domain (Bella et al. 2008). Substrates for the Cul5-MUF1 complex are unknown. Our attempt to confirm the interaction of MUF1 with MyoIXb and RBPMS by co-immunoprecipitation was not successful. These two proteins were identified in large scale yeast-two hybrid screenings (Rual et al. 2005, Stelzl et al. 2005); however it is possible that these interactions do not take place in mammalian cells *in vivo*.

4.6 MUF1 is a binding partner of RhoBTB proteins

MUF1 was identified as a putative binding partner of RhoBTB3 and is therefore a possible substrate for RhoBTB3-Cul3 ligase complexes. We have verified the interaction of MUF1 with all three RhoBTB proteins using an immunoprecipitation approach. The interaction of MUF1 and RhoBTB3 is not mediated by heterodimerisation of Cul3 and Cul5, as shown by co-immunoprecipitation of mutated proteins unable to bind their respective cullin. Interestingly, it seems that MUF1 may have multiple binding sites on RhoBTB3 and similarly, RhoBTB3 may have multiple binding sites on MUF1 as well. This observation did not come as a complete surprise. It has been shown recently that adaptor proteins can have multiple binding sites on their substrates. SPOP, a MATH-BTB domains containing protein, forms dimers and is in complex with two molecules of Cul3 (Zhuang et al. 2009). HIB/Roadkill, the *Drospohila* SPOP orthologue, controls degradation of the MAPK phosphatase Puc involved in TNF signalling in the fly eye (Liu et al. 2009). Crystallographic studies demonstrated that Puc has multiple SPOP binding sites and dimeric SPOP binds only one molecule of Puc *in vitro*. The SPOP-Cul3 complex ubiquitinates Puc in the presence of E1 and E2 and all three SPOP binding sites of Puc contribute to proper ubiquitination of the substrate (Zhuang et al. 2009). This is in agreement with previous observations that cyclin E, a substrate protein that is recognised by an F-box protein Fbw7 in an SCF complex, contains one optimal and one suboptimal

degron (Hao et al. 2007). It is possible that multiple binding sites on the substrate increase the efficiency of substrate-adaptor interaction.

MUF1 was identified as a binding partner of RhoBTB3 in a bacterio-match screening and this would strongly suggest that the interaction is likely to be direct. It was the C-terminal part of MUF1 (609-807 AA) that was identified in this screening to interact with the B1B2C region of RhoBTB3. It is possible that additional binding sites uncovered in our immunoprecipitation studies are not direct binding sites, as during co-immunoprecipitation additional proteins may be present in the complex that might mediate the interaction. Attempts to confirm a direct interaction using recombinant proteins were hampered by poor solubility of GST fusions of RhoBTB3 and its domains.

4.7 MUF1 as a substrate of Cul3-RhoBTB3 ubiquitin ligase

We show that MUF1 is apparently degraded by a Cul3-RhoBTB3 ubiquitin ligase complex. MUF1ΔSOCS, a mutant that lacks the entire SOCS-box and therefore cannot associate with Cul5, is rapidly degraded in the presence of RhoBTB3. We also found that the C-terminal part of RhoBTB3 (B1B2C) is sufficient to mediate this effect. MUF1 contains 27 lysine residues that in theory can serve as acceptor sites for ubiquitin. Now the question is in which subcellular compartment the degradation takes place. Some of the components of the proteasomal degradation system, like E1 and the proteasomes, have nuclear localisation signals and have been identified in the nucleus (McGrath et al. 1991, Schwartz et al. 1992, Wójcik and DeMartino 2003). The presence of the ubiquitin in the nucleus has also been reported (Schwartz et al. 1988) and in fact, it has been shown that Far1, a protein required for cell cycle arrest and establishing cell polarity during yeast mating, is degraded exclusively in the nucleus by an SCF-ubiquitin ligase complex after it has been phosphorylated (Blondel et al. 2000). Other proteins shuttle from the nucleus to the cytoplasm prior degradation, as it was shown for β-catenin, a transcriptional activator regulated by the Wnt signalling pathway (Henderson 2000).

MUF1 and RhoBTB3, when expressed alone, localise to different cellular compartments. MUF1 is predominantly nuclear and we did not observe its presence in cytoplasmic vesicles. The presence of RhoBTB3 in the nucleus has not been confirmed and most of the protein accumulates in the paranuclear area. Interestingly, when co-expressed with RhoBTB3, MUF1 is observed in the cytoplasm in vesicles and aggregates that overlap with RhoBTB3 localisation. Therefore it is possible that RhoBTB3 causes MUF1 to be partially

retained in the cytoplasm and degradation of MUF1 occurs here. It is not clear yet whether MUF1 is captured by RhoBTB3 before being transported into the nucleus or whether MUF1 shuttles from the nucleus to the cytoplasm where it binds RhoBTB3, in which case cellular stimuli that might mediate this event remain unknown.

Substrates of SCF and ECS/ECV ubiquitin ligases usually require post-translational modification before they can be recognised for proteasomal degradation. This modification is usually phosphorylation or prolyl-hydroxylation (Krek 2003). One of the many examples is cyclin D1 that must be phosphorylated prior to its transport to the cytoplasm. Once in the cytoplasm cyclin D1 is recognised by FBX4/αB-crystallin, an F-box protein that functions as a substrate-specific adaptor of the SCF ligase complex, and after ubiquitination cyclin D1 is degraded in the proteasome (Diehl et al. 1997, Lin et al. 2007). Interestingly, FBX4/αB-crystallin-SCF activity also requires FBX4 dimerisation that is mediated by phosphorylation of the D-domain of FBX4 (Barbash et al. 2008). To our knowledge, post-translational modifications that trigger substrates degradation via BTB-protein containing Cul3-ubiquitin ligases have not been identified yet. In the case of the already mentioned MATH-BTB domain containing protein SPOP, phosphorylation of SPOP-binding sites on the substrate abrogates binding to SPOP (Zhuang et al. 2009). On the other hand, the KBTBD2 (Kelch-repeat and BTB/POZ domain containing 2) protein was identified as a binding partner of phosphorylated ezrin (Heiska and Carpén 2005). Proteins containing simultaneously Kelch-repeats and BTB-fold serve as substrate-specific adaptors in Cul3-based ubiquitin ligase complexes, as has been shown for Keap1, which mediates the degradation of Nrf2, a protein implicated in the response to oxidative stress (Cullinan et al. 2004). However, involvement of KBTBD2 protein in Cul3-dependent ubiquitin ligase complexes has not been examined so far.

Large scale proteomic analysis of proteins phosphorylated by ATM (ataxia telangiectasia mutated) and ATR (ATM and Rad3 related) protein kinases revealed that MUF1 is phosphorylated upon DNA damage and the phosphorylation site was mapped to the region upstream to the LRR (Matsuoka et al. 2007). The relevance of MUF1 phosphorylation has not been examined so far. It is possible, that MUF1 plays specific roles in maintaining cell homeostasis in the DNA damage response. However, on the other hand, phosphorylation of MUF1 might be a signal for its export out of the nucleus and degradation in the cytoplasm, as has been proved for cyclin D1 (Diehl et al. 1997, Lin et al. 2007). Another option is that phosphorylation regulates MUF1 dimerisation, similarly to the F-box protein FBX4/αB-crystallin (Barbash et al. 2008).

4.8 Heterodimerisation of Cul3 and Cul5

Cullin-dependent ubiquitin ligases exist in the cell as dimers. The importance of these interactions might be in accumulation of the local concentration of substrate or E2, or in facilitating their optimal orientation (Tang et al. 2007). Evidence is accumulating indicating that both cullins and substrate-specific adaptors can dimerise.

Homodimerisation of cullins has been reported for Cul1 (Chew et al. 2007), Cul3 (Chew et al. 2007, Wimuttisuk and Singer 2007), Cul4A (Chew et al. 2007) and Cul7 (Skaar et al. 2005) but has not been confirmed for Cul2 and Cul5 (Chew et al. 2007). Heterodimerisation of cullins is also possible, as was shown for Cul1 and Cul3 (Wimuttisuk and Singer 2007). Based on these observations, we assumed that other cullins can also exist as heterodimers and we tested the interaction between Cul3 and Cul5. Using co-immunoprecipitation we show that Cul3 interacts with Cul5. It was proposed by Wimuttisuk and Singer (2007), that this interaction is mediated by Nedd8. Nedd8 is an ubiquitin like protein that is covalently attached to the C-terminus of cullin (K712) in a process called neddylation. Nedd8 conjugation to the cullin positively regulates ubiquitin ligase activity of cullin complexes by releasing the autoinhibition of cullin C-terminus, allowing structural flexibility of these complexes (Merlet et al. 2009). A point mutation of the Nedd8 binding site did not prevent Cul3-Cul3 interaction, however multiple mutations of the C-terminal region of both cullins completely abrogate dimerisation. Based on this and other data, Wimuttisuk and Singer (2007) proposed that dimerisation of Cul3 is mediated by a single Nedd8 molecule. Nedd8 covalently binds to one Cul3 molecule and non-covalently to the C-terminus of a second Cul3 molecule to form a Cul3 dimer . Our results do not support these observations. A Cul5 that lacks a substantial part of the C-terminus was successfully co-immunoprecipitated by both, Cul3 and Cul5, therefore it seems that the C-terminal part is not necessary for dimerisation. To our knowledge there is no structural evidence addressing the dimerisation of cullins that would identify the dimerisation interface.

As already mentioned (see section 4.5), substrate-specific adaptors in cullin-based ubiquitn ligases very often dimerise. Whether dimerisation of the adaptor subunits constitutes a prerequisite for cullin dimerisation is not clear. Chew et al. (2007) showed by co-immunoprecipitation analysis that dimerisation of Cul3, but not Cul1, is dependent on the substrate recognition adaptor. In this work we observed that heterodimerisation of Cul3

and Cul5 is not mediated by adaptor dimerisation as a Cul5 mutant lacking the N-terminus was still able to pull-down full length Cul3. Therefore heterodimerisation of Cul3 and Cul5 seems to be direct and not dependent on the N- or C-terminal part of the protein. The physiological relevance of cullin heterodimerisation still needs to be elucidated. We hypothesise that heterodimeric cullin complexes that engage different substrate-specific adaptors will function as a big catalytical centre for processing of diverse substrates.

4.9 A possible model of MUF1 function and degradation

Based on the observations mentioned above we proposed following model (Figure 4.2). MUF1 protein exists as a homodimer in a Cul5-ubiquitin ligase complex and would predominantly regulate the turnover of nuclear proteins by targeting them to the proteasome (Figure 4.2A). Although homodimerisation of Cul5 has not been demonstrated (Chew et al. 2007), it is possible that Cul5-MUF1 complex exists in the nucleus as a tetramer. Under some conditions (it may be e.g. phosphorylation in response to the DNA damage) MUF1 would shuttle to the cytoplasm. In the cytoplasm the Cul3-RhoBTB3 ubiquitin ligase exists as a tetrameric complex and binds MUF1 in order to mediate its proteasomal degradation (Figure 4.2B). We have not determined the precise dimerisation interface of MUF1 and the exact interaction sites of MUF1 and RhoBTB3; the binding sites depicted on figure 4.2 are hypothetical.

.
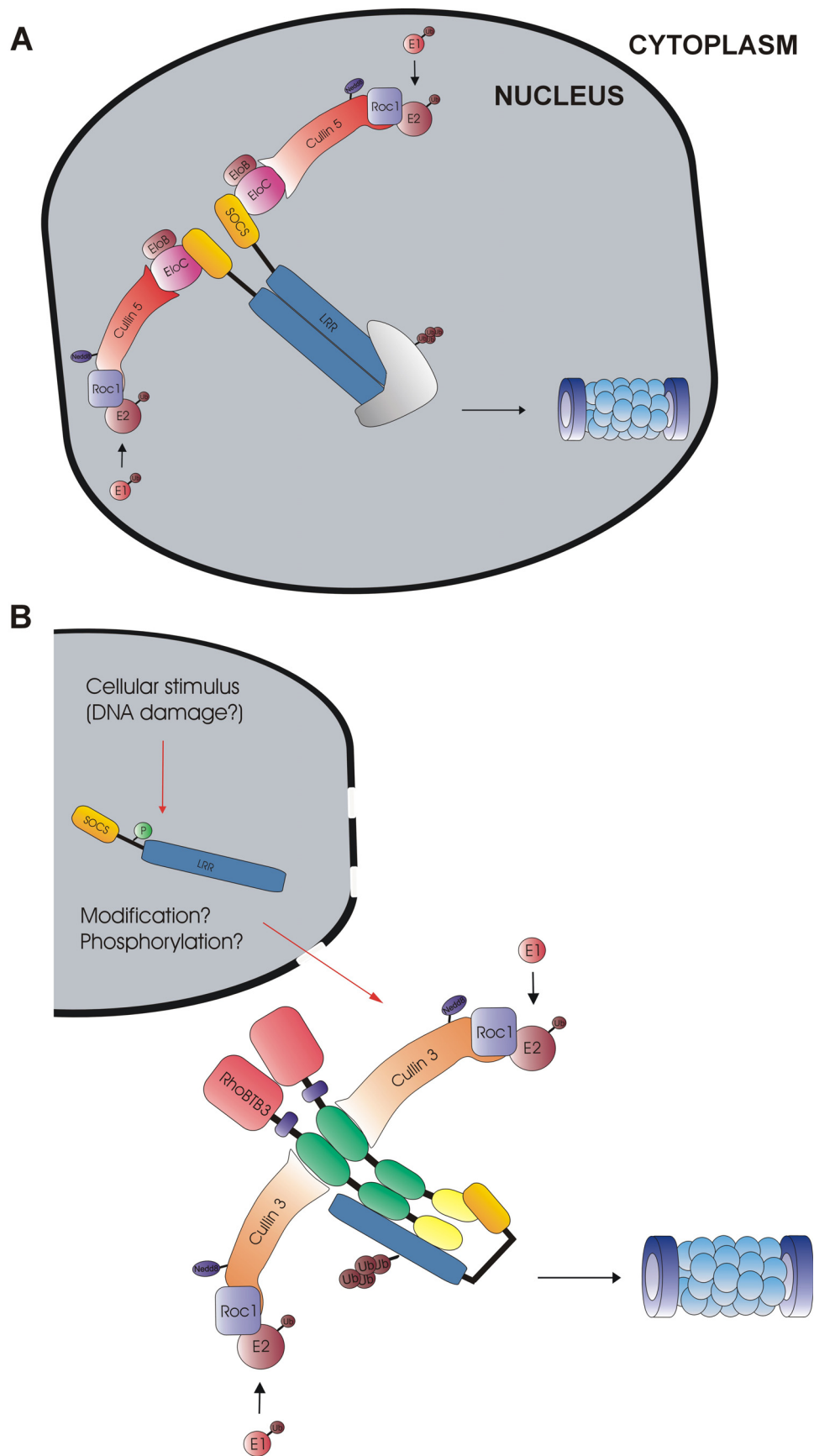
Figure 4.2: Model of MUF1 function and degradation. See text for details. Ub – ubiquitin, E1 – ubiquitin activating enzyme, E2 – ubiquitin conjugating enzyme, EloC – Elongin C, EloB – Elongin B, SOCS – SOCS-box of MUF1, LRR – leucine-rich repeat domain of MUF1, P – phosphorylation.

4.10 Kindlin is a binding partner of RhoBTB proteins

Kindlin-2 was another protein identified in a two-hybrid screening as a potential binding partner of RhoBTB3. Kindlins have received increased interest in the last decade, because it has been shown that they bind directly to the cytoplasmic tails of β1 and β3 subunits of integrins (Harburger et al. 2009, Moser et al. 2008, Ussar et al. 2008) and together with talin are key regulators of integrin activation (Moser et al. 2009). Using co-immunoprecipitation we confirmed the interaction of RhoBTB3 with kindlin-2 and showed that kindlin-1 as well as kindlin-2 interacts with RhoBTB2 and RhoBTB3. Similarly to MUF1, RhoBTB proteins have probably multiple binding sites on kindlins, at least on kindlin-1.

Kindlin-1 and kindlin-2 localises predominantly to focal adhesions in keratinocytes (Kloeker et al. 2004, Siegel et al. 2003, Tu et al. 2003, Ussar et al. 2006). However, cytoplasmic (including perinuclear) and nuclear localisation was observed for both kindlins depending on the cell type used (Kato et al. 2004, Kloeker et al. 2004, Lai-Cheong et al. 2008, Siegel et al. 2003). COS7 fibroblasts form focal adhesions and have been used for the study of proteins in these structures (Schmalzigaug et al. 2007). In immunofluorescence studies we examined mutual localisation of RhoBTB3 and kindlin-1 or kindlin-2 in COS7 cells. Both kindlin proteins were observed in the cytoplasm in the paranuclear area where they partially co-localised with RhoBTB3. In this cell line we did not observe any localisation of kindlins to focal adhesions. However, it is possible, that part of the RhoBTB vesicles that are dispersed through the whole cytoplasm might co-localise with kindlin in focal adhesions in a more suitable cell line (e.g. keratinocytes).

The relationship between RhoBTB and kindlin is currently unknown. Preliminary results from our laboratory showed that endogenous kindlin-1 maintains constant expression levels in HaCaT cells (a human keratinocyte cell line). Similarly in 293T HEK cells, exogenous kindlin-1 is not destabilised upon overexpression of RhoBTB3 and the cellular levels of kindlin-1 are not altered even in the presence of proteasomal inhibitor (Julia Lutz, personal communication). It is possible that the relationship between kindlins and RhoBTB proteins is different than it is in the case of MUF1 and that the function of RhoBTB proteins in complex with kindlin is other than ubiquitination and degradation.

The potential relevance of kindlin-RhoBTB3 interaction might lay in recruitment of the Cul3-ubiquitin ligase complex to the sites of focal adhesions. A number of plasma membrane proteins (e.g. growth factor-activated receptor tyrosine kinases, transporters

and ion channels as well as surface complexes involved in formation of cell junctions) are downregulated predominantly by clathrin-dependent endocytosis upon monoubiquitination or Lys-63 polyubiquitination. Internalised membrane proteins are either recycled back to the plasma membrane or targeted to multivesicular bodies (MVBs) for subsequent degradation in lysosomes. Downregulation of plasma membrane proteins serves as an important mechanism for terminating signalling. Ubiquitin ligases of the HECT- and RING- classes are involved in ubiquitination of plasma membrane proteins either upon direct binding to the substrate or through adaptor proteins (d'Azzo et al. 2005, Léon and Haguenauer-Tsapis 2009). It is tempting to speculate that kindlin might serve here as an adaptor protein bringing RhoBTB-Cul3 ligase complexes to the close proximity of integrins. In this scenario, a RhoBTB-Cul3 ubiquitin ligase would regulate internalisation and turnover of activated integrins by their ubiquitination. However, it is equally possible that Cul3 is not present in the RhoBTB3-kindlin complex. In fact, there is no evidence describing involvement of cullin ubiquitin-ligases in internalisation processes so far.

Supporting the possible role of RhoBTB proteins in this endocytic pathway, RhoBTB3 was recently identified in a proteomic screen as a binding partner of Hrs (hepatocyte growth factor-regulated tyrosine kinase substrate) (Pridgeon et al. 2009). Hrs recognises ubiquitinated membrane cargo proteins through ubiquitin-interacting motifs and is one of the subunits of the so-called ESCRT (endosomal sorting complex required for transport) complex. The ESCRT complex is cellular machinery that recognises ubiquitinated membrane cargo proteins at early endosomes and facilitates their sorting into MVBs for lysosomal degradation (Raiborg and Stenmark 2009). However, the importance of RhoBTB3-Hrs interaction has not been investigated yet.

Further investigations must be carried out to determine the link between RhoBTB proteins and kindlins and their involvement on integrin activation or turnover. Elucidation of the role of RhoBTB proteins with respect to kindlins will undoubtedly contribute to better understanding of RhoBTB function.

4.11 Uev1a is a binding partner of RhoBTB proteins

The last potential binding partner of RhoBTB3 that was investigated here is Uev1a. We confirmed that Uev1a interacts with RhoBTB3 using co-immunoprecipitation. This is in agreement with previous observations obtained by yeast-two hybrid analysis (Berthold 2006, dissertation thesis). Additionally, RhoBTB3 co-localises with Uev1a in the paranuclear area. When expressed in COS7 cells Uev1a localises to the nucleus and part of the signal is observed also in the cytoplasm in the paranuclear area. Early studies attempting to study the localisation of Uev1a revealed nuclear localisation of HA-tagged Uev1a in COS7 cells (Rothofsky and Lin 1997). Similarly, myc-Uev1a localises also to the nucleus in 3T3 (mouse fibroblasts) and HepG2 (hepatocellular carcinoma) cells, but some signal was also observed in the cytoplasm. A deletion mutant lacking the first 30 amino acids displays nuclear as well as cytoplasmic localisation (Andersen et al. 2005). Uev1a is expressed in the cells as four different transcript variants, at least two of them are generated by alternative splicing (Sancho et al. 1998). These variants share the same C-terminus including the domain homologous to the Ubc domain of E2 enzymes, but posses unique N-termini. We found that the Uev1a transcript variant used in our study is different form that one used by Rothofsky and Lin (1997) and Andersen et al. (2005). It lacks first 30 amino acids and in addition contains extra 8 amino acids N-terminally. This explains nuclear and cytoplasmic localisation that we observed in COS7 cells, similarly to Uev1aΔ30 used in the study by Andersen et al. (2005).

The significance of the interaction of RhoBTB3 with Uev1a is not clear so far. Both RhoBTB3 and Uev1a are involved in ubiquitination pathways, although their effectors seem to meet different fates. It is therefore tempting to speculate that these proteins might function in a completely novel pathway within the ubiquitination system. We propose two different hypotheses to explain the relevance of the RhoBTB3-Uev1a interaction.

Since the Uev1-Ubc13 complex is the only ubiquitin-conjugating enzyme that mediates the assembly of Lys63-linked poly-Ub chains (Hofmann and Pickart 1999), one of the possibilities is that RhoBTB3, together with Uev1a, is involved in substrate degradation in a Lys63 polyubiquitin dependent manner. Degradation of proteins modified by Lys63 polyubiquitin chains has been reported recently. Yeast Rsp5, a HECT-type E3 that catalyses the formation of Lys63 ubiquitin chains, ubiquitinates its substrate Mga-p120 and Lys63 ubiquitin chains are sufficient for recognition by the proteasome and Mga-p120 degradation (Saeki et al. 2009). In the RhoBTB3-Uev1a complex the interaction between

RhoBTB3 and Uev1a might be mediated by Cul3. This mode of interaction has been reported for example for RCBTB1, a BTB-domain containing protein linked to lymphocytic neoplasias. RCBTB1 binds together with UbcM2 (ubiquitin-conjugating enzyme) to the N-terminal substrate-binding region of Cul3 in a RING-finger protein independent manner and these interactions are not mutually exclusive. The physiological relevance of this interaction has not been clarified yet, although it has been shown that UbcM2 monoubiquitinates Cul3 (Plafker et al. 2009). In support of our observation that RhoBTB3 interacts with Uev1a, Plafker et al. (2009) reported interaction of RhoBTB1 with another ubiquitin-conjugating enzyme UbcM2.

The second possibility is even more attractive. RhoBTB3, in complex with Cul3-ubiquitin ligase, might ubiquitinate Uev1a in order to target it to the proteasome for degradation. Uev1a has been proposed as a candidate proto-oncogene as its expression is up-regulated in many cancer cell lines (Ma et al. 1998, Xiao et al. 1998). Moreover, Uev1a alone is capable of evoking NFκB signalling that results in anti-apoptotic response and Uev1a seems to be sufficient to drive cells toward tumourigenesis. Downregulation of the cellular pool of Uev1a by RhoBTB3 therefore might contribute to maintain the constant levels of Uev1a in the cell, thus RhoBTB3 would have proapoptotic and anti-cancerogenic effect in this complex. Downregulation of RhoBTB3 might disrupt this balance and direct cells for their cancer destiny. Since expression of RhoBTB proteins is decreased in many types of tumours, it might be interesting to examine if downregulation of RhoBTB3 correlates with upregulation of Uev1a in different types of tumours and cancer cell lines.

5 Abstract

RhoBTB proteins constitute a subfamily of atypical Rho GTPases represented by three isoforms in vertebrates. They serve as adaptors in the formation of Cul3-dependent ubiquitin ligase complexes. Although reports about the function of RhoBTB proteins are accumulating, their significance in cellular processes is far from being understood. Using markers for different subcellular compartments we examined the localisation of RhoBTB3 and found that this protein is localised in part at the GA and to a less extent at early endosomes. Overexpression of RhoBTB proteins significantly disrupted the GA morphology. Disruption of the microtubule, but not of the actin, network caused delocalisation of RhoBTB3 positive vesicles. Connecting to previous observations from our laboratory, we investigated more deeply the function of RhoBTB3 in multiprotein Cul3-dependent ubiquitin ligase complexes. Using immunoprecipitation we observed that RhoBTB3 interacts with endogenous Cul3 and is ubiquitinated by Cul3-dependent ubiquitin ligase complexes for subsequent degradation in the proteasome. This degradation is prevented by an intramolecular interaction between the GTPase domain and the C-terminus of RhoBTB3. We confirmed that RhoBTB proteins, similarly to other adaptors involved in Cul-dependent degradation, are able to dimerise and this interaction is not mediated by Cul3. We propose a model in which RhoBTB proteins play roles in targeting of substrates for ubiquitination and degradation via Cul3-dependent ubiquitin ligase complexes. In order to identify binding partners (and possible substrates) of RhoBTB3 a two-hybrid screening on a mouse brain cDNA library was performed previously in our laboratory. We confirmed the interactions with three potential binding partners, namely MUF1, kindlin-2 (that we further extended also to kindlin-1) and Uev1a by co-immunoprecipitation and co-localisation studies. We focused on MUF1, a largely uncharacterised protein that consist of a leucine-rich repeat region and a BC-box that serves as a linker in multicomponent, Cul5-based ubiquitin ligases. We found that MUF1 interacts with all three RhoBTB proteins and that the interaction between MUF1 and RhoBTB3 is direct and does not depend on Cul3 and Cul5. MUF1 localises in the nucleus but RhoBTB3 causes it to be partially retained in the cytoplasm where both proteins co-localise. MUF1 is able to make homodimers, a feature shared by many leucine-rich repeat containing proteins, and this homodimerisation is not mediated by Cul5. RhoBTB is an adaptor of Cul3-based ubiquitin ligases and MUF1 is an adaptor of Cul5-based ubiquitin ligases. This raises the question whether MUF1 and RhoBTB3 are together involved in

multiprotein complexes containing Cul3 and Cul5 simultaneously. It has been reported that cullins can assemble into dimers, and consistent with this, we found that Cul3 and Cul5 are able to heterodimerise. Our results suggest that MUF1 is degraded in the proteasome in a Cul5 independent manner by a Cul3-RhoBTB3 ligase complex. Our data shows that there is extensive cross-talk among cullin-dependent ubiquitin ligases. We envision a model in which MUF1 exists in a Cul5-ubiquitin ligase complex and predominantly regulates turnover of nuclear proteins by targeting them to the proteasome. RhoBTB3 may be able to regulate MUF1 functions by targeting it for proteasomal degradation in the cytoplasm.

6 Zusammenfassung

Die RhoBTB Proteine gründen eine Unterfamilie der atypischen Rho GTPasen und kommen in Vertebraten in drei Isoformen vor. Sie wirken ursprünglich als Adaptoren am Aufbau von Cul3-abhängigen Ubiquitin Ligase Komplexen. Obwohl es mittlerweile viele Berichte zu den Funktionen der RhoBTB Proteine gibt, ist ihre Bedeutung in zellulären Prozessen bislang kaum geklärt. Wir haben die subzelluläre Lokalisation von RhoBTB3 mit Hilfe von Markern für unterschiedliche subzelluläre Kompartimente untersucht und zeigen, dass RhoBTB3 teilweise am GA und in kleinerem Umfang an frühen Endosomen lokalisiert ist. Die Überexpression der RhoBTB Proteine führt zu signifikanten Störungen in der GA-Morphologie. Störungen des Mikrotubuli-, nicht aber des Aktinnetzwerks führten zu einer Delokalisation von RhoBTB3 positiven Vesikeln. Anknüpfend an frühere Beobachtungen unseres Labors, haben wir die Funktion von RhoBTB3 im Multiprotein Cul3-abhängiger Ubiquitin Ligase Komplexe genauer untersucht. Mit Hilfe von Immunopräzipitionsstudien haben wir bestätigt, dass RhoBTB3 mit endogenem Cul3 interagiert und vom Cul3-abhängigen Ubiquitin Ligase Komplex für den darauffolgenden Abbau im Proteasom ubiquitiniert wird. Dieser Abbau wird durch intramolekulare Wechselwirkungen zwischen der GTPase Domäne und dem C-Terminus von RhoBTB3 verhindert. Wir konnten bestätigen, dass RhoBTB Proteine dimerisieren können, vergleichbar mit anderen Adaptoren die am Cul-abhängigen Abbau beteiligt sind. Dieser Vorgang wird nicht von Cul3 vermittelt. Wir schlagen ein Modell vor, bei dem RhoBTB Proteine an der Markierung von Substraten für eine Ubiquitinierung und am Abbau durch Cul3-abhängige Ubiquitin Ligase Komplexe beteiligt sind. Um Bindungspartner (und potenzielle Substrate) von RhoBTB3 zu identifizieren, wurde in unserem Labor bereits früher ein two-hybrid screening mit einer cDNA Bibliothek aus murinem Gehirn durchgeführt. Wir konnten eine Wechselwirkung zu drei potenziellen Bindungspartnern durch Koimmunopräzipitations- und Kolokalisationsstudien bestätigen: MUF1, kindlin-2 (wir erweiterten es später zusätzlich auf kindlin-1) und Uev1a. Wir haben den Schwerpunkt auf MUF1 gelegt, ein kaum charakterisiertes Protein, dass aus einer leucinreichen Wiederholungsregion und einer BC-Box besteht, die als Verbindungsstelle in multikomponenten Cul5 basierenden Ubiquitin Ligasen dient. Wir bestätigten die Interaktion zwischen MUF1 und allen drei RhoBTB Proteinen, und konnten zeigen, dass eine direkte Interaktion zwischen MUF1 und RhoBTB3 auftritt, die nicht von Cul3 und Cal5 abhängt. MUF1 lokalisiert im Kern, wobei es von RhoBTB3 im Zytoplasma zurück

gehalten wird, indem beide Proteine kolokalisieren. Wir konnten beobachten, dass MUF1 in der Lage ist Homodimere zu bilden - eine Eigenschaft, die es mit vielen Proteinen, die leucinreiche Wiederholungen enthalten ,teilt. Diese Homodimerisation wird nicht von Cul5 vermittelt. RhoBTB ist ein Adaptor der Cul3-basierenden Ubiquitin Ligasen und MUF1 ein Adaptor der Cul5-basierenden Ubiquitin Ligasen. Dies führt zu der Frage, ob MUF1 und RhoBTB3 zusammen in Multiproteinkomplexen, die sowohl Cul3 als auch Cul5 enthalten, involviert sind. Es wurde berichtet, dass sich Culline zu Dimeren zusammenfügen können. Übereinstimmend damit fanden wir heraus, dass Cul3 und Cul5 in der Lage sind Heterodimere zu bilden. Unsere Ergebnisse zeigen, dass MUF1 im Proteasom in einer Cul5-unabhängigen Weise von einem Cul3-RhoBTB3 Ligase Komplex abgebaut wird. Dies deutet auf ein umfangreiches Zusammenspiel zwischen den Cullin-abhängigen Ubiquitin Ligasen untereinander hin. Wir stellen uns ein Modell vor, in dem MUF1 in einem Cul5-abhängigen Ubiquitin Ligase Komplex eingebunden ist, und hauptsächlich den turnover der Zellkernproteine beeinflusst, indem es sie für das Proteasom markiert. RhoBTB3 wäre in der Lage die Funktionen von MUF1 zu regulieren, indem RhoBTB3 MUF1 für den Abbau im Proteasom im Zytoplasma markiert.

7 References

Acconcia F, Sigismund S, Polo S. (2009). Ubiquitin in trafficking: the network at work. *Exp Cell Res.* 315: 1610-1618.

Andersen PL, Zhou H, Pastushok L, Moraes T, McKenna S, Ziola B, Ellison MJ, Dixit VM, Xiao W. (2005). Distinct regulation of Ubc13 functions by the two ubiquitin-conjugating enzyme variants Mms2 and Uev1A. *J Cell Biol.* 170: 745-755.

Angers S, Li T, Yi X, MacCoss MJ, Moon RT, Zheng N. (2006). Molecular architecture and assembly of the DDB1-CUL4A ubiquitin ligase machinery. *Nature.* 443: 590-593.

Aravind L, Koonin EV. (1999). Fold prediction and evolutionary analysis of the POZ domain: structural and evolutionary relationship with the potassium channel tetramerization domain. *J Mol Biol.* 285: 1353-1361.

Aspenström P, Fransson A, Saras J. (2004). Rho GTPases have diverse effects on the organization of the actin filament system. *Biochem J.* 377: 327-337.

Aspenström P, Ruusala A, Pacholsky D. (2007). Taking Rho GTPases to the next level: the cellular functions of atypical Rho GTPases. *Exp Cell Res.* 313: 3673-3679.

Barbash O, Zamfirova P, Lin DI, Chen X, Yang K, Nakagawa H, Lu F, Rustgi AK, Diehl JA. (2008). Mutations in Fbx4 inhibit dimerization of the SCF^{Fbx4} ligase and contribute to cyclin D1 overexpression in human cancer. *Cancer Cell.* 14: 68-78.

Beder LB, Gunduz M, Ouchida M, Gunduz E, Sakai A, Fukushima K, Nagatsuka H, Ito S, Honjo N, Nishizaki K, Shimizu K. (2006). Identification of a candidate tumor suppressor gene RHOBTB1 located at a novel allelic loss region 10q21 in head and neck cancer. *J Cancer Res Clin Oncol.* 132: 19-27.

Bella J, Hindle KL, McEwan PA, Lovell SC. (2008). The leucine-rich repeat structure. *Cell Mol Life Sci.* 65: 2307-2333.

Berthold J. (2006). Rho GTPases of the RhoBTB family: Characterisation and role in tumorigenesis. Dissertation thesis. University of Cologne, Germany.

Berthold J, Schenková K, Rivero F. (2008a). Rho GTPases of the RhoBTB subfamily and tumorigenesis. *Acta Pharmacol Sin.* 29: 285-295.

Berthold J, Schenková K, Ramos S, Miura Y, Furukawa M, Aspenström P, Rivero F. (2008b). Characterization of RhoBTB-dependent Cul3 ubiquitin ligase complexes – evidence for an autoregulatory mechanism. *Exp Cell Res.* 314: 3453-3465.

Bhoj VG, Chen ZJ. (2009). Ubiquitylation in innate and adaptive immunity. *Nature.* 458: 430-437.

Birnboim HC, Doly J. (1979). A rapid alkaline extraction procedure for screening recombinant plasmid DNA. *Nulceic Acid Res.* 7: 1513.

Blondel M, Galan J-M, Chi Y, Lafourcade C, Longaretti C, Deshaies RJ, Peter M. (2000). Nuclear-specific degradation of Far1 is controlled by the localization of the F-box protein Cdc4. *EMBO J.* 19: 6085-6097.

Bourne HR, Sanders DA, McCormick F. (1991). The GTPase superfamily: conserved structure and molecular mechanism. *Nature.* 349: 117-127.

Bullock WO. (1987). *Biotechniques.* 5: 376-378.

Burridge K, Wennerberg K. (2004). Rho and Rac take center stage. *Cell.* 116: 167-179.

Carroll KS, Hanna J, Simon I, Krise J, Barbero P, Pfeffer SR. (2001). Role of the Rab9 GTPase in facilitating receptor recruitment by TIP47. *Science.* 292: 1373-1377.

Colicelli J. (2004). Human RAS superfamily proteins and related GTPases. *Sci STKE.* 250: RE13.

Collado D, Yoshihara T, Hamaguchi M. (2007). DBC2 resistance is achieved by enhancing 26S proteasome-mediated protein degradation. *Biochem Biophys Res Commun.* 360: 600-603.

Cullinan SB, Gordan JD, Jin J, Harper JW, Diehl JA. (2004). The Keap1-BTB protein is an adaptor that bridges Nrf2 to a Cul3-based E3 ligase: oxidative stress sensing by a Cul3-Keap1 ligase. *Mol Cell Biol.* 24: 8477-8486.

d'Azzo A, Bongiovanni A, Nastasi T. (2005). E3 ubiquitin ligases as regulators of membrane protein trafficking and degradation. *Traffic.* 6: 429-441.

de la Roche M, Mahasneh A, Lee S-F, Rivero F, Coté GP. (2005). Cellular distribution and functions of wild-type and constitutively activated *Dictyostelium* PakB. *Mol Biol Cell.* 16: 238-247.

De Sepulveda P, Ilangumaran S, Rottapel R. (2000). Suppressor of cytokine signaling-1 inhibits VAV function through protein degradation. *J Biol Chem.* 275: 14005-14008.

DeGregori J, Johnson DG. (2006). Distinct and overlapping roles for E2F family members in transcription, proliferation and apoptosis. *Curr Mol Med.* 6: 739-748.

Deng L, Wang. C, Spencer E, Yang L, Braun A, You J, Slaughter C, Pickart C, Chen ZJ. (2000). Activation of the IκB kinase complex by TRAF6 requires a dimeric ubiquitin conjugating enzyme complex and a unique polyubiquitin chain. *Cell.* 103: 351-361.

Diehl JA, Zindy F, Sherr CJ. (1997). Inhibition of cyclin D1 phosphorylation on threonine-286 prevents its rapid degradation via the ubiquitin-proteasome pathway. *Genes Dev.* 11: 957-972.

Ea CK, Deng L, Xia ZP, Pineda G, Chen ZJ. (2006). Activation of IKK by TNFα requires site-specific ubiquitination of RIP1 and polyubiquitin binding by NEMO. *Mol Cell.* 22: 245-257.

Endo TA, Masuhara M, Yokouchi M, Suzuki R, Sakamoto H, Mitsui K, Matsumoto A, Tanimura S, Ohtsubo M, Misawa H, Miyazaki T, Leonor N, Taniguchi T, Fujita T, Kanakura Y, Komiya S, Yoshimura A. (1997). A new protein containing an SH2 domain that inhibits JAK kinases. *Nature.* 387: 921-924.

Espinosa EJ, Calero M, Sridevi K, Pfeffer SR. (2009). RhoBTB3: A Rho GTPase-family ATPase required for endosome to Golgi transport. *Cell.* 137: 938-948.

Flick JS, Johnston M. (1990). Two systems of glucose repression of the GAL1 promoter in *Saccharomyces cerevisiae. Mol Cell Biol.* 10: 4757-4769.

Freeman SN, Ma Y, Cress WD. (2007). RhoBTB2 (DBC2) is a mitotic E2F1 target gene with a novel role in apoptosis. *J Biol Chem.* 283: 2353-2362.

Furukawa M, He YJ, Borchers C, Xiong Y. (2003). Targeting of protein ubiquitination by BTB-Cullin 3-Roc1 ubiquitin ligases. *Nat Cell Biol.* 5: 1001-1007.

Furukawa M, Zhang Y, McCarville J, Ohta T, Xiong Y. (2000). The CUL1 C-terminal sequence and ROC1 are required for efficient nuclear accumulation, NEDD8 modification, and ubiquitin ligase activity of CUL1. *Mol Cell Biol.* 20: 8185-8197.

Ganley I, Carroll K, Bittova L, Pfeffer SR. (2004). Rab9 regulates late endosome size and requires effector interaction for stability. *Mol Biol Cell.* 15: 5420-5430.

Garrett KP, Tan S, Bradsher JN, Lane WS, Conaway JW, Conaway RC. (1994). Molecular cloning of an essential subunit of RNA polymerase II elongation factor SIII. *Proc Natl Acad Sci.* 91: 5237–5241.

Geyer R, Wee S, Anderson S, Yates JI, Wolf DA. (2003). BTB/POZ domain proteins are putative substrate adaptors for Cullin 3 ubiquitin ligases. *Molecular Cell.* 12: 783-790.

Glickman MH, Ciechanover A. (2002). The ubiquitin-proteasome proteolytic pathway: destruction for the sake of construction. *Physiol Rev.* 95: 2727-2730.

Goldenberg SJ, Cascio TC, Shumway SD, Garbutt KC, Liu J, Xiong Y, Zheng N. (2004). Structure of the Cand1-Cul1-Roc1 complex reveals regulatory mechanisms for the assembly of the multisubunit cullin-dependent ubiquitin ligases. *Cell.* 119: 517-528.

Goult BT, Bouaouina M, Harburger DS, Bate N, Patel B, Anthis NJ, Campbell ID, Calderwood DA, Barsukov IL, Roberts GC, Critchley DR. (2009). The structure of the N-terminus of kindlin-1: a domain important for αIIbβ3 integrin activation. *J Mol Biol.* 394: 944-956.

Grimm-Günter EM, Revenu C, Ramos S, Hurbain I, Smyth N, Ferrary E, Louvard D, Robine S, Rivero F. (2009). Plastin 1 binds to keratin and is required for the terminal web assembly in the intestinal epithelium. *Mol Biol Cell.* 20: 2549-2562.

Haas AL, Warms JVB, Hershko A, Rose IA. (1982). Ubiquitin-activating enzyme. Mechanism and role in protein-ubiquitin conjugation. *J Biol Chem.* 257: 2543-2548.

Hamaguchi M, Meth JL, von Klitzing C, Wei W, Esposito D, Rodgers L, Walsh T, Welcsh P, King MC, Wigler MH. (2002). DBC2, a candidate for a tumor suppressor gene involved in breast cancer. *Proc Natl Acad Sci U S A.* 99: 13647-13652.

Han JW, Leeper L, Rivero F, Chung CY. (2006). Role of RacC for the regulation of WASP and phosphatidylinositol 3-kinase during chemotaxis of *Dictyostelium*. *J Biol Chem.* 281: 35224-35234.

Hao B, Oehlmann S, Sowa ME, Harper JW, Pavletich NP. (2007). Structure of a Fbw7-Skp1-cyclin E complex: multisite-phosphorylated substrate recognition by SCF ubiquitin ligases. *Mol Cell.* 26: 131-143.

Harburger DS, Bouaouina M, Calderwood DA. (2009). Kindlin-1 and -2 directly bind the C-terminal region of β integrin cytoplasmic tails and exert integrin-specific activation effects. *J Biol Chem.* 284: 11485-11497.

Harper JW, Adami GR, Wei N, Keyomarsi K, Elledge SJ. (1993). The p21 Cdk-interacting protein Cip1 is a potent inhibitor of G1 cyclin-dependent kinases. *Cell.* 75: 805-816.

Hau DD, Lewis MJ, Saltibus LF, Pastushok L, Xiao W, Spyracopoulos L. (2006). Structure and interactions of the ubiquitin-conjugating enzyme variant human Uev1a: implications for enzymatic synthesis of polyubiquitin chains. *Biochemistry.* 45: 9866-9877.

Hayden MS, Ghosh S. (2004). Signaling to NF-κB. *Genes Dev.* 18: 2195-2224.

Heiska L, Carpén O. (2005). Src phosphorylates ezrin at tyrosine 477 and induces a phosphospecific association between ezrin and a Kelch-repeat protein family member. *J Biol Chem.* 280: 10244-10252.

Henderson BR. (2000). Nuclear-cytoplasmic shuttling of APC regulates β-catenin subcellular localization and turnover. *Nature Cell Biol.* 2: 653-660.

Hershko A, Heller H, Elias S, Ciechanover A. (1983). Components of the ubiquitin protein ligase system: resolution, affinity purification and role in protein breakdown. *J Biol Chem.* 258: 8206-8214.

Hershko A, Ciechanover A, Heller H, Haas AL, Rose IA. (1980). Proposed role of ATP in protein breakdown: conjugation of protein with multiple chains of the polypeptide of ATP-dependent proteolysis. *Proc Natl Acad Sci U S A.* 77: 1783-1786.

Hilton DJ, Richardson RT, Alexander WS, Viney EM, Willson TA, Sprigg NS, Starr R, Nicholson SE, Metcalf D, Nicola NA. (1998). Twenty proteins containing a C-terminal SOCS box form five structural classes. *Proc Natl Acad Sci U S A.* 95: 114-119.

Hirsch C, Gauss R, Horn S, Neuber O, Sommer T. (2009). The ubiquitylation machinery of the endoplasmic reticulum. *Nature.* 458: 453-460.

Hofmann RM, Pickart CM. (1999). Noncanonical MMS2-encoded ubiquitin-conjugating enzyme functions in assembly of novel polyubiquitin chains for DNA repair. *Cell.* 96: 645-653.

Hwang YW, Miller DL. (1987). A mutation that alters the nucleotide specificity of elongation factor Tu, a GTP regulatory protein. *J Biol Chem.* 262: 13081-13085.

Hynes RO. (2002). Integrins: bidirectional, allosteric signaling machines. *Cell* 110: 673-687.

Chang FK, Sato N, Kobayashi-Simorowski N, Yoshihara T, Meth JL, Hamaguchi M. (2006). DBC2 is essential for transporting vesicular stomatitis virus glycoprotein. *J Mol Biol.* 364: 302-308.

Chardin P. (2006). Function and regulation of Rnd proteins. *Nat Rev Mol Cell Biol.* 7: 54-62.

Chew E-H, Poobalasingam T, Hawkey CJ, Hagen T. (2007). Characterization of cullin-based E3 ubiquitin ligases in intact mammalian cells – Evidence for cullin dimerization. *Cell Signal.* 19: 1071-1080.

Cho YG, Choi BJ, Song JH, Zhang C, Nam SW, Lee JY, Park WS. (2007). Genetic analysis of the DBC2 gene in gastric cancer. *Acta Oncol.* 47: 366-371.

Chung J, Roberts AM, Chow J, Coady-Osberg N, Ohh M. (2006). Homotypic association between tumour associated VHL proteins leads to the restoration of HIF pathway. *Oncogene.* 25: 3079-3083.

Iwai K, Yamanaka K, Kamura T, Minato N, Conaway RC, Conaway JW, Klausner RD, Pause A. (1999). Identification of the von Hippel-Lindau tumor-suppressor protein as part of an active E3 ubiquitin ligase complex. *Proc Natl Acad Sci U S A.* 96: 12436-12441.

Jaffe AB, Hall A. (2005). Rho GTPases: biochemistry and biology. *Annu Rev Cell Dev Biol.* 21: 247-269.

Jung T, Catalgol B, Grune T. (2009). The proteasomal system. *Mol Aspects Med.* 30: 191-296.

Kajava AV. (1998). Structural diversity of leucine-rich repeat proteins. *J Mol Biol.* 277: 519-527.

Kamizono S, Hanada T, Yasukawa H, Minoguchi S, Kato R, Minoguchi M, Hattori K, Hatakeyama S, Yada M, Morita S, Kitamura T, Kato H, Nakayama K, Yoshimura A. (2001). The SOCS box of SOCS-1 accelerates ubiquitin-dependent proteolysis of TEL-JAK2. *J Biol Chem.* 276: 12530-12538.

Kamura T, Sato S, Haque D, Liu L, Kaelin Jr. WG, Conaway RC, Conaway JW. (1998). The Elongin BC complex interacts with the conserved SOCS-box motif present in members of the SOCS, ras, WD-40 repeat, and ankyrin repeat families. *Genes & Dev.* 12: 3872-3881.

Kamura T, Maenaka K, Kotoshiba S, Matsumoto M, Kohda D, Conaway RC, Conaway JW, Nakayama KI. (2004). VHL-box and SOCS-box domains determine binding specificity for Cul2-Rbx1 and Cul5-Rbx2 modules of ubiquitin ligases. *Genes Dev.* 18: 3055-3065.

Kamura T, Burian D, Yan Q, Schmidt SL, Lane WS, Querido E, Branton PE, Shilatifard A, Conaway RC, Conaway JW. (2001). MUF1, a novel Elongin BC-interacting leucine-rich repeat protein that can assemble with Cul5 and Rbx1 to reconstitute a ubiquitin ligase. *J Biol Chem.* 276: 29748-29753.

Kato K, Shiozawa T, Mitsushita J, Toda A, Horiuchi A, Nikaido T, Fujii S, Konishi I. (2004). Expression of the mitogen-inducible gene-2 (mig-2) is elevated in human uterine leiomyomas but not in leiomyosarcomas. *Hum Pathol.* 35: 55-60.

Kay BK, Williamson MP, Sudol M. (2000). The importance of being proline: the interaction of proline-rich motifs in signaling proteins with their cognate domains. *FASEB J.* 14: 231-241.

Kim HT, Kim KP, Lledias F, Kisselev AF, Scaglione KM, Skowyra D, Gygi SP, Goldberg AL. (2007). Certain pairs of ubiquitin-conjugating enzymes (E2 s) and ubiquitin-protein ligases (E3 s) synthesize nondegradable forked ubiquitin chains containing all possible isopeptide linkages. *J Biol Chem.* 282: 17375-17386.

Kloeker S, Major MB, Calderwood DA, Ginsberg MH, Jones DA, Beckerle MC. (2004). The klindler syndrome protein is regulated by transforming growth factor-ß and involved in integrin-mediated adhesion. *J Biol Chem.* 279: 6824-6833.

Knowles MA, Aveyard JS, Taylor CF, Harnden P, Bass S. (2005). Mutation analysis of the 8p candidate tumour suppressor genes DBC2 (RHOBTB2) and LZTS1 in bladder cancer. *Cancer Lett.* 225: 121-130.

Kobe B, Deisenhofer J. (1993). Crystal structure of porcine ribonuclease inhibitor, a protein with leucine-rich repeats. *Nature.* 366: 751-756.

Kobe B, Kajava AV. (2001). The leucine-rich repeat as a protein recognition motif. *Curr Opin Struct Biol.* 11: 725-732.

Kopp M. (2006). Characterisation of the binding partners of the atypical RhoGTPase RhoBTB3. Diploma thesis. University of Cologne, Germany.

Krek W. (2003). BTB proteins as henchmen of Cul3-based ubiquitin ligases. *Nat Cell Biol.* 5: 950-951.

Kucharczak J, Simmons MJ, Fan Y, Gelinas C. (2003). To be, or not to be: NF-κB is the answer – Role of Rel/NF-κB in the regulation of apoptosis. *Oncogene.* 22: 8961-8982.

Kurian SM, Le-Niculescu H, Patel SD, Bertram D, Davis J, Dike C, Yehyawi N, Lysaker P, Dustin J, Caligiuri M, Lohr J, Lahiri DK, Nurnberger JI Jr, Faraone SV, Geyer MA, Tsuang MT, Schork NJ, Salomon DR, Niculescu AB. (2009). Identification of blood biomarkers for psychosis using convergent functional genomics. *Mol Psychiatry.* [Epub ahead of print]

Lai-Cheong JE, Parsons M, McGrath JA. (2009). The role of kindlins in cell biology and relevance to human disease. *Int J Biochem Cell Biol.* 42: 595-603.

Lai-Cheong JE, Ussar S, Arita K, Hart IR, McGrath JA. (2008). Colocalization of kindlin-1, kindlin-2, and migfilin at keratinocyte focal adhesion and relevance to the pathophysiology of Kindler syndrome. *J Invest Dermatol.* 128: 2156-2165.

Laviolette MJ, Nunes P, Peyre J-B, Aigaki T, Stewart BA. (2005). A genetic screen for suppressors of *Drosophila* NSF2 neuromuscular junction overgrowth. *Genetics.* 170: 779-792.

Lee C-Y, Clough EA, Yellon P, Teslovich TM, Stephan DA, Baehrecke EH. (2003). Genome-wide analyses of steroid- and radiation-triggered programmed cell death in *Drosophila*. *Curr Biol.* 13: 350-357.

Léon S, Haguenauer-Tsapis R. (2009). Ubiquitin ligase adaptors: Regulators of ubiquitylation and endocytosis of plasma membrane proteins. *Exp Cell Res.* 315: 1574-1583.

Li S. (2005). Specificity and versatility of SH3 and other proline-recognition domains: structural basis and implications for cellular signal transduction. *Biochem J.* 390: 641-653.

Li X, Bu X, Lu B, Avraham H, Flavell RA, Lim B. (2002). The hematopoiesis-specific GTP-binding protein RhoH is GTPase deficient and modulates activities of other Rho GTPases by an inhibitory function. *Mol Cell Biol.* 22: 1158-1171.

Lin A, Karin M. (2003). NF-κB in cancer: a marked target. *Semin Cancer Biol.* 13: 107-114.

Lin DI, Lessie MD, Gladden AB, Bassing CH, Wagner KU, Diehl JA. (2007). Disruption of cyclin D1 nuclear export and proteolysis accelerates mammary carcinogenesis. *Oncogene.* 27: 1231-1242.

Liu J, Ghanim M, Xue L, Brown CD, Iossifov I, Angeletti C, Hua S, Nĕgre N, Ludwig M, Stricker T, Al-Ahmadie HA, Tretiakova M, Camp RL, Perera-Alberto M, Rimm DL, Xu T, Rzhetsky A, White KP. (2009). Analysis of Drosophila segmentation network identifies a JNK pathway factor overexpressed in kidney cancer. *Science.* 323: 1218-1222.

Lombardi D, Soldati T, Riederer MA, Goda Y, Zerial M, Pfeffer SR. (1993). Rab9 functions in transport between late endosomes and the trans Golgi network in vitro. *EMBO J.* 12: 677-682.

Ma L, Broomfield S, Lavery C, Lin SL, Xiao W, Bacchetti S. (1998). Up-regulation of CIR1/CROC1 expression upon cell immortalization and in tumor-derived human cell lines. *Oncogene.* 17: 1321-1326.

Masuhara M, Sakamoto H, Matsumoto A, Suzuki R, Yasukawa H, Mitsui K, Wakioka T, Tanimura S, Sasaki A, Misawa H, Yokouchi M, Ohtsubo M, Yoshimura A. (1997). Cloning and characterization of novel CIS family genes. *Biochem Biophys Res Commun.* 239: 439-446.

Matsuoka S, Ballif BA, Smogorzewska A, McDonald ER 3rd, Hurov KE, Luo J, Bakalarski CE, Zhao Z, Solimini N, Lerenthal Y, Shiloh Y, Gygi SP, Elledge SJ. (2007). ATM and ATR substrate analysis reveals extensive protein networks responsive to DNA damage. *Science.* 316: 1160-1166.

Matsushima N, Tachi N, Kuroki Y, Enkhbayar P, Osaki M, Kamiya M, Kretsinger RH. (2005). Structural analysis of leucine-rich-repeat variants in proteins associated with human diseases. *Cell Mol Life Sci.* 62: 2771-2791.

Mayer BJ. (2001). SH3 domains: complexity in moderation. *J Cell Sci.* 114: 1253-1263.

McGrath JP, Jentsch S, Varshavsky A. (1991). UBA 1: an essential yeast gene encoding ubiquitin-activating enzyme. *EMBO J.* 10: 227-236.

McKenna S, Spyracopoulos L, Moraes T, Pastushok L, Ptak C, Xiao W, Ellison MJ. (2001). Noncovalent interaction between ubiquitin and the human DNA repair protein Mms2 is required for Ubc13-mediated polyubiquitination. *J Biol Chem.* 276: 40120-40126.

McKinnon CM, Lygoe KA, Skelton L, Mitter R, Mellor H. (2008). The atypical Rho GTPase RhoBTB2 is required for expression of the chemokine CXCL14 in normal and cancerous epithelial cells. *Oncogene.* 27: 6856-6865.

McMahon M, Thomas N, Itoh K, Yamamoto M, Hayes JD. (2006). Dimerization of substrate adaptors can facilitate cullin-mediated ubiquitinylation of proteins by a "tethering" mechanism. *J Biol Chem.* 281: 24756-24768.

Melnick A, Ahmad KF, Arai S, Polinger A, Ball H, Borden KL, Carlile GW, Prive GG, Licht JD. (2000). In-depth mutational analysis of the promyelocytic leukemia zink finger BTB/POZ domain reveals motifs and residues required for biological and transcriptional functions. *Mol Cell Biol.* 20: 6550-6567.

Merlet J, Burger J, Gomes JE, Pintard L. (2009). Regulation of cullin-RING E3 ubiquitin-ligases by neddylation and dimerization. *Cell Mol Life Sci.* 66: 1924-1938.

Meves A, Stremmel C, Gottschalk K, Fässler R. (2009). The Kindlin protein family: new members to the club of focal adhesion proteins. *Trends Cell Biol.* 19: 504-513.

Mondal S, Neelamegan D, Rivero F, Noegel AA. (2007). GxcDD, a putative RacGEF, is involved in *Dictyostelium* development. *BMC Cell Biol.* 8: 23.

Moser M, Legate KR, Zent R, Fässler R. (2009). The tail of integrins, talin, and kindlins. *Science.* 324: 895-899.

Moser M, Nieswandt B, Ussar S, Pozgajova M, Fassler R. (2008). Kindlin-3 is essential for integrin activation and platelet aggregation. *Nat Med.* 14: 325-330.

Müller RT, Honnert U, Reinhard J, Bähler M. (1997). The rat myosin myr 5 is a GTPase-activating protein for Rho in vivo: essential role of arginine 1695. *Mol Biol Cell.* 8: 2039–2053.

Nagase T, Ishikawa K-I, Suyama M, Kikuno R, Miyajima N, Kotani H, Nomura N, Ohara O. (1998a). Prediction of the coding sequences of unidentified human genes. XI. The complete sequence of 100 new cDNA clones from brain which code for large proteins in vitro. *DNA Res.* 5: 277-286.

Nagase T, Ishikawa K-I, Suyama M, Kikuno R, Hirosawa M, Miyajima N, Tanaka A, Kotani H, Nomura N, Ohara O. (1998b). Prediction of the coding sequences of unidentified human genes. XII. The complete sequence of 100 new cDNA clones from brain which code for large proteins in vitro. *DNA Res.* 5: 355-364.

Naka T, Narazaki M, Hirata M, Matsumoto T, Minamoto S, Aono A, Nishimoto N, Kajita T, Taga T, Yoshizaki K, Akira S, Kishimoto T. (1997). Structure and function of a new STAT-induced STAT inhibitor. *Nature.* 387: 924-929.

Ohadi M, Totonchi M, Maguire P, Lindblom A, Habibi R, Afshin Alavi B, Keyhani E, Najmabadi H. (2007). Mutation analysis of the DBC2 gene in sporadic and familial breast cancer. *Acta Oncol.* 46: 770-772.

Ohta T, Michel JJ, Schottelius AJ, Xiong Y. (1999). ROC1, a homolog of APC11, represents a family of cullin partners with an associated ubiquitin ligase activity. *Mol Cell.* 3: 535-541.

Olusanya O, Andrews PD, Swedlow JR, Smythe S. (2001). Phosphorylation of threonine 156 of the μ2 subunit of the AP2 complex is essential for endocytosis in vitro and in vivo. *Curr Biol.* 11: 896-900.

Park KC, Rivero F, Meili R, Lee S, Apone F, Firtel RA. (2004). Rac regulation of chemotaxis and morphogenesis. *EMBO J.* 23: 4177-4189.

Patnaik A, Chau V, Wills JV. (2000). Ubiquitin is part of the retrovirus budding machinery. *Proc Natl Acad Sci U S A.* 97: 13069-13074.

Peng J, Schwartz D, Elias JE, Thoreen CC, Cheng D, Marsischky G, Roelofs J, Finley D, Gyigi SP. (2003). A proteomics approach to understanding protein ubiquitination. *Nat Biotechnol.* 21: 921-926.

Petroski MD, Deshaies RJ. (2005). Function and regulation of cullin-RING ubiquitin ligases. *Nat Rev Mol Cell Biol.* 6: 9-20.

Pickart CM. (1997). Targeting of substrates to the 26S proteasome. *FASEB J.* 11: 1055-1066.

Pintard L, Willis JH, Willems A, Johnson JL, Srayko M, Kurz T, Glaser S, Mains PE, Tyers M, Bowerman B, Peter M. (2003). The BTB protein MEL-26 is a substrate-specific adaptor of the CUL-3 ubiquitin-ligase. *Nature.* 425: 311-316.

Plafker KS, Singer JD, Plafker SM. (2009). The ubiquitin conjugating enzyme, UbcM2, engages in novel interactions with components of Cullin-3 based E3 ligases. *Biochemistry.* 48: 3527-3537.

Pridgeon JW, Webber EA, Sha D, Li L, Chin L-S. (2009). Proteomic analysis reveals Hrs ubiquitin-interacting motif-mediated ubiquitin signalling in multiple cellular processes. *FEBS J.* 276: 118-131.

Raiborg C, Stenmark H. (2009). The ESCRT machinery in endosomal sorting of ubiquitylated membrane proteins. *Nature.* 458: 445-452.

Ramos S, Khademi F, Somesh BP, Rivero F. (2002). Genomic organization and expression profile of the small GTPases of the RhoBTB family in human and mouse. *Gene.* 298: 147-157.

Reinhard J, Scheel AA, Diekmann D, Hall A, Ruppert C, Bähler M. (1995). A novel type of myosin implicated in signalling by rho family GTPases. *EMBO J.* 14: 697-704.

Riederer MA, Soldati T, Shapiro AD, Lin J, Pfeffer SR. (1994). Lysosome biogenesis requires mannose 6-phosphate receptor recycling from endosomes to the trans Golgi network. *J Cell Biol.* 125: 573-582.

Rivero F, Dislich H, Glockner G, Noegel AA. (2001). The Dictyostelium discoideum family of Rho-related proteins. *Nucleic Acids Res.* 29: 1068-1079.

Rogers SL, Wiedemann U, Stuurman N, Vale RD. (2003). Molecular requirements for actin-based lamella formation in *Drosophila* S2 cells. *J Cell Biol.* 162: 1079-1088.

Rothofsky ML, Lin SL. (1997). CROC-1 encodes a protein which mediates transcriptional activation of the human FOS promoter. *Gene.* 195: 141-149.

Rual JF, Venkatesan K, Hao T, Hirozane-Kishikawa T, Dricot A, Li N, Berriz GF, Gibbons FD, Dreze M, Ayivi-Guedehoussou N, Klitgord N, Simon C, Boxem M, Milstein S, Rosenberg J, Goldberg DS, Zhang LV, Wong SL, Franklin G, Li S, Albala JS, Lim J, Fraughton C, Llamosas E, Cevik S, Bex C, Lamesch P, Sikorski RS, Vandenhaute J, Zoghbi HY, Smolyar A, Bosak S, Sequerra R, Doucette-Stamm L, Cusick ME, Hill DE, Roth FP, Vidal M. (2005). Towards a proteome-scale map of the human protein–protein interaction network. *Nature.* 437: 1173-1178.

Saeki Y, Kudo T, Sone T, Kikuchi Y, Yokosawa H, Toh-e A, Tanaka K. (2009). Lysine 63-linked polyubiquitin chain may serve as a targeting signal for the 26S proteasome. *EMBO J.* 28: 359-371.

Sancho E, Vila MR, Sanchez-Pulido L, Lozano JJ, Paciucci R, Nadal M, Fox M, Harvey C, Bercovich B, Loukili N, Ciechanover A, Lin SL, Sanz F, Estivill X, Valencia A, Thomson TM. (1998). Role of UEV-1, an inactive variant of the E2 ubiquitin-conjugating enzymes, in in vitro differentiation and cell cycle behavior of HT-29-M6 intestinal mucosecretory cells. *Mol Cell Biol.* 18: 576-589.

Saras J, Wollberg P, Aspenström P. (2004). Wrch1 is a GTPase deficient Cdc42-like protein with unusual binding characteristics and cellular effects. *Exp Cell Res.* 299: 356-369.

Seibert V, Prohl C, Schoultz I, Rhee E, Lopez R, Abderazzaq K, Zhou C, Wolf DA. (2002). Combinatorial diversity of fission yeast SCF ubiquitin ligases by homo- and heterooligomeric assemblies of the F-box proteins Pop1p and Pop2p. *BMC Biochem.* 3: 22.

Shi CS, Kehrl JH. (2003). Tumor necrosis factor (TNF)-induced germinal center kinase-related (GCKR) and stress-activated protein kinase (SAPK) activation depends upon the E2/E3 complex Ubc13-Uev1A/TNF receptor-associated factor 2 (TRAF2). *J Biol Chem.* 278: 15429-15434.

Shi X, Ma Y-Q, Tu Y, Chen K, Wu S, Fukuda K, Qin J, Plow EF, Wu C. (2007). The MIG-2/Integrin Interaction Strengthens Cell-Matrix Adhesion and Modulates Cell Motility. *J Biol Chem.* 282: 20455-20466.

Shimamoto A, Kitao S, Ichikawa K, Suzuki N, Yamabe Y, Imamura O, Tokutake Y, Satoh M, Matsumoto T, Kuromitsu J, Kataoka H, Sugawara K, Sugawara M, Sugimoto M, Goto M, Furuichi Y. (1996). A unique human gene that spans over 230 kb in the human chromosome 8p11-12 and codes multiple family proteins sharing RNA-binding motifs. *Proc Natl Acad Sci U S A.* 93: 10913-10917.

Shukla A, Chaurasia P, Bhaumik SR. (2009). Histone methylation and ubiquitination with their cros-talk and roles in gene expression and stability. *Cell Mol Life Sci.* 66: 1419-1433.

Shutes A, Berzat AC, Cox AD, Der CJ. (2004). Atypical mechanisms of regulation of the Wrc-1 Rho family small GTPase. *Curr Biol.* 14: 2052-2056.

Schmalzigaug R, Garron ML, Roseman JT, Xing Y, Davidson CE, Arold ST, Premont RT. (2007). GIT1 utilizes a focal adhesion targeting-homology domain to bind paxillin. *Cell Signal.* 19: 1733-1744.

Schubert U, Ott DE, Chertova EN, Welker R, Tessmer U, Princiotta MF, Bennink JR, Kräusslich H-G, Yewdell JW. (2000). Proteasome inhibition interferes with Gag polyprotein processing, release, and maturation of HIV-1 and HIV-2. *Proc Natl Acad Sci U S A.* 97: 13057-13062.

Schwartz AL, Ciechanover A, Brandt RA, Geuze HJ. (1988). Immunoelectron microscopic localization of ubiquitin in hepatoma cells. *EMBO J.* 10: 2961-2966.

Schwartz AL, Trausch JS, Ciechanover A, Slot JW, Geuze H. (1992). Immunoelectron microscopic localization of the ubiquitin-activating enzyme El in HepG2 cells. *Proc Nati Acad Sci U S A.* 89: 5542-5546.

Siegel DH, Ashton GH, Penagos HG, Lee JV, Feiler HS, Wilhelmsen KC, South AP, Smith FJ, Prescott AR, Wessagowit V, Oyama N, Akiyama M, Al Aboud D, Al Aboud K, Al Githami A, Al Hawsawi K, Al Ismaily A, Al-Suwaid R, Atherton DJ, Caputo R, Fine JD, Frieden IJ, Fuchs E, Haber RM, Harada T, Kitajima Y, Mallory SB, Ogawa H, Sahin S, Shimizu H, Suga Y, Tadini G, Tsuchiya K, Wiebe CB, Wojnarowska F, Zaghloul AB, Hamada T, Mallipeddi R, Eady RA, McLean WH, McGrath JA, Epstein EH. (2003). Loss of kindlin-1, a human homolog of the *Caenorhabditis elegans* actin-extracellular-matrix linker protein UNC-112, causes Kindler syndrome. *Am J Hum Genet.* 73: 174-187.

Skaar JR, Arai T, DeCaprio JA. (2005). Dimerization of CUL7 and PARC is not required for all CUL7 functions and mouse development. *Mol Cell Biol.* 25: 5579-5589.

Spence J, Sadis S, Haas AL, Finley D. (1995). A ubiquitin mutant with specific defects in DNA repair and multiubiquitination. *Mol Cell Biol.* 15: 1265-1273.

St-Pierre B, Jiang Z, Egan SE, Zacksenhaus E. (2004). High expression during neurogenesis but not mammogenesis of a murine homologue of the Deleted in Breast Cancer2/Rhobtb2 tumor suppressor. *Gene Expr Patterns.* 5: 245-251.

Starr R, Willson TA, Viney EM, Murray LJ, Rayner JR, Jenkins BJ, Gonda TJ, Alexander WS, Metcalf D, Nicola NA, Hilton DJ. (1997). A family of cytokine-inducible inhibitors of signalling. *Nature.* 387: 917-291.

Stebbins CE, Kaelin Jr. WG, Pavletich NP. (1999). Structure of the VHL–ElonginC–ElonginB complex: Implications for VHL tumor suppressor function. *Science.* 284: 455-461.

Stelzl U, Worm U, Lalowski M, Haenig C, Brembeck FH, Goehler H, Stroedicke M, Zenkner M, Schoenherr A, Koeppen S, Timm J, Mintzlaff S, Abraham C, Bock N, Kietzmann S, Goedde A, Toksöz E, Droege A, Krobitsch S, Korn B, Birchmeier W, Lehrach H, Wanker EE. (2005). A human-human protein interaction network: A resource for annotating the proteome. *Cell.* 122: 957-968.

Stogios PJ, Downs GS, Jauhal JJ, Nandra SK, Prive GG. (2005). Sequence and structural analysis of BTB domain proteins. *Genome Biol.* 6: R82.

Strack B, Calistri A, Accola MA, Palú G, Göttlinger HG. (2000). A role for ubiquitin ligase recruitment in retrovirus release. *Proc Natl Acad Sci U S A.*: 13063-13068.

Sun Y, Ding L, Zhang H, Han J, Yang X, Yan J, Zhu Y, Li J, Song H, Ye Q. (2006). Potentiation of Smad-mediated transcriptional activation by the RNA-binding protein RBPMS. *Nucleic Acids Res.* 34: 6314-6326.

Suzuki H, Chiba T, Suzuki T, Fujita T, Ikenoue T, Omata M, Furuichi K, Shikama H, Tanaka K. (2000). Homodimer of two F-box proteins βTrCP1 or βTrCP2 binds to IκBα for signal-dependent ubiquitination. *J Biol Chem.* 275: 2877-2884.

Syed NA, Andersen PL, Warrington RC, Xiao W. (2006). Uev1A, a ubiquitin conjugating enzyme variant, inhibits stress-induced apoptosis through NF-κB activation. *Apoptosis.* 11: 2147-2157.

Takai Y, Sasaki T, Matozaki T. (2001). Small GTP-Binding Proteins. *Physiol Rev.* 81: 153-208.

Tang X, Orlicky S, Lin Z, Willems A, Neculai D, Ceccarelli D, Mercurio F, Shilton BH, Sicheri F, Tyers M. (2007). Suprafacial orientation of the SCF^{Cdc4} dimer accommodates multiple geometries for substrate ubiquitination. *Cell.* 129: 1165-1176.

Thrower JS, Hoffman L, Rechsteiner M, Pickart CM. (2000). Recognition of the polyubiqitin proteolytic signal. *EMBO J.* 19: 94-102.

Tu Y, Wu S, Shi X, Chen K, Wu C. (2003). Migfilin and Mig-2 link focal adhesions to filamin and the actin cytoskeleton and function in cell shape modulation. *Cell.* 113: 37-47.

Ussar S, Wang HV, Linder S, Fassler R, Moser M. (2006). The Kindlins: subcellular localization and expression during murine development. *Exp Cell Res.* 312: 3142-3151.

Ussar S, Moser M, Widmaier M, Rognoni E, Harrer C, Genzel-Boroviczeny O, Fässler R. (2008). Loss of Kindlin-1 causes skin atrophy and lethal neonatal intestinal epithelial dysfunction. *PLoS Genet.* 4: e1000289.

Valencia A, Chardin P, Wittinghofer A, Sander C. (1991). The ras protein family: evolutionary tree and role of conserved amino acids. *Biochemistry.* 30: 4637-4648.

van den Boom F, Düssmann H, Uhlenbrock K, Abouhamed M, Bähler M. (2007). The myosin IXb motor activity targets the myosin IXb RhoGAP domain as cargo to sites of actin polymerization. *Mol Biol Cell.* 18: 1507-1518.

Vega FM, Ridley AJ. (2007). SnapShot: Rho family GTPases. *Cell.* 129: 1430

Wang C, Deng L, Hong M, Akkaraju GR, Inoue J, Chen ZJ. (2001). TAK1 is a ubiquitin-dependent kinase of MKK and IKK. *Nature.*: 346-351.

Wegener KL, Partridge AW, Han J, Pickford AR, Liddington RC, Ginsberg MH, Campbell ID. (2007). Structural basis of integrin activation by talin. *Cell.* 128: 171-182.

Weissman AM. (2001). Themes and variations on ubiquitylation. *Nat Rev Mol Cell Biol.* 2: 169-178.

Wennerberg K, Der C. (2004). Rho-family GTPases: it's not only Rac and Rho (and I like it). *J Cell Sci.* 117: 1301-1312.

Wennerberg K, Rossman K, Der C. (2005). The Ras superfamily at a glance. *J Cell Sci.* 118: 843-846.

Wick M, Bürger C, Brüsselbach S, Lucibello FC, Müller R. (1994). Identification of serum-inducible genes: different patterns of gene regulation during G0→S and G1→S progression. *J Cell Sci.* 107: 227-239.

Wilkins A, Ping Q, Carpenter CL. (2004). RhoBTB2 is a substrate of the mammalian Cul3 ubiquitin ligase complex. *Genes Dev.* 18: 856-861.

Wimuttisuk W, Singer JD. (2007). The cullin3 ubiquitin ligase functions as a Nedd8-bound heterodimer. *Mol Biol Cell.* 18: 899-909.

Wójcik C, DeMartino DN. (2003). Intracellular localization of proteasomes. *Int J Biochem Cell Biol.* 35: 579-589.

Wolf DA, McKeon F, Jackson PK. (1999). F-box/WD-repeat proteins pop1p and Sud1p/Pop2p form complexes that bind and direct the proteolysis of cdc18p. *Curr Biol.* 9: 373-376.

Xiao W, Lin SL, Broomfield S, Chow BL, Wei YF. (1998). The products of the yeast MMS2 and two human homologs (hMMS2and CROC-1) define a structurally and functionally conserved Ubc-like protein family. *Nucleic Acids Res.* 26: 3908-3914.

Xu L, Wei Y, Reboul J, Vaglio P, Shin TH, Vidal M, Elledge SJ, Harper JW. (2003). BTB proteins are substrate-specific adaptors in an SCF-like modular ubiquitin ligase containing CUL-3. *Nature.* 425: 316-321.

Yoshihara T, Collado D, Hamaguchi M. (2007). Cyclin D1 downregulation is essential for DBC2's tumor suppressor function. *Biochem Biophys Res Commun.* 358: 1076-1079.

Zhang DD, Lo SC, Cross JV, Templeton DJ, Hannink M. (2004). Keap1 is a redox-regulated substrate adaptor protein for a Cul3-dependent ubiquitin ligase complex. *Mol Cell Biol.* 24: 10941-10953.

Zhang JG, Farley A, Nicholson SE, Willson TA, Zugaro LM, Simpson RJ, Moritz RL, Cary D, Richardson R, Hausmann G, Kile BJ, Kent SB, Alexander WS, Metcalf D, Hilton DJ, Nicola NA, Baca M. (1999). The conserved SOCS box motif in suppressors of cytokine signaling binds to elongins B and C and may couple bound proteins to proteasomal degradation. *Proc Natl Acad Sci.* 96: 2071-2076.

Zhang X, Jiang G, Cai Y, Monkley SJ, Critchley DR, Sheetz MP. (2008). Talin depletion reveals independence of initial cell spreading from integrin activation and traction. *Nature Cell Biol.* 10: 1062-1068.

Zhao C, Slevin JT, Whiteheart SW. (2007). Cellular functions of NSF: not just SNAPs and SNAREs. *FEBS Lett.* 581: 2140-2149.

Zheng N, Schulman BA, Song L, Miller JJ, Jeffrey PD, Wang P, Chu C, Koepp DM, Elledge SJ, Pagano M, Conaway RC, Conaway JW, Harper JW, Pavletich NP. (2002). Structure of the Cul1-Rbx1-Skp1-F boxSkp2 SCF ubiquitin ligase complex. *Nature.* 416: 703-709.

Zhong JM, Chen-Hwang MC, Hwang YW. (1995). Switching nucleotide specificity of Ha-Ras p21 by a single amino acid substitution at aspartate 119. *J Biol Chem.* 270: 10002-10007.

Zhuang M, Calabrese MF, Liu J, Waddell MB, Nourse A, Hammel M, Miller DJ, Walden H, Duda DM, Seyedin SN, Hoggard T, Harper JW, White KP, Schulman BA. (2009). Structures of SPOP-substrate complexes: insights into molecular architectures of BTB-Cul3 ubiquitin ligases. *Mol Cell.* 36: 39-50.

8 Abbreviations

%	Percent
˚C	Celsius degree
AA	Amino acid(s)
APS	Ammonium persulfate
ATP	Adenosine triphosphate
bp	Baise pair(s)
BSA	Bovine serum albumin
cDNA	Complementary DNA
Cul	cullin
DAPI	4´, 6´- diamidino - 2 phenylindol
DME medium	Dulbeccos´ Modified Eagle Medium
DMSO	Dimethylsulfoxide
DNA	Deoxyribonucleic acid
dNTP	Desoxyribonucleotide triphosphate
DTT	Dithiothreitol
E1	Ubiquitin-activating enzyme
E2	Ubiquitin-conjugating enzyme
E3	Ubiquitin ligase
E. coli	*Escherichia coli*
ECS	EloB/C-Cul5-SOCS-box protein
ECV	EloB/C-Cul2-VHL-box protein
EDTA	Ethylen-Diamine-Tetra-Acetate
ER	Endoplasmic reticulum
FBS	Fetal bovine serum
g	relative centrifugation force
GA	Golgi apparatus
GAPDH	Glyceraldehyde-3-phosphate dehydrogenase
GFP	Green fluorescent protein of *Aequorea victoria*
GTP	Guanosine triphosphate
HEPES	4-(2-Hydroxyethyl)-1-piperazineethanesulfonic acid
h	hours
IPTG	Isopropyl β-D-1-thiogalactopyranoside
KDa	Kilodalton
λ	Wave length
LRR	Leucine-rich repeat
M	Molar
min	minute
MTOC	Microtubule organising center
MPR	Mannose 6-phosphate receptor
mRNA	Messenger ribonucleic acid
NP-40	Nonidet P-40
PAGE	Polyacrylamide gel electrophoresis
PBS	Phosphate buffered saline
PCR	Polymerase chain reaction
PIPES	Piperazine-N,N'-bis (2-ethanesulfonic acid)
Ponceau S	3-Hydroxy-4-[2-sulfo-4-(sulfo-phenylazo)phenylazo]-2,7-naphthalindisulfonacid

RT-PCR	Reverse transcription polymerase chain reaction
SAP	Shrimp alkaline phosphatase
SCF	Skp1/Cul1/F-box complex
SDS	Sodium dodecyl sulphate
sec	Second
TAE	Tris-Acetate-EDTA
Taq	*Thermus aquaticus*
TBE	Tris-Borate-EDTA
TBS-T	Tris buffered saline with Tween
TE	Tris-EDTA
TEMED	N,N,N´,N´-Tetramethyl-ethylendiamin
Tris	Trishydroxyaminomethan
U	Unit
Ub	Ubiquitin
Uev	Ubiquitin-conjugating E2 enzyme variant
UV	Ultraviolet light
V	Volt
v/v	Volume per volume
w/v	Weight per volume
X-Gal	5-bromo-4-chloro-3-indolyl-β-D-galactopyranoside

Erklärung

Ich versichere, daß ich die von mir vorgelegte Dissertation selbstständig angefertigt, die benutzten Quellen und Hilfsmittel vollständig angegeben und die Stellen der Arbeit – einschließlich Tabellen, Karten und Abbildungen –, die anderen Werken in Wortlaut oder dem Sinn nach entnommen sind, in jedem Einzelfall als Entlehnung kenntlich gemacht habe; daß diese Dissertation noch keiner anderen Fakultät oder Universität zur Prüfung vorgelegen hat; daß sie – abgesehen von unten angegebenen Teilpublikationen – noch nicht veröffentlicht worden ist sowie, daß ich eine solche Veröffentlichung vor Abschluß des Promotionsverfahrens nicht vornehmen werde.

Die Bestimmungen dieser Promotionsordnung sind mir bekannt. Die von mir vorgelegte Dissertation ist von Prof. Dr. Angelika A. Noegel und PD Dr. Francisco Rivero betreut worden.

Köln, im Mai 2010

_____

Kristína Schenková

Teilpublikationen:

● J. Berthold, K. Schenková, F. Rivero (2008). Rho GTPases of the RhoBTB subfamily and tumorigenesis Acta Pharmacol. Sin. 29: 285-295.

● J. Berthold, K. Schenková, S. Ramos, Y. Miura, M. Furukawa, P. Aspenström, F. Rivero (2008). Characterization of RhoBTB-dependent Cul3 ubiquitin ligase complexes — Evidence for an autoregulatory mechanism, Exp. Cell Res. 314: 3453-3465.

● Schenková K, Rivero F (2008). RHOBTB1 (Rho-related BTB domain containing 1). Atlas Genet Cytogenet Oncol Haematol.

● Schenková K, Rivero F (2008). RHOBTB2 (Rho-related BTB domain containing 2). Atlas Genet Cytogenet Oncol Haematol.

Curriculum vitae

Name   Kristína Schenková
Date of birth   11th December 1982
Place of birth   Nitra, Slovakia
Nationality   Slovak
eMail   kristina.schenkova@hyms.ac.uk

Academic records:

Nov 2006 – May 2010   **PhD studies.** Faculty of Mathematics and Natural Science, University of Cologne
Title: Characterisation of atypical Rho GTPases of the RhoBTB family and their binding partners
Supervisors: Prof. Dr. Angelika A. Noegel, Dr. Francisco Rivero Center for Biochemistry, Medical Faculty, University of Cologne, Germany

Aug 2008 – May 2010   PhD studies (continuation). Centre for Biomedical Research, The Hull York Medical School, University of Hull, United Kingdom

2001-2006   **Diploma studies.** Natural Science Faculty, Charles University in Prague, Czech Republic
Main study programme - Biology
Name of the qualification: Magistr (Mgr.)

27.09.2006 – Final state examination
Subjects: Virology, Molecular biology, Genetic engineering

26.09.2006 – Diploma thesis examination
Title: Studies of delivery of the mouse polyomavirus genome into the cell nucleus
Advisor: Doc. RNDr. Jitka Forstová, CSc., Department of Genetics and Microbiology, Charles University in Prague, Czech Republic

1993-2001   **Secondary school.** Parovska street, Nitra, Slovakia

1989-1993   **Primary school.** Vajanskeho street, Nitra, Slovakia

Lebenslauf

Name	Kristína Schenková
Geburtsdatum	11. Dezember 1982
Geburtsort	Nitra, Slowakei
Staatangehörigkeit	slowakisch
Email	kristina.schenkova@hyms.ac.uk

Bildung:

Nov 2006 – Mai 2010 — **Promotionsstudium.** Matematisch-Naturwissenschaftliche Fakultät, Universität zu Köln
Titel: Charakterisierung der atypischen Rho GTPasen der RhoBTB Familie und deren Bindungspartner
Betreuer: Prof. Dr. Angelika A. Noegel, Dr. Francisco Rivero
Institut für Biochemie, Medizinische Fakultät, Universität zu Köln

Aug 2008 – Mai 2010 — Promotionsstudium (Fortsetzung). Centre for Biomedical Research,
The Hull York Medical School, University of Hull, Großbritannien

2001-2006 — **Diplomstudium.** Naturwissenschaftliche Fakultät,
Karls Universität zu Prag, Tschechische Republik
Hauptfach - Biologie
Name der Qualifikation: Magistr (Mgr.)

27.09.2006 – Staatsexamen
Fächer: Virologie, Molekularbiologie, Gentechnik

26.09.2006 – Diplomprüfung
Titel: Untersuchungen zum Transport des Genoms des murinen Polyomavirus in den Zellkern
Betreuer: Doc. RNDr. Jitka Forstová, CSc., Institut für Genetik und Mikrobiologie, Karls Universität zu Prag, Tschechische Republik

1993-2001 — **Gymnasium.** Parovska Strasse, Nitra, Slowakei

1989-1993 — **Grundschule.** Vajanskeho Strasse, Nitra, Slowakei